University of Alberta

Poly (*N*-isopropylacrylamide) Based Microgels and Their Assemblies for
Organic Molecule Removal from Water

by

Deepika Parasuraman

A thesis submitted to the Faculty of Graduate Studies and Research
in partial fulfillment of the requirements for the degree of

Master of Science

Department of Chemistry

ABSTRACT

This dissertation focuses on the application of poly (N-isopropylacrylamide) (pNIPAm) microgels and their assemblies for the removal of an azo dye molecule, Orange II, from water. Chapter 1 gives an overview of the different techniques that are used for water treatment and remediation. Chapter 2 focuses on hydrogel materials and their properties, with special focus on pNIPAm based microgels. Chapter 3 details the effect of increasing the concentration of percent AAc present in the microgels on the removal of Orange II from water and the concentration of the microgels in the solution. Chapter 4 describes the effect of aggregating the poly (N-isopropylacrylamide)-*co*-acrylic acid (pNIPAm-*co*-AAc) microgels on the uptake efficiencies. Chapter 5 describes the effect of the microgel diameter in the aggregates on the removal efficiency. Chapter 6 describes the possibility of reusing these microgel based systems for further remediation. Finally, Chapter 7 gives a brief outlook on the future directions.

ACKNOWLEDGEMENTS

TABLE OF CONTENTS

LIST OF TABLES

LIST OF FIGURES

LIST OF ABBREVIATIONS

AAc – Acrylic Acid

AC – Activated Carbon

AOPs – Advanced Oxidation Processes

APS – Ammonium Persulphate

BIS – *N,N'*- Methylene bisacrylamide

BMPO – 5-tert-butoxy carbonyl 5-methyl-1-pyrroline N-oxide

BSA – Bovine Serum Albumin

CMC – Critical Micelle Concentration

CNTs – Carbon Nano Tubes

DI – De Ionized

DIC- Differential Interference Contrast

DLS – Dynamic Light Scattering

DNA – Deoxyribonucleic acid

GAC – Granular Activated Carbon

HMX – Octahydro – 1,3,5,7 – tetranitro – 1,3,5,7 – tetrazocine

LCST – Lower Critical Solution Temperature

MEUF – Micellar Enhanced Ultra Filtration

MWCNTs – Multi Walled Carbon Nano Tubes

NADP – Nicotinamide Adenine Dinucleotide Phosphate

NF – Nano Filtration

NOM – Natural Organic Matter

nZVI – Zero Valent Iron Nanoparticles

PAHs – Poly Aromatic Hydrocarbons

PCBs – Polychlorinated Biphenyls

PEUF – Polymer Enhanced Ultra Filtration

pNIPAm – Poly(N-isopropylacrylamide)

pNIPAm-*co*-AAc- Poly (N-isopropylacrylamide-*co*-acrylic acid)

POEOMA – poly (ethylene glycol) monomethyl ether methacrylate

POPs – Persistent Organic Pollutants

RBF – Round Bottom Flask

RDX – Hexahydro – 1, 3, 5 – trinitro – 1, 3, 5 triazocine

RNA – Ribonucleic acid

RO – Reverse Osmosis

SDS – Sodium dodecyl sulphate

SWCNTs – Single Walled Carbon Nano Tubes

SOCs – Synthetic Organic Compounds

THMs – Tri halomethanes

UF – Ultra Filtration

UV – Ultra Violet

VPTT – Vapour Phase Transition Temperature

VPT – Vapour Phase Transition

CHAPTER 1

WATER TREATMENT AND REMEDIATION

1.1. Introduction

Water treatment and remediation techniques have been evolving over many decades to provide pure and clean water that is free from harmful chemicals and pathogens. There are close to 1 billion people in the world who do not have access to potable drinking water and more than a billion who lack access to adequate water sanitation facilities.[1] The world has been facing formidable challenges to meet the rising demands of water quality. Water treatment can be defined as: "The manipulation of water from sources to achieve a water quality that meets specific goals or standard set by the community through its regulatory agencies".[2]

The scope of this Chapter is to give a brief historical overview of water treatment techniques and discuss the current treatment methods in detail. Treatment of dyes stuffs in wastewater will be discussed in a separate section, with special focus on hydrogel and microgel materials used for these purposes.

One of the earliest methods of water treatment was invented by Fuller's team in Louisville, Kentucky and his team in the late 1800's that involved a series of steps namely: screening, coagulation, flocculation/sedimentation and disinfection. These methods are still being used to date in most conventional wastewater treatment plants.[2-4] There have been numerous attempts to improve on this process including experiments to: improve the coagulants available, obtain a better understanding the flocculation process, create more effective filtration systems, and control the amount of chlorine used in the disinfection process in order to curb adverse health effects of excess residual chlorine. Figure 1-1 (adapted from Water Treatment: Principles and Design, 2nd edition)[2] shows a schematic flow diagram of drinking water treatment

using the conventional technology. In this figure, the influent surface water is first screened to remove larger solid particles including pebbles and twigs. The water is then mixed with chemical coagulants such as salts of aluminum and iron which induce the suspended and dissolved solids to bind together or coagulate to form flocs. Flocs are large and heavy particles which settle down in the sedimentation step. Any solids that remain afloat are filtered out in the granular filtration step. The water is then treated with disinfectants such as chlorine or ammonia to kill harmful microorganisms. The disinfected water is finally sent to a clearwell from where it is distributed.
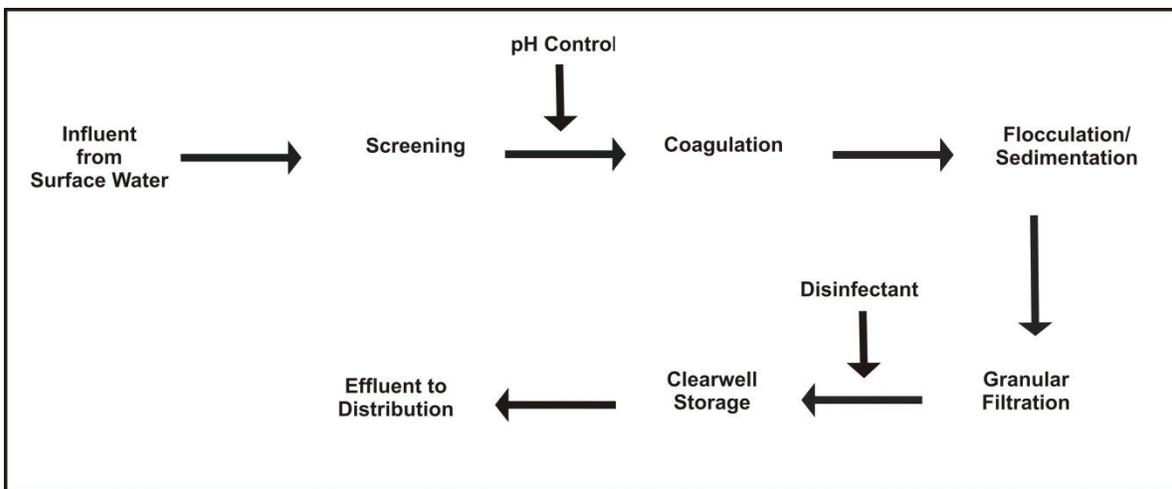
Figure 1-1. Process flow train in conventional drinking water treatment

Wastewater generated from municipal, institutional and commercial sources is collected along with storm water drainage and sent to a wastewater treatment plant. The water is treated before discharging the water back into the supply, e.g., rivers or stream, to control the level of contamination. Waste water treatment involves multiple steps[.5] Firstly, preliminary treatment involves screening of gross solids including rags, grit and any large objects. This is followed by a sedimentation step to remove any floating and settleable materials. This step is termed primary treatment. In an additional step called advanced primary treatment chemicals such as alum (coagulants) are added to remove suspended solids and dissolved solids as well. Secondly,

biological and chemical treatments follow where most of the organic matter is removed. This is known as secondary treatment. One of the biological treatment methods is called suspended growth treatment where waste water is constantly stirred in a bio reactor to enable indigenous microbes to degrade organic matter present in the wastewater. Another method of biological treatment involves attached growth systems such as rotating biological contactors which act as a support for microbes to grow on and gradually degrade any substrates present in the wastewater.

Three different processes namely aerobic, anaerobic and anoxic are used for degradation of organic matter by biological methods.[5] Aerobic processes involve biodegradation in the presence of oxygen, while anaerobic processes involve biodegradation in the absence of oxygen. In anoxic processes, nitrate is converted into nitrogen in the absence of oxygen. These mechanisms can be employed in either suspended growth or attached growth systems depending on the contaminants present in the wastewater. Sometimes a combined process in employed in order to get the best possible degradation results.

1.2. Biological and Chemical Constituents in Water

Biological constituents. Some of the most dangerous diseases including cholera, typhoid and gastroenteritis are water borne.[2] They spread easily and have a short incubation time (usually 2 − 3 days) and are sometimes fatal. They spread through the water distribution system and are capable of affecting a large portion of a population. Some microorganisms that originally affect animals evolve into new strains, which are capable of affecting humans as well. Examples include giargiasis, cryptosporidiosos, bird flu and swine flu.[2]

Hence, it is imperative that potable water be properly disinfected prior to distribution. Common examples of microorganisms present in water are viruses including Hepatitis,

Rotavirus, Echovirus and Enterovirus; bacteria including *Vibrio cholera, Salmonella typhi, Lysterium botulinum and Pseudomonas aeruginosa*; protozoa including *Entamoeba histolytica, Entamoeba dispar, Giardia lamblia and Cryptosporidium parvum.*[2] Conventional disinfection techniques include using oxidants such as chlorine, ammonia, ozone and UV disinfection techniques.

Chemical constituents. In the late twentieth century, two main developments were made in the fields of water quality and improving the effectiveness of water treatment. In water quality, it was realized that chlorine used in the disinfection process reacts with natural organic matter present in water to form harmful chemical byproducts some of which are potential carcinogens. The other most significant development was the introduction of membrane technology that had the potential for complete rejection of harmful pathogens and various other contaminants by size exclusion.[2, 6-9] There have been many more developments in water treatment technologies and remediation methods to face the rising standards of water quality. These have been detailed further in this Chapter with specific examples.

Numerous inorganic, organic and biological impurities can be found in untreated water. The sources of these contaminants are both natural and anthropogenic. Naturally present inorganic constituents that are present in significant amounts (1.0 to 1000 mg/mL) in water include calcium, magnesium, potassium, bicarbonate, chloride, sulphate and nitrate.[2] Other inorganic constituents that are generally present in lesser amounts (0.01 to 10 mg/mL) include arsenic, copper, fluoride, iron, lead, magnesium and silica. These inorganic constituents are found mainly due to reactions during rock weathering and soil and sediment leaching caused by minerals. Examples of inorganic constituents that are present in water due to human activity include, copper, arsenic, silver, mercury, zinc, chromium, nickel.[2,8,10-13] Organic contaminants

from natural sources are called natural organic matter (NOM), formed as a result of chemical and microbial degradation of vegetation.[2,14-17] Synthetic organic compounds (SOCs) are organic contaminants of anthropogenic origin which mainly include industries, careless disposal of chemical wastes in landfills and various other commercial activities. [2, 6,9, 18,19]

1.3. Removal of Heavy Metal Ions from Wastewater

Among the several inorganic constituents present in contaminated water, toxic heavy metal ion contamination originating from industrial, municipal, agricultural and anthropogenic activities has been proven to be hazardous and a serious environmental problem. [2, 8,10-13] If the concentration levels of these heavy metals go beyond a set limit, they can lead to severe health problems. For example, high levels of Ni can result in lung and kidney problem; mercury is known neurotoxin and can damage the central nervous system; lead damages liver and central nervous system.[2,20-22] Several techniques have been reported for the removal of these contaminants from wastewater; this Chapter will focus on chemical precipitation (coagulation), adsorption, ion-exchange, membrane filtration, electro chemical treatments, and nanomaterials.

1.3.1. Chemical Coagulation/Flocculation

Chemical coagulation and flocculation involves addition of chemical compounds called coagulants that react with the contaminants and precipitate them in solution. The precipitate is subsequently separated by sedimentation/filtration. [8] Common coagulants used for this purpose are Ca $(OH)_2$, NaOH, $CaCO_3$, Al_2 $(SO_4)_3$, some organic polymers and sulphides like pyrite (FeS_2) and synthetic FeS [8,10] This technique has been used to specifically remove Cu (II), Cr (VI), Cd (II), Pb (II), As, Cd, Ni, Zn, Mn and Mg from wastewater and groundwater.[23-30]

1.3.2. Adsorption

Another effective and more economic technique for remediation of heavy metal contaminated water is adsorption. The other main advantages of this technique are its operational flexibility and potential for regeneration for further reuse.[8] Among most adsorbents, activated carbon (AC) is one of the most widely used materials for removal of heavy metal ions. AC has been prepared from a variety of sources like coconut shells, wood char, lignin, petroleum coke, peat and sawdust.[12] AC has an amorphous structure, the crucial property being their high surface area as a consequence of large micropore and mesopore volumes. Cd (II), Zn (II), Cr (III) and Cr (VI) have been effectively removed using AC.[8,31-36]A major drawback of AC is its cost depends on its quality. In other words, higher the quality higher is the cost. More importantly, it often needs complexing agents to improve its efficiency and making it unattractive for industries because of low cost efficiency. In order to address this issue, many low cost adsorbents like chitosan, zeolites, clay, fly ash, peat moss, materials of coal (kaolinite, smectite, bentonite), have been employed to remove heavy metal ions like Cu (II), Hg (II), Cd (II), Ni (II), Zn (II), Co (II), Pb (II) and Cr (III) from wastewater and contaminated water. Other less commonly used adsorbents like industrial wastes containing iron (III) hydroxide and lignin, xanthate, rice husk and rice husk carbon have also been reported before for such remediation purposes. [12,22,33,37-43]

1.3.3. Ion Exchange

Ion exchange process employs certain natural and synthetic resins that have a unique ability to exchange their cations with the metals present in the water to be treated. Among the most commonly used synthetic resins, cation exchange resins are known to be strongly acidic in nature and functionalized with sulphonic groups ($-SO_3H$), while the weakly acid resins have

carboxylic acid groups (-COOH). The advantages of this technique include high water treatment capacity, high removal efficiency of metal ion contaminants and fast kinetics.[8,44] The factors governing the uptake of heavy metal ions by these resins are pH, temperature, concentration of metal, ionic charge and contact time.[45] Typical ions like Ce (IV), Fe (III) and Pb (II) have been removed from wastewater and aqueous solution by ion exchange processes. [45,46] There are reports of zeolites, a naturally occurring ion exchange resin for the removal of heavy metal ions but they are not as efficient as the synthetic resins and have been used only in the laboratory scale. Synthetic micron scale zeolites have been widely used for applications in removal of Cr (III), Ni (II), Zn (II), Cu (II) and Cd (II) from metal electroplating wastewaters. [1,47-51]

1.3.4. *Membrane Filtration*

As mentioned earlier, membrane filtration methods are a very significant development for the water treatment. Membrane processes involve a cross-flow filtration technique in which the feed is pumped at high velocity parallel to the surface of the membrane to reduce the collection of species retained at the surface.[2] Among the well-known membrane filtration methods, is ultrafiltration (UF). UF works on low transmembrane pressures that involve creating a constant low pressure drop across the membrane to avoid occurrence of pressure gradients caused by increasing cross flow velocity. The pore size of these membranes is generally bigger than the metal ions, these ions pass through the membrane with ease. [6-9] So in order to improve the retention efficiencies of these membrane , surfactants like Sodium dodecyl sulphate (SDS) are added to result in membranes called micellar enhanced UF (MEUF).[10] The removal efficiency of MEUF is governed by the concentration of the metals, pH and ionic strength. Often surfactants like Sodium dodecyl sulphate (SDS) are added to result in membranes called micellar enhanced UF (MEUF), used to improve the retention efficiency of these UF membranes. Metal ions like

Zn (II), Cu (II), Cd (II), Ni (II) and Pb (II) have been removed by this technique from waste water.[52-54] Another type of UF, called polymer enhanced UF (PEUF), works by water soluble polymers to complex the metal ions.[8] In this process, water soluble polymers with high electron density functional groups (carboxylic acids, thiols, amines) are added to the water contaminated with heavy metal ions. Complexation occurs due to the formation of a coordinate covalent bond between the metal ion and the functional groups. These membranes are widely reported to remove Cr (III), Ni (II), Cu (II), and many more heavy metal ions from aqueous streams.[55-58]

Reverse osmosis (RO), is another membrane filtration technique that uses a semi permeable membrane to remove ions and large molecules from liquid effluents. In this process, pressure is applied to one side of a semi permeable membrane and the contaminants are retained in the pressurized side of the membrane, while the clean water is allowed to pass through to the other side.[3,8] There have been a few reports of appropriate RO operated under specific conditions used previously to remove As, Ni (II), Cu (II) and Cr (III), but this technique is yet to be applied more widely.[59-61]

Nanofiltration (NF) is an intermediate technique between UF and RO with pore size typically about 1 nm. It is an emerging and a very promising technique used for the removal As, Cr and Cu from waste water, recently reported by several researchers.[62-67]

1.3.5. Electrochemical Methods

This technique involves plating out of metal ions on the surface of cathode and recovery of metals in their elemental state. This technology is known to be very expensive, so has not been very widely used, but their importance has gained momentum for past two decades because of the evolving water quality standards.[8] Electrocoagulation is a well established technique that

involves generation of coagulants by dissolving aluminum or iron ions from their respective electrodes. Metal ion is generated at the anode, while hydrogen gas is released at the cathode and this gas helps the flocculated particles to float out of the water.[68] The performance of this technique using aluminum electrode was investigated recently to remove Ag (I), Cu (II), Zn (II) and Ni (II), and reported that higher concentrations of these metals led to higher rates and eventually converted hydroxide precipitates.[68,69]

1.3.6. Nanomaterials

Recent advances in nanoscale science and engineering have shown great promise in contributing to water treatment and remediation by the use of nanosorbents, nanocatalysts, nanoparticles, nanoparticle enhanced ultrafiltration and nanostructured membranes.[1,70] One reason why these materials are so promising and attractive is their ability to reduce the concentrations of toxic substances to sub ppb (parts per billion) levels and help achieve high water quality standards.[70] Zero valent iron nanoparticles (nZVI) have been extensively used to study the transformation of heavy metal ions including As (III), Pb (II), Cu (II), Ni (II) and Cr (VI).[71-77] Another relatively new adsorption material used for these purposes is carbon nanotubes (CNTs) which have proven to have great ability to adsorb Pb (II), Cd (II), Cu (II), Ni (II) and Cr (III) from wastewater. The mechanism of adsorption of these contaminants are still under study, but is mostly attributed to electrostatic attraction, sorption-precipitation and interaction between the metal ions and the reactive functional groups on the CNTs.[78-83]

1.4 Organic Contaminants Removal from Wastewater

As detailed previously, one of the major sources of organic contamination in water is from SOCs. Several industries like leather, pharmaceuticals, pesticides, textile, paper and even

wastewater treatment plants are the major source of SOCs. A few examples of SOCs include antibiotics, pesticides, herbicides, polychlorinated biphenyls (PCBs), poly aromatic hydrocarbons (PAHs), organochlorine compounds, and explosives. [2,3,6,9,18,19,84] Some of these contaminants are referred to as persistent organic pollutants (POPs) are resistant to biological degradation. SOCs and POPs are generally present in low concentrations, but are of significant health concern leading to chronic health conditions that are usually detected late. Biodegradation and photodegradation are the two main routes for destroying toxic organic compounds present in water.[85] Many compounds including aromatic and chlorinated hydrocarbons, chlorinated phenols, and other pesticides degrade by direct or indirect photolysis (photodegredation). During photolysis, photosensitizers including nitrates and humic acids present in natural water absorb light and transfer this energy to the contaminants present in the water that get degraded. For biodegradation, metabolic activity of microorganisms, fungi and bacteria that live in natural water eliminates the contaminants present in water. But these techniques sometimes are not effective for organic pollutants (POPs) that are toxic and resistant to these natural biological treatments.[86-90] This section discusses the most common treatment techniques that have been developed to remediate wastewater contaminated with SOCs and POPs including advanced oxidation processes (AOPs), use of nanomaterials, membrane technology, adsorption by activated charcoal, conventional techniques (filtration, coagulation, flocculation, and sedimentation). Treatment of wastewaters contaminated with synthetic dyes will be discussed as a separate section in this Chapter, with special focus on polymeric materials employed for their remediation purposes.

1.4.1. Advanced Oxidation Processes (AOPs)

AOPs involve generation of an extremely reactive and less selective intermediate radicals (OH$^\bullet$), compared to the conventional oxidants, chlorine and molecular ozone.[91-94] The standard oxidation potential of these radicals is typically, $E^0 = 2.8$ V which is much higher than the conventional oxidants,[3] thus making them more effective in oxidation of greater variety of organic compounds. Multiple oxidizing agents including Ozone (O_3), hydrogen peroxide (H_2O_2), combined with metallic or semiconductor catalyst and UV light, generate these reactive radicals.[3,95,96]

Ozonation is an example of AOP that generates OH$^-$ radical by decomposition of ozone (O_3) in water which can be artificially accelerated by increasing the pH[97]. This technique is known to be applied to systems that have fluctuating composition of effluents and flow rate. Ozonation has been applied to wastewater systems containing antibiotics including β-lactams, lincosamides, macrolides, sulphonamides[98-100], pesticides,[101] textile industry effluents,[102,103] Though ozonation has been widely used for such remediation purposes, it suffers from mass transfer limitations in which it requires greater amounts of the oxidant compared to other AOPs which need much lower quantities of oxidant to treat a given load of pollutants.[3]

Fenton's reagent was developed by Henry John Horstman Fenton in the 1890s, which is a solution of strong oxidising agents consisting of hydrogen peroxide (H_2O_2) and ferrous ions.[3,104] Among the two Fenton's oxidation systems namely homogeneous and heterogeneous systems, the former has been more widely used. Fenton's reagent in the homogeneous oxidation system uses H_2O_2 and iron (ferrous or ferric ions) catalyst in an acidic medium that generates the hydroxyl radical.[97] The efficiency of the oxidation process is most commonly increased by conjugation with UV radiation, in which case the process is termed photo-Fenton.[105-107] UV

radiation increases the oxidation efficiency by regenerating ferrous ions resulting in production of more hydroxyl radicals. The main factors that govern the performance of Fenton and photo-Fenton are pH, temperature, catalyst, H_2O_2 and pollutant concentrations.[3] The major advantages of these systems are that the reagents are inexpensive, Fe is readily available in abundance and H_2O_2 is relatively easy to handle. These systems have been used for several applications for degradation of imidazoles, quinolones, tetracyclines and sulphonamides, [96,105,106,108-114] wastewater containing pesticides and herbicides; treating effluents from paper mills, textile industries, petrochemical industries, distilleries and tanneries. [115-127]

Photolysis involves dissociation of organic compounds by using natural or artificial light. These are of two types: direct and indirect photolysis.[3] In the former case, organic compounds absorb UV light and react with the constituents in the water matrix and sometime even undergo self-decomposition. [107,128-130] Whereas indirect photolysis involves photo degradation of sensitizers like oxygen, hydroxyl and/or peroxyl radicals.[109,129] Photolysis of humic acid and other inorganic constituents present in water matrices and external addition of H_2O_2 produce the oxidants necessary for this type of photocatalysis. The main factors that affect the performance of this technique are absorption spectrum of the pollutant, intensity of radiation and frequency, concentration of H_2O_2 and the type of matrix.[131] More importantly only compounds that are photo sensitive are easily degraded, i.e., the technique is very dependent on the chemical structure of the compound. Previous reports mention the use of this technique to study the degradation of metronidazole, tetracyclines, and chlorophenols.[4,107,109,130,132] But this technique has proven to be less effective than other AOPs especially in which UV radiation is combined with H_2O_2, ozone or catalysis.[3]

Semiconductor photocatalysis involves degradation by oxidation in the presence of three components: a catalytic photo-sensitive surface (semiconductor such as titanium dioxide is often used), photon energy source and an oxidizing agent. [111,133-140] Semiconductor photocatalysis is a promising technique to treat wastewaters contaminated with pesticides and antibiotics, effluents from textile industries, leather tanning industries and paper industries. [111,123,133,134-148]

1.4.2. Use of Nanomaterials

As detailed in the previous section, nanomaterials have emerged as one of the most widely used techniques for water remediation purposes. Specifically, single-walled carbon nanotubes (SWCNTs) that have typical diameters ranging from 0.3 nm to 3 nm and multi-walled carbon nanotubes (MWCNTs) with diameters that reach up to 100 nm, are known for their interesting structural, mechanical and chemical properties.[149,150] Moreover, their large surface area and tubular structure make them very good adsorbent materials.[1] There have been several reports where both SWCNTs and MWCNTs have been used for removal of carcinogenic trihalomethanes (THMs) including $CHCl_3$, $CHBrCl_2$, $CHBr_2Cl$ and $CHBr_3$ that were present in water as a result of chlorination of drinking water. [151-154] There have also been reports of treating water contaminated with herbicides.[155-158] Though these materials are known for their high adsorption capabilities for contaminants in both drinking water and environmental water, there applications are often hindered by high cost and poor solubility.[1] In other examples, zero valent iron nanoparticles (nZVI) are known for their higher reactivity when compared to their microscale counterparts because of their greater density and higher reactive surface.[73,74] Several laboratory reports have used nZVI for transformation of wide variety of contaminants including chlorinated organic compounds and polychlorinated biphenyls (PCBs).[159-162] Although nZVI have been proven effective in degrading these organic pollutants, the structure of these particles

may limit the rate of reaction over time. This is attributed to formation of oxide layers on the surface of these particles upon contact or reaction with air.[77,163] In order to address this issue, bimetallic iron particles were physically mixed with either palladium or nickel and were reported to better degrade the chlorinated organics.[163,164] These materials have been used mostly for chlorinated organics which are highly toxic, but there have been reports where bimetallic Fe/Pd have been used for dechlorination of chlorinated aliphatic compounds, chlorinated aromatics and PCBs. [161,162,165-170]

1.4.3. Membrane Processes

Membrane technology has been detailed in previous section for remediation of wastewaters contaminated with heavy metal ions. These methods have been used widely for removal of organic contaminants as well. Specifically, reverse osmosis (RO), nano and ultrafiltration techniques (NF, UF) have been employed for removal of Levamisole, Sulfaguanidine, Sulfadiazine, Sulfamethazine and various others from model wastewaters of a pharmaceutical industry.[4,171-174] More recently, taking into consideration the cost efficiency and the ability to remove pesticides, endocrine disrupters and other industrial pollutants, a 'tight' nanofiltration (NF) membranes modified with polyamide were used as a substitute for RO.[7]

1.4.4. Activated Carbon

Granular activated carbon (GAC) is known for its relatively larger surface area, microporous structure, high adsorption capacities and surface reactivity compared to powdered activated carbon.[9] Among a few examples, activated charcoal has been used for adsorption of trimethoprim, sulphonamides, imidazoles, ampoxicillin;[5,175-177] pentachorophenol, propetamphos[17]8; hexahydro- 1,3,5-trinitro- 1,3,5-triazocine (RDX) and octahydro-1,3,5,7-

tetranitro-1,3,5,7- tetrazocine (HMX)[179]. Activated carbon has also been chemically, physically or thermally modified to better remove fungicides, herbicides, phenols, aniline and nitrobenzene.[180]

1.4.5. Conventional Methods

As discussed before, one of the commonly used techniques in water treatment coagulation and flocculation, involves addition of alum, iron salts, lime and polymers to enhance the precipitation of pollutants, solids sedimentation and colloids formation. [8,10] There are several examples including removal of non-biodegradable contaminants from landfill leachates[9] (highly polluted water from landfills or municipal solid waste disposal); treatment of tannery wastewater [181], removal of pesticides; removal of natural organic matter (NOM) during drinking water treatment processes[84,182] and treating textile wastewaters.[183-188]

1.5. Synthetic Dyes in Wastewater: Occurrences, Health Concerns and Remediation Techniques

Synthetic dyes are extensively used in the textile, paper production, leather tanning, food technology, photoelectrochemical cells, hair coloring industries.[189-194] Large scale production and applications of synthetic dyes leading to considerable environmental pollution have become a serious health risk concern.[189] According to a recent estimate in 2008, it was reported that the amount of dye stuff produced worldwide was about 7×10^5 tons.[195,196] Synthetic dyes are widely classified based on their structure as azo, anthraquinone, indigoid, oxazine, triphenylmethyl, and phthalocyanine. Of these, azo, anthraquinone and oxazine fall under the class of reactive dyes, which react with the fibres of the material to be dyed.[197] Azo dyes form a large portion (~ 60%) of these reactive dyes and are heavily relied on in the textile industries. Specifically, synthetic

azo dyes transform into colorless aromatic amines, some of which are carcinogenic by nicotinamide adenine dinucleotide phosphate NAD (P) H-dependent reduction, catalyzed by azoreductases. [198]

Most synthetic dyes are highly stable when exposed to sunlight and also resistant to microbial attack and high temperature, making it a challenge to degrade most of these dyes by traditional wastewater treatment methods.[186] But there is continuous research involved in addressing this issue. The most common techniques that are used to degrade or decolourize the dyes in wastewater effluents include physico-chemical methods, biological treatments and electrochemical methods that already been discussed in detail in the previous sections.

1.5.1. Remediation Methods

Briefly, activated carbon is one of the most extensively used adsorbents for treating a wide variety of cationic dyes, reactive dyes and acid dyes for treatment of waste water. [199-207] In addition many lost cost adsorbents including carbon materials from solid wastes and coal based sorbents, industrial by products, chitosan, zeolites and biosorbents.[196,208,209] Coagulation/flocculation is another widely used technique for removal of several synthetic dyes from wastewater.[187,188,210,211] But a main disadvantage of this technique is that it leads to secondary pollution. Advanced oxidation process is another example which has been used as a widespread tool mostly by using Fenton's reagent and photocatalysis for degradation of a wide variety of dyes, but there have been concerns regarding the cost and operational methods. [186,212] Application of microorganisms for biodegradation of synthetic dyes has also been reported before, but these are often inefficient because most of these dyes are resistant to their attack.[213,214] Electrochemical methods have gained a lot of significance for over the past decade

for treatment of dyestuff wastewaters, which include electrocoagulation, electrochemical reduction, electrochemical oxidation and photo assisted electrochemical methods.[213,215-217]

1.5.2. Polymeric Materials for Remediation

Relevant to the work in this thesis are polymeric materials based adsorbents and sorbents on hydrogels and microgels (colloidal hydrogel particles), which have been used in recent years for water remediation. As detailed in the previous section, adsorption on activated carbon is one of the most commonly used techniques for removal of dyes from water. However activated carbon has been recognized to still suffer from costly regeneration processes. Though there have been many low cost adsorbents substituents, they still suffer from low adsorption capacities. In the past decades, polymer based adsorbents have been explored as another alternative for removal of organic contaminants from water. [218-232] The main advantages of these materials being adjustable surface chemistry and regeneration under mild conditions, in addition to having large surface area and mechanical strength. A variety of cationic and anionic dyes have been removed using many hydrogel systems based on poly (acrylic acid), poly (*N*-Isopropylacrylamide), poly (N,N- dimethylacrylamide), poly (vinylpyrrolidone), poly (vinyl alcohol). Of these dyes, an azo dye 4-(2-Hyrodxy-1-napthylazo) benzenesulfonic acid sodium salt (Orange II) is of specific relevance to this work, and in recent reports pNIPAm based hydrogels have been employed to determine the partition coefficient of these dyes in the system. Orange II has been considered as a contaminant from various industrial effluents and treated using many physical and chemical methods.[233-235]

The aim of this Chapter was to give an overview of the most common remediation techniques used for the removal of inorganic and organic contaminants from wastewater. Removal of synthetic dyes using the common methods with specific focus on polymeric

materials was highlighted in a separate section. The following Chapter will give an introduction to a special class of materials called microstructured hydrogels or microgels with specific focus on poly (N-isopropylacrylamide) microgels (pNIPAm), their syntheses, properties and characterization techniques.

CHAPTER 2

MICROSTRUCTURED HYDROGELS

This Chapter will serve as a brief overview of hydrogel materials with special focus on microstructured hydrogel particles, known as microgels. The synthesis and properties of microgels based on *N*-Isopropylacrylamide (NIPAm) will be discussed in detail.

2.1. Hydrogels Overview

Hydrogels are materials that are composed of a crosslinked hydrophilic organic polymer network held together by covalent or noncovalent bonds, and are able to swell in aqueous media absorbing water about a thousand times their dry weight.[236-242] The crosslinks maintain the stability of the hydrogel network, and the solvent content within the hydrogels provide them fluid-like properties.[236] Hydrogels can be: crosslinked chemically or physically; responsive or non-responsive to stimuli; and either of macroscopic or microscopic dimensions.

2.1.1. Physically and Chemically Crosslinked Hydrogels

Physically crosslinked hydrogels arise from non-covalent attractive forces that typically include hydrophobic and electrostatic forces, present between polymer chains. Hydrogels of this class are capable of degrading, i.e., they can undergo a transition from a three dimensional structure to a polymer solution under certain conditions. These are commonly called degradable or reversible hydrogels..[236,243] Their most common application is the encapsulation of small molecule species, and their release, triggered when the gel dissolves.[244-246]

Chemically crosslinked hydrogels on the other hand are formed by covalent bonds between the polymers in the network, and are therefore more stable than physically crosslinked hydrogels. They have a "permanent" structure except when labile chemical bonds are added to

the network. These hydrogels are formed by polymerizing monomers in the presence of a crosslinker, which contains polymerizable groups.[236,237] Several methods have been reported for synthesis of chemically crosslinked hydrogels that employ radical polymerization, chemical reactivity between complementary functional groups, high energy irradiation using gamma radiation or electron beam and enzymes.[236,247] These hydrogels serve as useful tools for applications in drug delivery systems, matrices for tissue engineering, biosensing and bio adhesives.[239,248-252]

2.1.2. *Macrogels and Microgels*

Based on the dimensions of a hydrogel, it can be classified as either a macrogel or microgel. Macrogels are "bulk" hydrogels that have at least one dimension greater than one millimeter.[253-255] Microgels are colloidally stable hydrogels with dimensions typically of the tens of nanometer to micrometers range.[256-259] Microgel with submicron dimensions are known as nanogels. Microgels can be synthesized from a variety of monomers, but this Chapter will focus on microgels based on pNIPAm and is discussed in detail later in this Chapter.

2.1.3. *Stimuli Responsive Hydrogels*

Hydrogels that undergo physical and chemical changes in response to the application of external stimuli are known as stimuli responsive hydrogels.[260,261] These external stimuli can be either physical or chemical stimuli. Physical stimuli include temperature, electric or magnetic field, while chemical stimuli include pH, ionic strength and biomolecules.[250,258,262-276] In general, depending on the applied stimulus, the hydrogel containing the stimuli responsive component undergoes some changes such as swelling/deswelling. A stimuli responsive polymer hydrogel may undergo a phase transition from a random coil to globule conformation as a result of change in the solution properties brought about by the above mentioned factors.[236,264,277] This change in

conformation is depicted in Figure 2-1. Hydrogels of this kind are also known as 'smart' materials and have a huge potential in many diverse applications. Examples include pH and temperature sensitive hydrogels used for site specific drug delivery,[250,264-283] biomolecule specific hydrogels upon addition of glucose or antigens used for biosensing.[250,252,264,284-286] Upon combining a pH responsive hydrogel with glucose oxidase, the release of insulin is regulated by the swelling of hydrogels in response to the concentration of glucose.[252] In other examples, hydrogels responsive to light have been used for development of artificial muscles, and in drug delivery,[250,276,287] and tissue engineering.[241,288] Non responsive hydrogels on the other hand, are materials that just swell in water, because they absorb water.

Temperature, pH
Ionic strength, [Analyte]
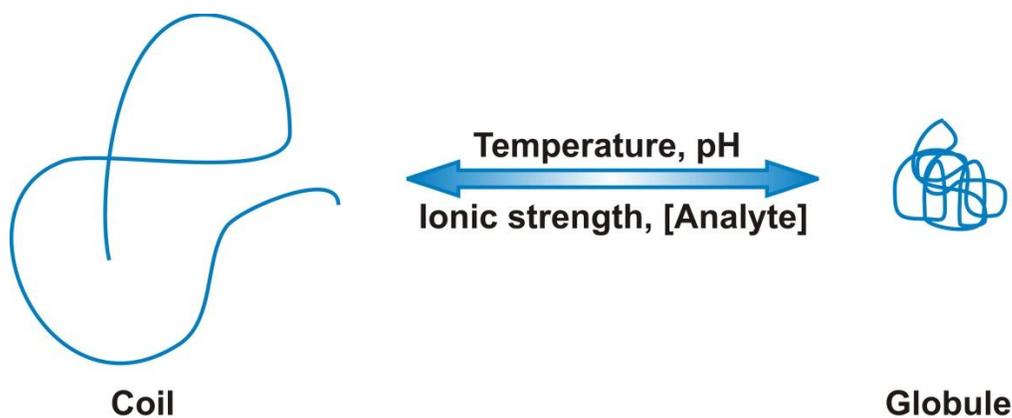
Coil

Globule

Figure 2-1. Coil to globule phase transformation of polymer in the hydrogel

2.2. Poly (N-isopropylacrylamide) Based Hydrogels

Poly (N-substituted acrylamide) based hydrogels are a representative of a group of responsive polymers that are thermoresponsive and have a very unusual behaviour in solution. Specifically, poly (N-isopropylacrylamide) (pNIPAm) is arguably the most thoroughly studied

stimuli responsive polymer.[289-300] The solution characteristics, synthesis and characterization will be discussed in detail in this section.

2.2.1. Solution Characteristics of pNIPAm

PNIPAm is fully water soluble and is known for its thermoresponsive nature, in which it undergoes a conformational change from a random coil in aqueous solution at T < ~32 ˚C to a compact globule at T > ~32 ˚C by expelling much of its water of solvation.[290,291,297,298] The earliest studies on the properties of pNIPAm in solution revealed that this phase transition is driven by entropy and is endothermic.[301] In general, for any polymer in a solvent, the behaviour is related to the balance between the solvent-solvent, solvent-polymer and polymer-polymer interactions. If the polymer is stimuli responsive, the solvation changes due to strengthening of one these interactions while weakening one of the others. In the case of pNIPAm in water, the water bonds to the amide side chains in the polymer at room temperature.[236,300] The isopropyl side chain imparts hydrophobic structuring on the water. This structured water leads to an entropically driven polymer-polymer interactions by the hydrophobic effect.[236] The hydrogen bonding between the polymer and water gets disrupted upon heating causing the water to act as a poor solvent leading to a chain collapse. Above LCST, the intra and inter polymer hydrogen bonding and polymer-polymer hydrophobic interactions are dominant that leads to a globular conformation.[300,302]

2.2.2. Swelling Behaviour of PNIPAm Hydrogels (Macrogels)

PNIPAm macrogels typically have one dimension and are of a millimeter or more in size and exhibit a volume phase transition temperature (VPTT) of T ~32 ˚C. At this temperature, also known as the lower critical solution temperature (LCST) the macrogels transform from a water swollen (hydrophilic) state to a deswollen (hydrophobic) state.[236] The main factors that affect the

VPTT of the gels are cross-link density, balance between the hydrophobic-hydrophilic states, ionic strength and the composition of solvent . Extensive studies on the deswelling kinetics of pNIPAm were performed by Tanaka and coworkers reveal that the ionic thermoresponsive gels display a discontinuous or discrete transition in contrast to nonionic gels. In a discrete transition, an infinitesimal change in the solvent composition or temperature brings about a finite change in the gel volume. Also, it was observed that the deswelling rate is inversely proportional to the square of the smallest dimension of the gel.[255,303-306] In order to achieve higher swelling rates, studies have shown that by synthesizing pNIPAm gels at a temperature above their LCST, which results in larger pore size.[307,308]

2.2.3. PNIPAm Microgels

As discussed before, microgels are colloidally stable counterparts of bulk macrogels and their size typically ranges between tens of nanometer and micrometer. Microgels based on pNIPAm also exhibit a volume phase transition (VPT) similar to pNIPAm based macrogels where they transform from a swollen to a deswollen state above their LCST (T ~32 ˚C) and this change is ideally reversible. [236,299,300] Microgels have an advantage over macrogels in terms of faster deswelling kinetics because of their smaller size.[309] An interesting study done by Wu et al revealed a very specific difference pNIPAm macrogel and microgel in terms of the phase behavior. It was observed that the VPTT of the pNIPAm microgels was slightly greater than the LCST of linear pNIPAm and the region of the transition was broader than the bulk gels.[310] They attributed this continuous transition to the higher heterogeneity present in the subchain lengths of the microgels. When T > VPTT, the regions with longer subchains (which depend on the number of cross links) collapsed at a lower temperature compared to the region with smaller subchains. In other words, different regions of the polymer microgel undergo phase transition at

different temperatures. Other characteristics of pNIPAm microgels include colloidal dispersions like zeta potential.[300,311-314]

There has been tremendous interest in modifying pNIPAm microgels to broaden their responsivity to various other stimuli, the most common being addition of carboxylic acid groups like acrylic acid or methacrylic acid. [258,293,299,300,315-318] Specifically copolymerization of acrylic acid, with a pKa of ~ 4.25 into the pNIPAm microgel network hinders the VPT or thermoresponsivity at pH > pKa (4.25) of the AAc groups causing the microgels to swell due to Coulombic repulsion.[267,293,319,320]

2.2.4. Synthesis of PNIPAm Microgels

Microgels can be synthesized via a variety of routes such as: precipitation polymerization, anionic copolymerization, crosslinking of neighbouring polymer chains, microemulsion and miniemulsion polymerization.[299, 300, 310, 321-327] Colloidal particles syntheses of pNIPAm have been reported widely. [258,290,291,293,298-300,315,328-330] This dissertation focuses on synthesis of pNIPAm based microgels through free radical precipitation polymerization and this will be discussed in detail.

Free radical precipitation polymerization of pNIPAm microgels consists of NIPAm as the major monomer and a cross-linker *N,N'*- methylene bisacrylamide (BIS) dissolved in water. This solution is transferred to a three-necked round bottom flask. Dissolved oxygen prevents the polymerization from occurring and so the solution in the RBF is purged with nitrogen throughout. The solution is then heated to ~ 70 ˚C upon stirring and under the nitrogen blanket. Once this temperature is reached, comonomers can be added to the reaction mixture. Acrylic acid (AAc) comonomer was used throughout this dissertation. The initiator ammonium persulphate (APS) is then added to this mixture and the reaction is allowed to proceed for ~ 4h. Finally the

solution is cooled and filtered. For synthesis of microgels of smaller size, some concentration of the surfactant, sodium dodecyl sulphate (SDS) is added along with the monomer and the crosslinker. The concentration of the surfactant is kept below the critical micelle concentration (CMC). Figure 2-2 shows the scheme for the synthetic scheme of pNIPAm microgels.

NIPAm   BIS   AAc pKa ~ 4.25
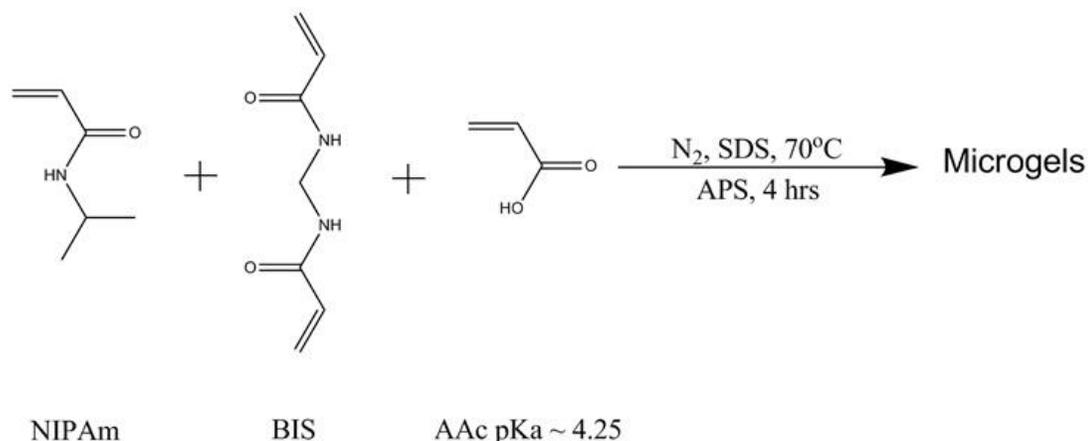
Figure 2-2. Synthesis scheme for pNIPAm microgels. All the monomers are dissolved in water. Specifically, for the synthesis of a) 'small' size microgels (~ 250 nm), conditions include addition of SDS prior to initiation at solution temperature of ~ 70 ˚C, b) 'medium' size microgels (~ 1 μm), conditions include initiation after the solution temperature reaches ~ 70 ˚C and c) 'large' size microgels (~ 1.5 μm) conditions include addition of AAc prior to initiation at a solution temperature of 45 ˚C and the temperature is again ramped up to reach ~ 70 ˚C.

The mechanism of the formation of microgels involves homogenous nucleation.[299] Addition of APS at high temperature results in the generation of sulphate radicals which initiate the polymerization. Also, after initiation the NIPAm monomer starts to polymerize and the chain grows till it reaches a critical chain length, after which it collapses on itself giving precursor particles. This chain collapse happens because the polymerization temperature is higher than the LCST of the polymer resulting in phase separation. The precursor particles act as nuclei to promote the growth of microgel leading to a colloidally stable structure whose diameter is determined by the amount of SDS present in the reaction mixture. Figure 2-3 represents a schematic of steps that take place in a precipitation polymerization. To synthesize small

microgels, the precursor particles have to be stabilized by high concentration of SDS while low concentration of SDS is needed for large microgels.

Growing Chain   **Collapsed Chain**   **Precursor Particle**   **Microgel Particle**
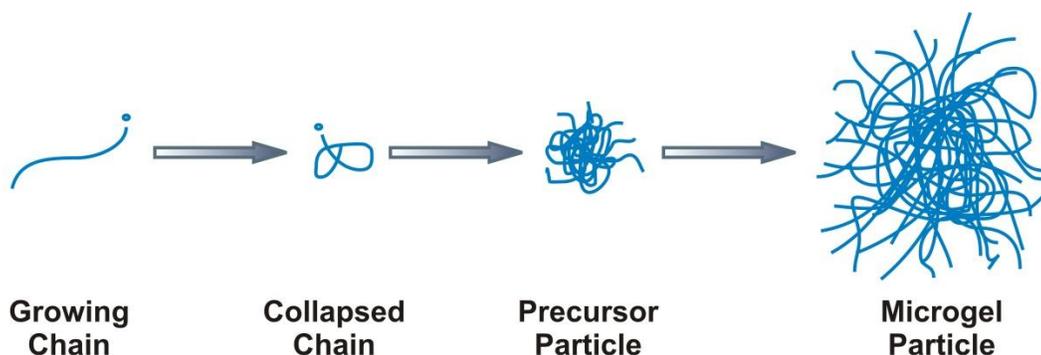
Figure 2-3. Free radical precipitation polymerization schematic. After initiation, the polymer chain slowly grows and collapses upon reaching a critical length. This collapsed chain then serves as a precursor particle for the formation of a stable microgel.

2.3. Applications of Microgels

Responsive microgel materials also known as smart materials, as mentioned above, have found have been used for a variety of applications including biosensing,[331,332] optical materials,[294,296,329,333] catalysis,[335,336] tissue engineering.[302,337]

Of interest to this dissertation is the application of polymer microgels for encapsulation of organic molecules. Incorporation of DNA, RNA, small organic molecules, proteins and drug molecules within the microgel network have been reported widely.[236] A schematic for encapsulation of molecules by the microgels is shown in scheme 2-4. For biomolecules with low molecular weights like anti-cancer drugs (and release them subsequently), and polypeptides, encapsulation was performed by directly mixing these molecules with microgels,[338-341] and in some cases hydrophilic-hydrophobic interactions were used to encapsulate a drug called doxorubicin into biodegradable poly (ethylene glycol) monomethyl ether methacrylate

(POEOMA) nanogels with disulfide crosslinking in water for drug delivery applications.[342] Higher molecular weight biomolecules including proteins, carbohydrates and genes have been incorporated into microgels using inverse microemulsion polymerization, to confine water-soluble biomolecules in water-soluble droplets.[343] For instance plasmid DNA was encapsulated by PAAm based microgels synthesized by inverse emulsion polymerization and subsequently released upon degradation in response to pH change. Same method was used to incorporate for various other molecules including ovalbumin, BSA, lysozyme, various carbohydrate model drugs incorporated into micro/nanogels.[344-346]
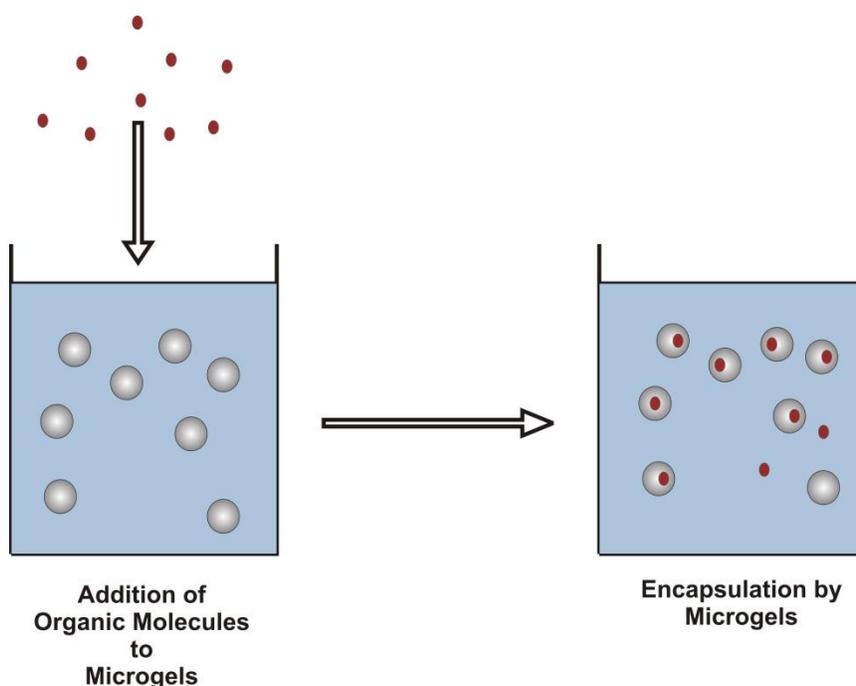
Figure 2-4. Encapsulation of small organic molecules (•) by microgels.

In the following Chapters (3-5), the ability of pNIPAm based microgels and their assemblies (aggregates) for the encapsulation (removal) of an azo dye molecule Orange II from water at both room temperature and elevated temperature (~ 50 ˚C) has been discussed in detail. Chapter 3 also discusses the efficiency of pNIPAm based microgels for the removal of 5-tert-

butoxycarbonyl 5-methyl-1-pyrroline N-oxide (BMPO). The removal efficiency of the dye is greatly affected by the solution temperature, structure and hydrophobicity of these systems. The overall efficiency to retain the dye within these systems has also been discussed. In Chapter 6, the reusability of the microgels and microgel aggregates has been monitored.

CHAPTER 3

POLY (N-ISOPROPYLACRYAMIDE) BASED MICROGELS FOR SMALL ORGANIC MOLECULES REMOVAL FROM WATER

3.1. Research Outline [1]

As detailed in Chapter 1, treatment of wastewater containing a variety of pollutants is an ongoing challenge to provide clean and potable water. This dissertation focuses on investigating poly (N-isopropylacrylamide)-*co*-acrylic acid (pNIPAm-*co*-AAc) microgels for the removal of an organic, azo dye molecule, 4-(2-Hydroxy-1-naphthylazo) benzenesulfonic acid sodium salt (Orange II, an azo dye) from aqueous solutions. It was observed that these microgels removed 29.5% of the dye at room temperature within a very short period of time, while at elevated temperature, 56.6% of the dye was removed. We attribute the enhanced uptake at elevated temperature of ~ 50 ˚C to the thermoresponsive nature of the microgels, which expel water of solvation and deswell at high temperature and reswell when they are cooled back to room temperature. In attempts to further improve the removal efficiency of the pNIPAm based microgels, assemblies (or aggregates) of the microgels were synthesized. We observed a maximum removal efficiency of 73.1% at an elevated temperature as detailed in Chapter 4. The effect of changing the size of the microgels within the aggregates was also investigated and it was concluded that for aggregates with larger microgel diameters the removal efficiency increased to a maximum of 85.3% at an elevated temperature. The details of this study are discussed in Chapter 5. Finally, the reusability of the microgels, and their aggregates, for water remediation was investigated, as outline in Chapter 6. Chapter 3 also discusses the results from

---

[1] This dissertation has been adapted from references 361, 362 and 363.

the uptake experiments of an organic molecule, 5-tert-butoxycarbonyl 5-methyl-1-pyrroline N-oxide (BMPO) from aqueous solutions.

3.2. Chapter Introduction

As mentioned in Chapter 1, azo dyes are a class of synthetic dyes that constitute a large portion of reactive dyes. These compounds are mainly used as colorants in textile, cosmetic, food and drug industries. Many physico-chemical methods have been reported to remove azo dyes from water including electrochemical, biological, photo catalytic methods and adsorption.[189,212,217,347-350] Most of these techniques are often expensive, not easy to implement and not very efficient.[186,351-354] In recent years, many hydrogel based systems have been used to remove azo dyes, cationic and anionic dyes from water.[218-221,224] Specifically, hydrogels of pNIPAm modified with polyacrylamide have been employed to determine the partition coefficient of Orange II and methylene blue in the system at different temperatures. It was reported that the permeability of Orange II through the hydrogels increased when temperature was raised above 32˚C.[355,356]

This Chapter focuses on studies performed to assess the ability of pNIPAm-co-AAc microgels for the removing the organic, azo dye molecule, Orange II (Figure 3-1) from water. These studies were performed at both room and elevated temperature. At room temperature, the percent uptake of the dye increased with increasing concentration of the microgels and acrylic acid. The removal efficiency of the microgels was greatly affected by the increase in the solution temperature, which is a result of the thermoresponsive nature of pNIPAm-based microgels which deswell at elevated temperature expelling their solvating water and when the microgels are cooled back down they reswell with the Orange II containing water. Sorption studies of the dye

on the microgels were fit by a Langmuir sorption isotherm model. Studies based on removal of BMPO (Figure 3-1).at room temperature are also discussed in this Chapter. BMPO is used for electro paramagnetic resonance spectroscopy studies as a nitrone spin trap used for detection of short lived radicals like superoxide and hydroxyl in vivo and in vitro.[357-360] Finally the overall efficiency of the microgels to retain the dye and BMPO was assessed by leaking studies.
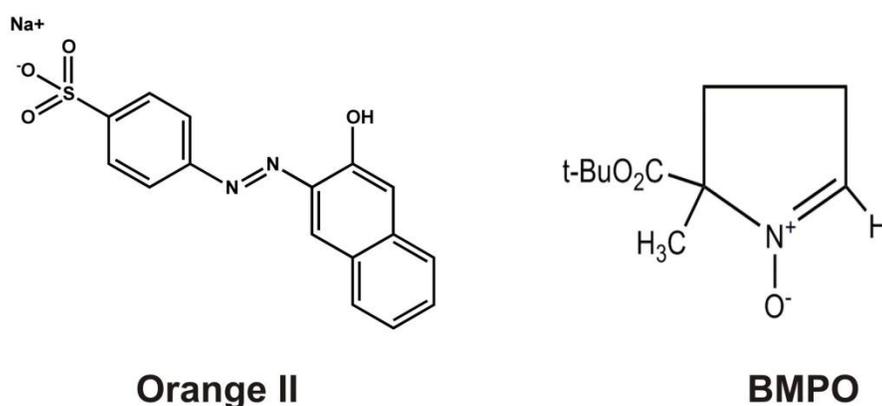
Figure 3-1. Chemical structures of Orange II and BMPO.

3.3. Materials and Methods

Materials. The monomer, *N*-isopropylacrylamide was purchased from TCI (Portland, Oregon) and purified by recrystallization from hexanes (ACS reagent grade, EMD, Gibbstown, NJ). *N,N'*-methylenebisacrylamide (BIS) (~99%), acrylic acid (AAc) (~99%), and ammonium persulphate (APS) (~98%) were obtained from Sigma-Aldrich (Oakville, Ontario) and were used as received. Orange II was obtained from Eastman Organic Chemicals (Rochester, New York) and BMPO was kindly provided by Dr. Jie Sun of Academic Instruments, Bradenton, FL. All the phosphate salts used for preparing buffer solutions of pH 7, with an ionic strength of 0.235 M, were obtained from EMD and were used as received. Deionized (DI) water with a resistivity of

18.2 MΩ·cm was obtained from a Milli-Q Plus system from Millipore (Billerica, MA), and filtered through a 0.2μm filter, prior to use. Microgel samples were lyophilized using a VirTis benchtop K-manifold freeze dryer (Stone Ridge, New York).

Synthesis of microgels. Microgels composed of poly (N-isopropylacrylamide) were prepared by a surfactant free, free radical precipitation polymerization as described previously.[293] The total monomer concentration was 140 mM, and was 95% N-isopropylacrylamide (NIPAm) and 5% N, N'-methylenebisacrylamide (BIS) crosslinker. The monomer, NIPAm (13.3 mmol), and the crosslinker, BIS (0.700 mmol), were dissolved in deionized water (75 mL) with stirring in a small beaker. The mixture was filtered through a 0.2 μm filter affixed to a 20 mL syringe into a 250 mL, 3-neck round bottom flask. An additional aliquot of deionized water (24 mL) was used to wash the beaker, which was filtered and transferred to the round bottom flask. The flask was then fitted with a thermometer, a condenser, stir bar, and a N_2 inlet. The temperature was set to 65°C and N_2 was bubbled through the solution for ~ 1 h, after which 0.197 mmoles of 1 mL aqueous solution of APS initiator solution was added to the reaction mixture and was left to stir in the flask for 4 h, under N_2 atmosphere. The solution was allowed to cool, while stirring overnight.

Microgels composed of pNIPAM-*co*-AAc were prepared in a similar way by adding 0.700 mmol, 1.40 mmol and 2.10 mmol of AAc to the reaction mixture to synthesize 5%, AAc, 10%, and 15% pNIPAm-*co*-AAc microgels, respectively. The AAc was always added just prior to initiation, and the concentration of NIPAm was adjusted accordingly to maintain the monomer/crosslinker concentration constant at 140 mM for all microgel syntheses. The AAc% in the microgels will be represented as pNIPAM-*co*-XAAc, where X = 0, 5, 10, and 15 % AAc. The hydrodynamic diameter (D_H) of these microgels was determined by dynamic light scattering

studies using a ALV/CGS-3 Compact Goniometer System (Hesse, Germany). In brief, a dilute solution of microgels in DI water, maintained at ~23 °C, was irradiated by a 22 mW HeNe laser, and scattered light collected. . Data was analyzed using ALV-5000/EPP correlator software, from which the hydrodynamic diameter was determined. For microgels of varying concentration of AAc, three sets of samples each were analyzed using this protocol and the average sizes were determined to be 795.4 nm, 945.2 nm, 1.103 μm and 1.384 μm for pNIPAm-*co*-XAAc where X=0, 5, 10 and 15% respectively.

Table 3-1. DLS data for the different sizes of pNIPAm-co-XAAc (X=0, 5, 10 and 15%)

%AAc	Diameter of the Microgels	Standard Deviation
0	0.795 μm	±0.008 μm
5	0.94 μm	±0.01 μm
10	1.10 μm	±0.02 μm
15	1.38 μm	±0.01 μm

Following stirring overnight, the microgels were filtered through a type 1 Whatman filter paper, under vacuum and then rinsed with deionized water. To remove unreacted monomer and crosslinker, as well as linear polymer from the microgels, the microgel reaction solution was separated into 15 mL centrifuge tubes obtained from Corning Incorporated (Corning, NY) (~ 12 mL microgel solution/tube) and centrifuged at a speed of ~8400 relative centrifugal force (rcf) in a Baxter, biofuge 17R (Mount Holly, NJ) at 23 °C, for 30 min. Centrifugation yielded a pellet of microgels at the bottom of the centrifuge tube, and the supernatant was removed. ~12 mL of

fresh DI water was added and the microgel pellet was redispersed using a Fisher Vortex, Genie 2 vortexer (Pittsburgh, PA). This cleaning protocol was repeated six times.

Uptake studies. Microgels were lyophilized, and 52.1 mg of each was redispersed in 10 mL of pH 7 buffer solution of 0.235 M ionic strength in a volumetric flask. The concentration of the stock microgel solution was 5.21 mg microgels/mL. A stock solution of 0.023 M Orange II in deionized water was prepared. Using a micropipette 300 μL of microgels and 15 μL of Orange II were transferred separately into different 15 mL centrifuge tubes obtained from Corning Incorporated (Corning, NY). A buffer solution of pH 7 of ionic strength 0.235 M was added to the tubes to give a total volume of 3 mL (final concentrations of microgels and Orange II are 521 μg microgels/mL and 114 μM, respectively). For studies based on removal efficiency as a function of microgel concentration, a series of tests were conducted, in which 50, 100, 200, 300 and 400 μL of pNIPAm-*co*-10 AAc were exposed to 15 μL of the dye in a volume of 3 mL. For all the experiments the buffer was added only after the dye was exposed to the microgels. This solution was allowed to sit for five minutes and then centrifuged for 30 minutes, at ~8400 rcf to pack the microgels at the bottom of the centrifuge tube. This centrifugation time was used to ensure that all the dispersed microgels were removed from solution (as confirmed from differential interference contrast microscopy, data not shown). The supernatant was carefully removed from the tube without disturbing the microgel pellet at the bottom of the centrifuge tube and transferred to a quartz cuvette and the absorbance measured using a HP8452A UV-Vis spectrophotometer with a diode array detector (previously Agilent Technologies, Inc., Santa Clara, CA). The initial concentration of Orange II for all the uptake studies was maintained at 114 μM and it was also observed that the pH of Orange II solution does not change when microgels are added to it. The initial absorbance of Orange II without microgels was also

measured as a function of time the solution stayed in the tube. It was confirmed that the tube did

not have any effect on increasing/decreasing the absorbance of Orange II, independent of time.

To study the uptake of Orange II as a function of temperature, the solution of Orange II and

microgels was held at 50 ˚C, for different intervals of time (microgels deswell) and then cooled

down to room temperature (microgels reswell). This solution was then centrifuged and the

supernatant was used to perform UV-Vis studies. A schematic representing uptake studies is

depicted in Figure 3-2.

For studies on BMPO, the stock solution of BMPO was 0.2 M, out of which a volume of

15 μL was exposed to 100, 200, 300 and 400 μL of pNIPAm-*co*-10 AAc (173, 346, 521 and 693

μg microgels/mL) made up to 3 mL using the same pH 7 buffer solution. The initial

concentration of BMPO for all the studies was maintained to be 1000 μM. The uptake studies

were performed using the same protocol as above, for room temperature alone.
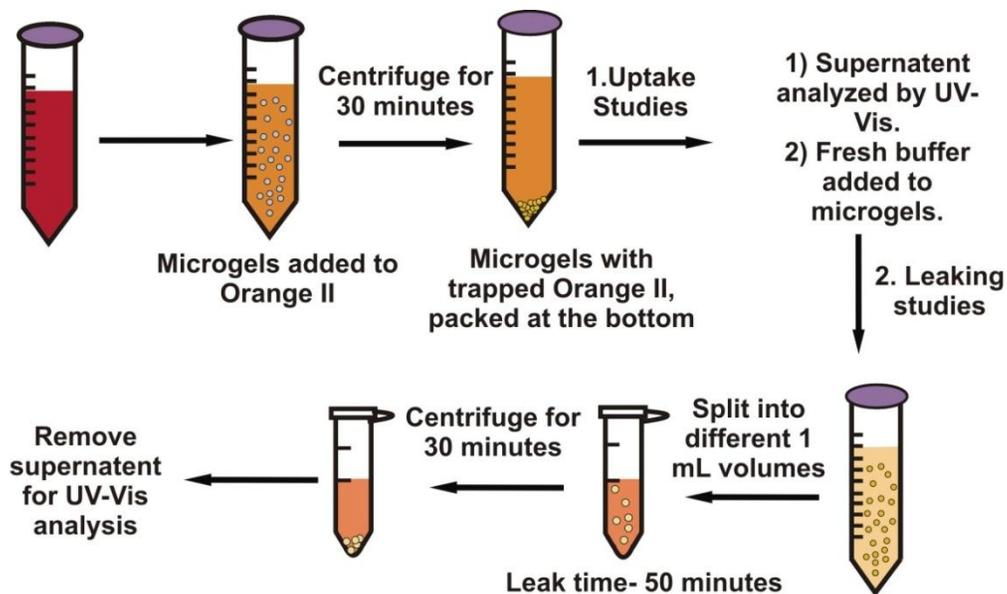
Figure 3-2. Schematic for the uptake and leaking studies of Orange II by the microgels.

Leaking studies. To evaluate the ability of the microgels to retain Orange II, the concentrations, and volumes from the previous section were scaled up three times. So in this case, 900 µL of microgels were exposed to 114 µM Orange II in a total volume of 9 mL using the same buffer that was used for the uptake studies. This scaling up was done to get a detectable absorbance signal from the solutions after leaking. As for the Orange II removal studies above, the solution was allowed to sit for five minutes followed by centrifugation for 30 minutes. The supernatant solution was then carefully removed without disturbing the microgels packed at the bottom. To this tube, 9.0 mL of fresh buffer solution (the same buffer that was used for the uptake studies) was added and then the microgels were redispersed by vortexing. This was immediately divided into nine, one mL samples in 1.5 mL Eppendorf tubes obtained from Fisher Scientific, (Ottawa, ON) and the solutions were allowed to incubate for various intervals of times. For example, immediately following splitting up the original solution, one tube was centrifuged for 30 min and the supernatant solution removed and UV-Vis performed on the supernatant solution, this was considered t = 0. We allowed the other tubes to incubate for 10, 20, 30, 40, 50, 60, 80 and 100 minutes respectively, before each was centrifuged. Figure 3-2 depicts a schematic of leaking studies of Orange II.

Leaking studies for BMPO were also conducted using the similar protocol as above, with the only differences being the durations of leaking (incubation time) were maintained at 30, 60, 90, 120 and 180 minutes and the initial volumes of BMPO and microgels were 30 µL and 600 µL respectively. The initial concentration of BMPO was maintained at 1000 µM.

Light scattering studies. This experiment was performed using a PTI fluorescence system (Birmingham, NJ, Model MP1, ser# 1621,) and analyzed using the FeliX32 Analysis Module (v1.2). Scattering intensity as a function of temperature was monitored. For this, 10 µL

pNIPAm-co-10AAc was added to a 3 mL pH 7 buffer, of ionic strength 0.235M. This solution was irradiated at a wavelength of 600 nm with slits open to 0.62 mm and the temperature was ramped up from 23 ˚C to 50 ˚C in 3 ˚C increments. The scattering intensity was measured for 300 s at every temperature. A stabilization period of 300 s was given between every temperature. The scattering intensity data was averaged at for every 300 s measurement and the standard deviation was obtained from the average value. The data shows the thermoresponsive behavior of the microgels where the scattering intensity increases as the temperature is increased.

3.4. Results and Discussion

Uptake studies at room temperature. The ability of microgels to remove organic azo dyes from aqueous solutions was investigated by exposing them to Orange II. Initially, we investigated the effect of adding the weak acid AAc to the microgel structure. The experiment was performed by recording an initial absorbance spectrum of 114 μM Orange II before the addition of 300 μL of microgels (521 μg/mL), and comparing that to the absorbance of the supernatant after the addition of microgels. If Orange II was removed from the solution a decrease in absorbance will be observed. The number of moles in the solution before and after microgel addition was determined using a calibration curve shown in Figure 3-3. The percent of Orange II removed from the solution was subsequently calculated. Figure 3-4 (a) shows the percent uptake as a function AAc concentration in the microgels. The percent uptake was found to depend critically on the AAc concentration, increasing from 6.63% for the pNIPAM-co-0AAc to 31.2% for pNIPAM-*co*-15AAc microgels. This trend could be due to the increase in the size of the microgels as the %AAc increases, as determined by DLS, where the size of the microgel increased from 795.4 nm for pNIPAm-co-0AAc to 1.384 μm for pNIPAm-co-15AAc. The

uptake percent using pNIPAm-co-10AAc was 29.5% (only about 2% less than the 15% AAc system) and these microgels were used for subsequent experiments.
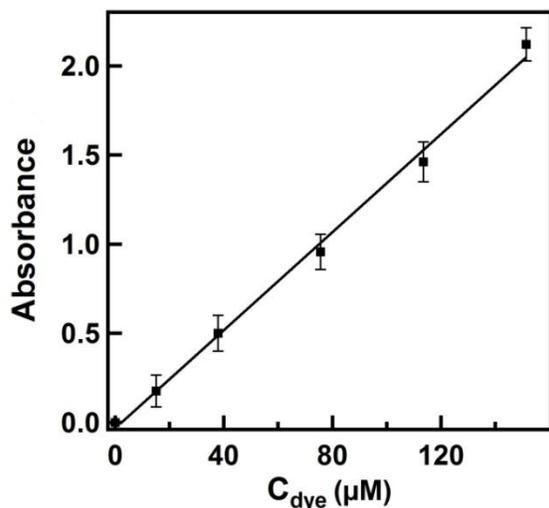
Figure 3-3. Calibration curve for Orange II. Each point on the plot represents an average of three replicate experiments and the error bars denote the standard deviation. The R^2 value was analyzed to be 0.9951. The equation of the line to calculate the concentrations of Orange II was y= 0.0138*x - 0.0327.
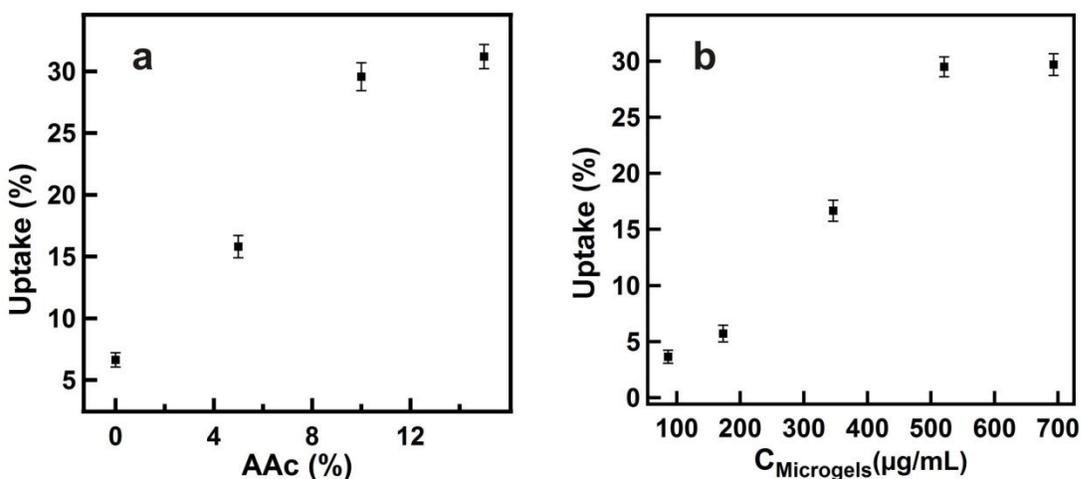
Figure 3-4. Uptake of Orange II as a function of (a) percentage of AAc (0%, 5%, 10% and 15%) present in the pNIPAm microgel system and (b) concentration of pNIPAm-*co*-10AAc. All the solutions were in a total volume of 3 mL and pH 7 buffer. Each point on the plots represents an average of three replicate experiments of uptake studies and the error bars denote the standard deviation.

The effect of microgel concentration on the removal efficiency was also investigated, and the results are depicted in Figure 3-4 (b). The removal efficiency steadily increased from 3.60% to 29.5% as the amount of pNIPAM-*co*-10AAc microgels was increased (86.6, 173, 346 and 521 μg microgels/mL), but did not increase for 693 μg microgels/mL). We hypothesize that this behavior is observed because the removal of dye is an equilibrium process and addition of more microgels to the solution, past a certain concentration, will not result in extra moles of the dye being removed.

The uptake studies with BMPO were conducted at room temperature, following the protocol outlined in the experimental. Briefly, from a stock solution of 0.2 M solution of BMPO a volume of 15 μL was pipetted out and added to 100, 200, 300 and 400 μL of pNIPAm-*co*-10 AAc made up to 3 mL using the same pH 7 buffer solution. The initial concentration of BMPO was maintained at 1000 μM. The experiment was performed by recording an initial absorbance spectrum of 1000 μM BMPO in the absence of microgels and comparing that to the absorbance of the supernatant after the addition of microgels. A decrease in absorbance of the supernatant will be observed if the microgels took up any BMPO. The number of moles in the solution before and after microgel addition was determined using a calibration curve as shown in Figure 3-5. From this, the percent uptake of BMPO by the microgels was calculated. Figure 3-6 shows the trend of removal efficiency of the microgels as a function of their concentrations. It was observed that as the concentration of microgels increased from 173 to 521 μg microgels/mL, the percent uptake increased from 10.4% to 33.5%. Upon increasing the concentration of microgels to 693 μg microgels/mL, the removal efficiency increased only up to 35.1%, which is not a very significant increase. This behavior again can be attributed to equilibrium present within the system which does not allow the microgels to remove any further BMPO.
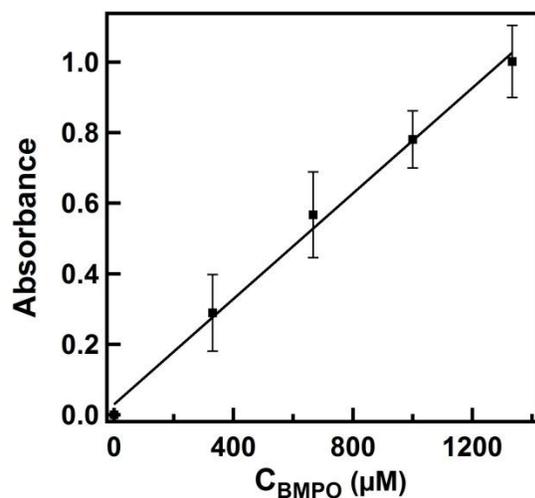
Figure 3-5. Calibration curve for BMPO. Each point on the plot represents an average of three replicate experiments and the error bars denote the standard deviation. The R^2 value was analyzed to be 0.9949. The equation of the line to calculate the concentrations of Orange II was y= 0.0007*x + 0.0297.
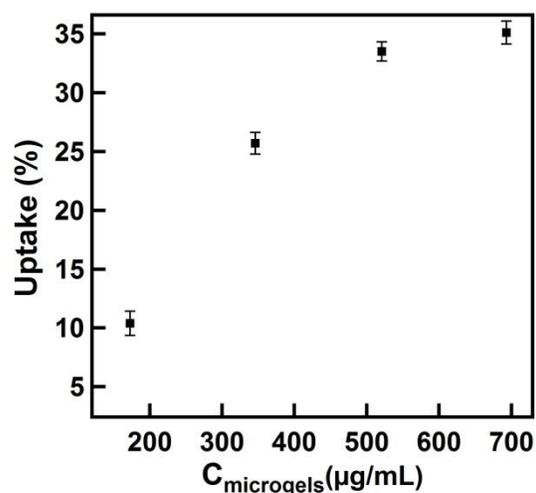
Figure 3-6. Uptake of BMPO as a function of concentration of pNIPAm-*co*-10AAc. All the solutions were in a total volume of 3 mL and pH 7 buffer. Each point on the plots represents an average of three replicate experiments of uptake studies and the error bars denote the standard deviation.

Removal efficiency as a function of temperature-Single cycle. PNIPAm microgels are well known to be thermoresponsive. That is, at T > ~32 ˚C they decrease in diameter by expelling their water of solvation, as result of which they become more hydrophobic. This process is reversible, so at T < ~32 ˚C the microgels rehydrate and return to their initial state. At this pH and ionic strength, the thermoresponsivity was still observed, as confirmed from light scattering experiments in Figure 3-7.
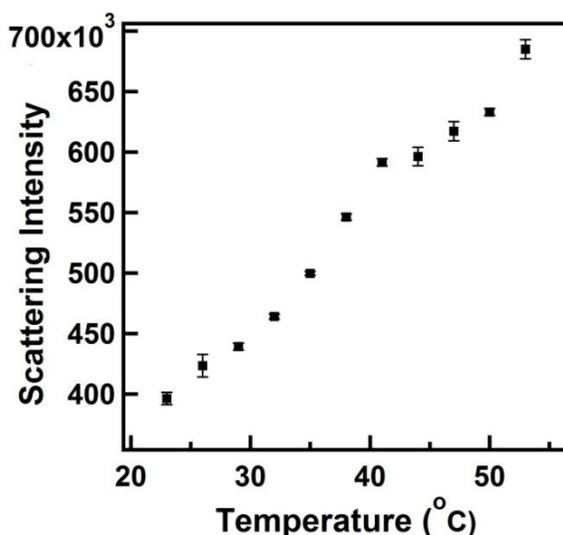
Figure 3-7. Light scattering data for thermoresponsivity of microgels

For the uptake studies, we exposed 300 µL (521µg/mL) pNIPAM-*co*-10AAc microgels to 15 µL of Orange II, and cycled the temperature above and below 32 ˚C and calculated the percent removal. We hypothesize that when the microgels rehydrate, they will absorb excess Orange II from solution. Additionally, we characterized the uptake efficiency as a function of time that the microgels were held at an elevated temperature. Specifically, the microgels were exposed to Orange II for five minutes and heated to 50˚C for periods of 20, 40, 60, 90 and 120

minutes. The solution was immediately cooled to room temperature (~23 ˚C) for 30 minutes and centrifuged. The absorbance of the supernatant solution was then evaluated and percent removal determined. Figure 3-8 shows that the percent of Orange II removed from solution increased from 29.5% (at RT) to 50.3% as the time the solution was held at elevated temperature increased to 120 minutes. The figure also suggests that no more dye is taken up after the 90 minute heating and 30 minute cooling experiment. A control experiment was performed by heating Orange II of the same concentration (in buffer) in the absence of microgels. It was shown that the absorbance intensity of Orange II decreased by only 3.5% due to heating alone as shown in Figure 3-9, which confirms that the improved uptake efficiency of the microgels by heating was indeed due to the thermoresponsive nature of the microgels.
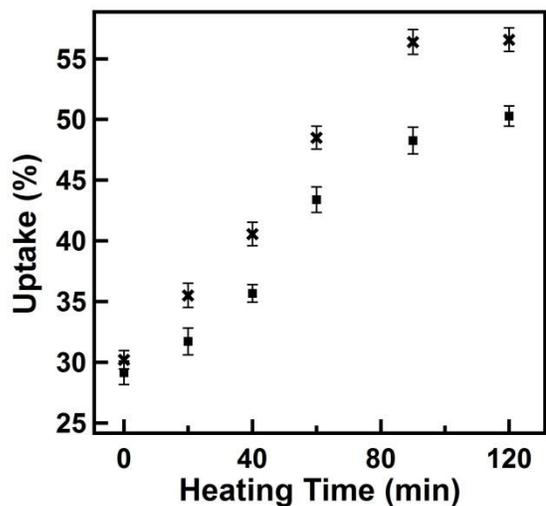
Figure 3-8. Uptake of Orange II as a function of the time the microgels were held at elevated temperature for (■) one and (x) two cycles. Each point on the plot represents an average of three replicate experiments of uptake studies and the error bars denote the standard deviation.
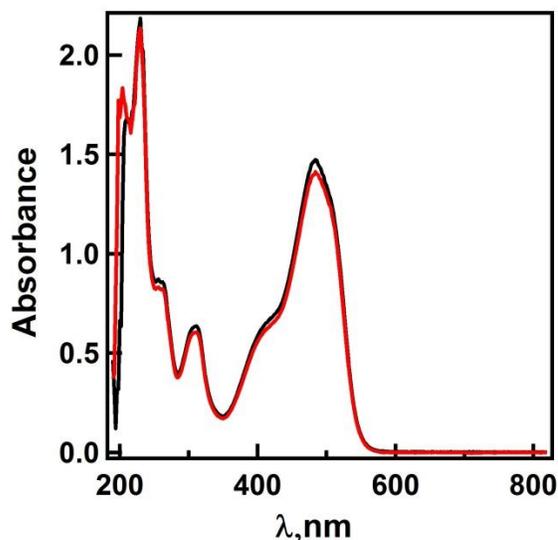
Figure 3-9. UV-Vis spectra for 113.5 μM Orange II at room temperature (shown in black) and after heating at 50 ˚C for 120 minutes (shown in red). No significant difference in the absorbance was observed under these conditions.

Removal efficiency as a function of temperature-Multiple cycles. Results from the previous section indicate that temperature affects the removal efficiency of the microgels, which is hypothesized to be due to the thermoresponsive nature of the microgels. The effect of multiple heating cycles was also investigated. This was done by heating 300 μL (521 μg/mL) of pNIPAM-*co*-10AAc microgels exposed to 15 μL of Orange II to 50 ˚C two times, followed by cooling cycles. The heating times were chosen such that the total time the microgels were held at elevated temperature matched the times for the single cycle, the only difference being the number of times the microgels were heated and cooled. For example, a solution of microgels was exposed to Orange II for five minutes, brought to 50 ˚C for 10 minutes, cooled for 15 minutes, heated again for 10 minutes, followed by cooling for 15 minutes. Overall, the microgels were at elevated temperature for 20 and at RT for 30 minutes, equivalent to the microgels that were heated 1 time for 20 minutes. This was repeated for all the single cycle heating times. Figure 3 -8

shows that the uptake of Orange II increased after an additional heating cycle. The maximum

uptake was increased from a maximum of 50.3% from one hot cycle to 56.6% for an extra hot

cycle. The uptake also levels off after 90 min, similar to the single hot cycle data. We also

investigated the effect of the cycling the temperature one more time, and didn't observe a

significant increase in in the removal efficiency (Figure 3-10).
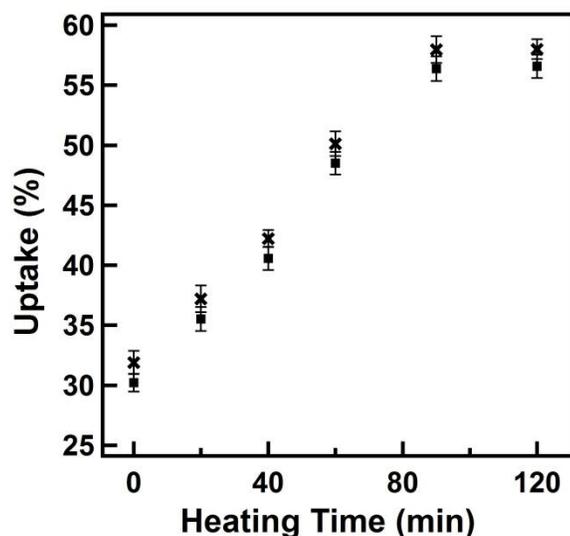
Figure 3-10. Trend for the uptake of Orange II as a function of heating and cooling cycles. The uptake of the dye for triple heating and cooling cycle (shown by 'x') is almost the same as the trend observed for the double heating and cooling cycle (shown by squares). Each point on the plot represents an average of three replicate experiments of uptake studies and the error bars denote the standard deviation.

Leaking studies. While the maximum removal efficiency of the microgels was shown to

be ~56.6%, with two 45 min heating cycles, it is important to evaluate the ability of the

microgels to retain the Orange II that was removed from the water. To evaluate this, we exposed

900 μL of pNIPAm-*co*-10AAc to Orange II for five minutes in a total volume of 9 mL using the

same buffer as in the uptake studies, and the solution was centrifuged and the supernatant

solution removed. The resulting microgel pellet was redispersed in 9 mL of fresh buffer by

vortexing and divided into 9 different Eppendorf tubes and allowed to incubate for various time intervals, from 0 to 100 minutes and then centrifuged, as indicated in the Experimental Section. The supernatant solution was then evaluated and the percent Orange II leaked calculated. The percentage of Orange II that was leaked was determined by calculating the number of moles Orange II that was initially removed from the solution and then determining how much was expelled after a given incubation time interval. The concentrations of Orange II were determined from a calibration curve, as indicated above. For example, the "0 min" sample was immediately centrifuged after splitting the solution up and the supernatant solution evaluated. The number of moles in this solution was compared to how many moles were initially in the microgels. Figure 3-11 shows the trend for the percent leaking of Orange II as a function of leaking time. The figure indicates that percentage of Orange II that leaked from the microgels increased with time up to 50 minutes and leveled off after this time. We calculated that a maximum of 25.6% of the absorbed dye leaks out of the microgels. This translates to a 74.4% retention efficiency. We also addressed the possibility of Orange II leaking out further with the addition of fresh buffer. We removed the supernatant from the sample that was allowed to incubate for 100 minutes and added 1.0 mL fresh buffer to this system and allowed the solution to incubate for 60 minutes. This was then centrifuged and the supernatant was removed to record the absorbance; no significant increase in leaked Orange II was observed. Additionally, we studied the possibility of microgels leaking out Orange II at elevated temperature. The microgels deswell by expelling water of solvation when heated above their LCST. In order to test if the microgels leak out more Orange II at higher temperatures, we redispersed the supernatant from the tube that was allowed to incubate for 100 minutes (at room temperature) with the microgels. This solution was then allowed to incubate for another 100 minutes on a hot plate at 50°C and was immediately

centrifuged for 30 minutes at 50°C by regulating the thermostat in the centrifuge. The supernatant was removed and the absorbance was measured. The results in Figure 3-12 show that leaking is not affected by temperature.
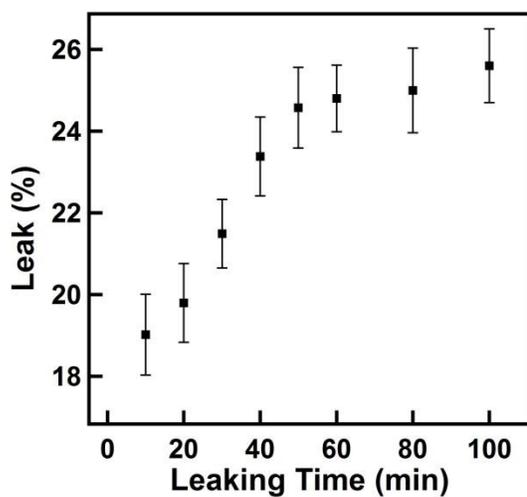
Figure 3-11. Leaking of Orange II from pNIPAm-*co*-10AAc microgels as a function of leak time. Each point on the plot represents an average of three replicate experiments of leaking studies and the error bars denote the standard deviation.
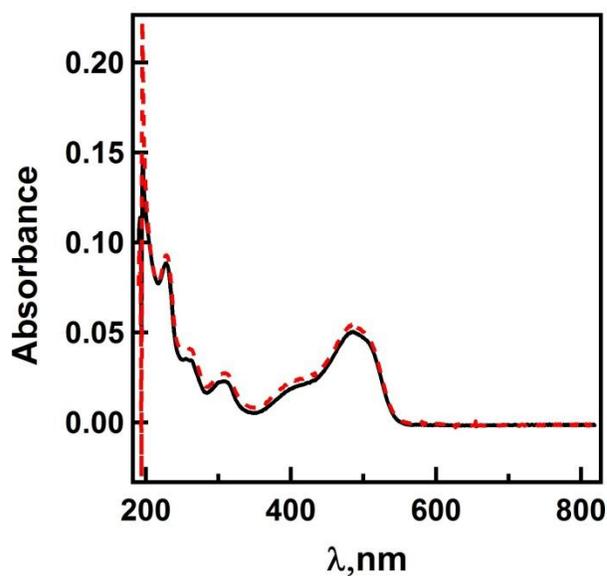

Figure 3-12.. UV-Vis spectra for the leaking of Orange II from pNIPAm-*co*-10AAc microgels at room temperature after 100 minutes (shown in black) and at 50 °C (shown in red). There is no significant difference in absorbance, i.e. no more leakage of Orange II even after heating.

Similar experiment was performed to monitor the leaking of BMPO from the microgels. Briefly, 600 μL of pNIPAm-*co*-10AAc were exposed to 30 μL of BMPO in a total volume of 6 mL using the same buffer solution. The solution was centrifuged after five minutes and and the supernatant solution was removed. The microgel pellet was redispersed in 6 mL of fresh buffer by vortexing and divided into 6 different Eppendorf tubes and allowed to incubate for various time intervals, from 0 to 180 minutes and then centrifuged. The calibration curve was used to determine the percent leak of BMPO after a given incubation time interval. The concentrations of Orange II were determined from a calibration curve, as indicated above. Figure 3-13 shows the trend for the percent leak of BMPO from the microgels as a function of incubation time (leaking time). It was observed that as the time increased from 30 minutes to 120 minutes, 14.3% to 23.4% of BMPO leaked out of the microgels. After 180 minutes, only 24.1% of BMPO leaked out. So the overall efficiency of the microgels to retain BMPO was determined to be 75.9%. The possibility of BMPO leaking further at higher temperatures, were monitored using the same protocol used for Orange II mentioned, using the sample that was incubated for 180 minutes. The results in Figure 3-14 show that leaking is not affected by temperature.
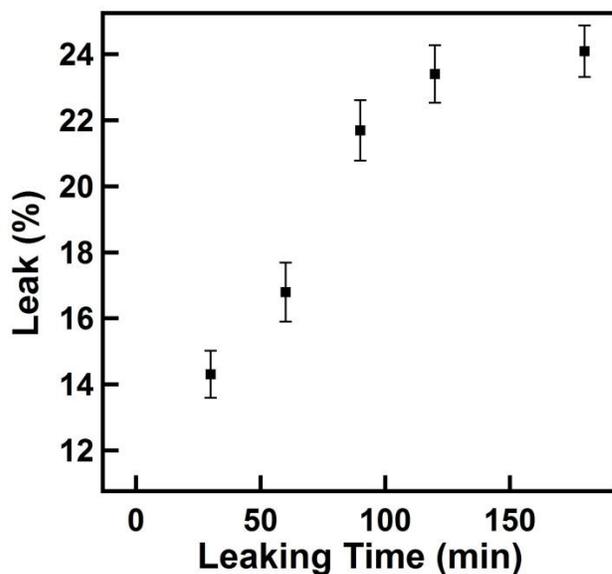
Figure 3-13. Leaking of BMPO from pNIPAm-*co*-10AAc microgels as a function of leak time. Each point on the plot represents an average of three replicate experiments of leaking studies and the error bars denote the standard deviation.
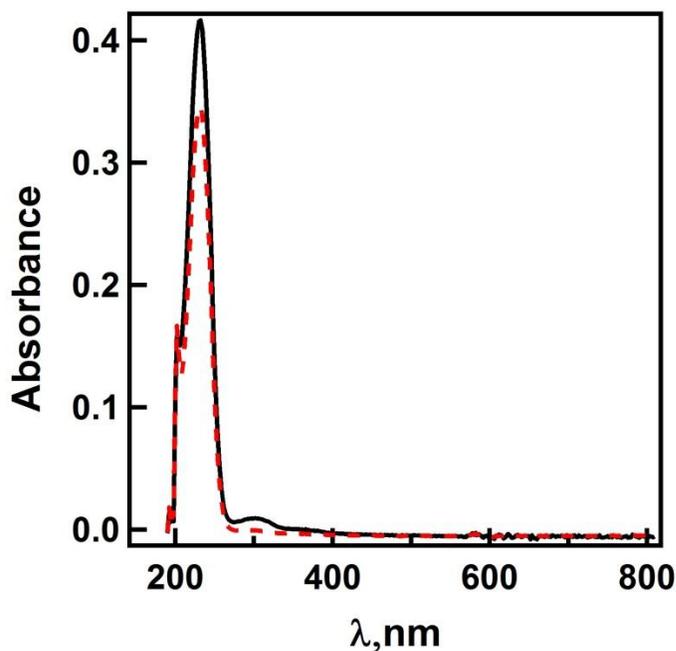
Figure3-14. UV-Vis spectra for the leaking of BMPO from pNIPAm-*co*-10AAc microgels at room temperature after 180 minutes (shown in black) and at 50 ˚C (shown in red). There is no significant difference in absorbance, i.e. no more leakage of Orange II even after heating.

Uptake studies as a function of Orange II concentration-Langmuir isotherm. We also investigated the ability of the pNIPAm-*co*-10AAc microgels to remove Orange II from aqueous solution as a function of Orange II concentration. We exposed 300 µL (521µg/mL) of pNIPAM-co-10AAc microgels to 5, 10, 15, 20, 25, 30 and 35 µL of Orange II from the stock solution in a total of 3 mL buffer (pH 7, 0.235M ionic strength). The microgels were then centrifuged for 30 minutes and the supernatant was analyzed by UV-Vis, as explained above. The data in Figure 3-15 was fit with a Langmuir isotherm (equation 1), which yielded a maximum concentration of Orange II adsorbed on the microgels as 139.9 µmoles/g (0.049 g Orange II/g microgels) and a Langmuir coefficient of 0.01143 ± 0.00134 g/µmoles was calculated.

$$C_{i,s} = C_{i,smax} * K_{ads} * C_{i,m}/(1 + K_{ads} * C_{i,m}) \hspace{2cm} (1)$$

$C_{i,s}$ is the concentration of the dye in sorbent (microgels)

$C_{i,m}$ is the concentration of the dye in the mobile phase (in buffer after centrifugation)

K_{ads} is the Langmuir coefficient

Previously, pNIPAm based gels were used for adsorption of naphthalene disulfonic acid (NS-2). The authors report the loading of NS-2 on the microgels to follow the Langmuir isotherm model, reporting R^2 values of ~ 0.97 and a maximum uptake of 13 mmoles/L of gel (3.747g NS-2/L of gel).[364] Assuming the density of the solution to be 1.000 g/mL, the maximum loading capacity would be 0.0037 g NS-2/g of gel. In comparison, it is evident that the microgels reported in this submission achieved higher uptake efficiencies.
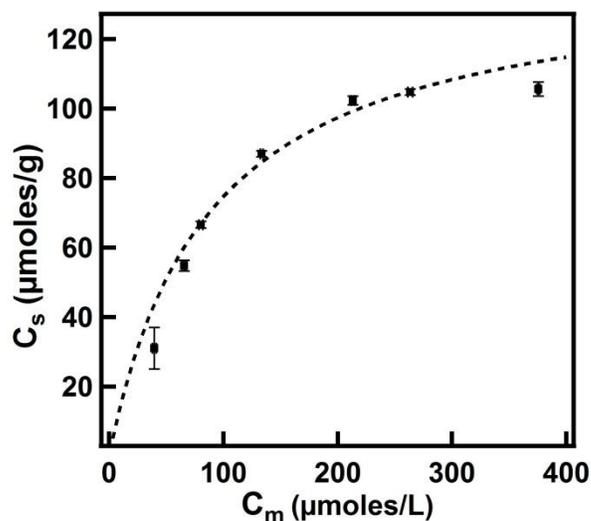
Figure 3-15. Langmuir sorption isotherm for the removal of Orange II by the microgels. C_m is the concentration of the dye remaining in the aqueous phase and C_s is the concentration of the dye sorbed to the microgels. The goodness of fit (R^2) value was calculated as 0.9518. Each point on the plot represents an average of three replicate experiments and the error bars denote the standard deviation.

3.5. Conclusion

Microgel systems of pNIPAm modified with varying concentrations of AAc were determined to be efficient to absorb an azo dye Orange II the most efficient of these systems being pNIPAm with 10%AAc. The same microgel system was used for removal for BMPO at room temperature, which gave a maximum uptake of 35.1%. The results from Orange II uptake studies indicate that by exploiting the thermoresponsive nature of these microgels, the percent absorption of Orange improved significantly by heating and cooling the microgels for a single cycle when compared with room temperature studies. The control experiments performed prove that the decrease in absorbance observed were due to the uptake of Orange II by the microgels and not merely due to any effect in the absorbance of Orange II at higher temperatures. Furthermore, the leaking studies show that the microgels leak out 25.6% of the Orange II that was originally removed from solution, with no more leaking occurring after 50 minutes.. The

Langmuir coefficient of 0.01143±0.00134 was calculated by fitting a curve using Langmuir equation for the concentration of Orange II encapsulated in the microgels vs. the concentration of Orange II in solution.

POLY (N-ISOPROPYLACRYLAMIDE) BASED ASSEMBLIES FOR ORGANIC DYE REMOVAL FROM WATER

4.1. Introduction[2]

As discussed in previous Chapter, poly (*N*-isopropylacrylamide)-*co*-acrylic acid microgels are capable of removing 29.5% of Orange II at room temperature and 56.6% at elevated temperature. This Chapter discusses the uptake efficiency of microgel assemblies, or aggregates. The aggregates from pNIPAm-*co*-AAc were synthesized via polymerization of the crosslinker *N,N'*-methylenebisacrylamide (BIS) in the presence of the microgels. In other words, the microgels were entrapped within the polymerized network of the crosslinker. Upon monitoring the ability of the aggregates to remove Orange II from water, the maximum percent uptake was determined to be 73.1% at elevated temperature. This is a significant improvement compared to the unaggregated microgels (an increase by ~ 16%) as mentioned in the previous Chapter under similar experimental conditions. This can be attributed to an increase in the interstitial or the void space between the aggregated microgels, which in turn can accommodate more Orange II in comparison with the unaggregated microgels. Figure 4-1 represents a schematic that represents the hypothesis for the enhanced uptake of the dye by the aggregates microgels compared to the unaggregated microgels. Among other studies in this Chapter, the uptake of the dye as a function of increasing concentration of BIS crosslinker present in the aggregates was monitored. It was determined that removal efficiency improved with the increasing concentration of the crosslinker, which can be attributed to either the increasing

---

[2] This dissertation has been adapted from references 361, 362 and 363.

hydrophobicity (structure) of the aggregates or increase in the number of aggregates, as confirmed by a counting experiment. The uptake studies of the dye by the aggregates were fit by a Langmuir isotherm model. The results indicate that the microgel aggregates follow the model more accurately compared to the unaggregated microgels. Finally, leaking studies were performed to assess the overall retention efficiency of the aggregates.
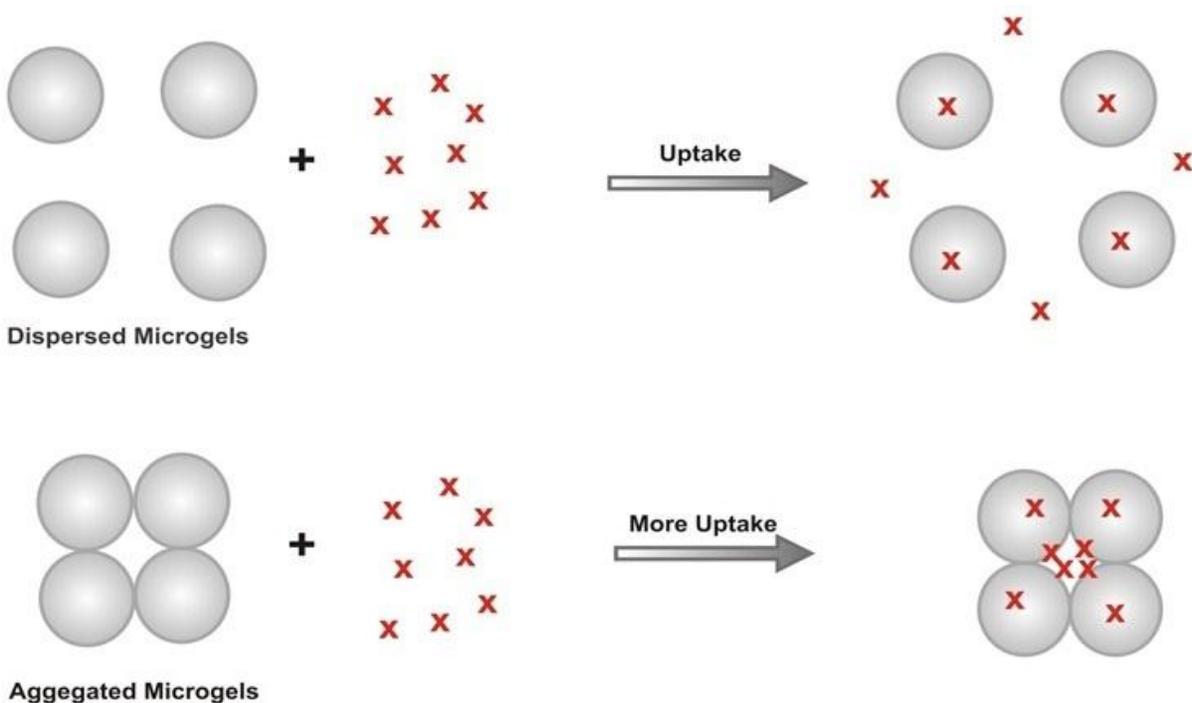
Figure 4-1. Schematic illustrating the uptake of (**x**) Orange II by the unaggregated microgels vs. the aggregated microgels. The aggregates take up more dye molecules because of larger void volume.

4.2. Materials and Methods

Materials. The monomer, *N*-isopropylacrylamide was purchased from TCI (Portland, Oregon) and purified by recrystallization from hexanes (ACS reagent grade, EMD, Gibbstown, NJ). *N,N'*-methylenebisacrylamide (BIS) (~99%), acrylic acid (AAc) (~99%), and ammonium persulphate (APS) (~98%) were obtained from Sigma-Aldrich (Oakville, Ontario) and were used as received. Orange II was obtained from Eastman Organic Chemicals (Rochester, New York). All the phosphate salts used for preparing buffer solutions of pH 7, with an ionic strength of 0.235 M, were obtained from EMD and were used as received. Deionized (DI) water with a resistivity of 18.2 $M\Omega \cdot cm$ was obtained from a Milli-Q Plus system from Millipore (Billerica, MA), and filtered through a 0.2µm filter, prior to use. Microgel samples were lyophilized using a VirTis benchtop K-manifold freeze dryer (Stone Ridge, New York).

Synthesis of microgels PNIPAm-*co*-AAc microgels of ~ 1.1 µm (the same microgels mentioned in the previous Chapter) diameter were prepared by a surfactant free, free radical precipitation polymerization as described previously.[293] The total monomer concentration was 140 mM, and was 85% *N*-isopropylacrylamide (NIPAm), 5% *N,N'*-methylenebisacrylamide (BIS) crosslinker and 10% acrylic acid (AAc) . The microgels will be indicated as pNIPAm-*co*-10AAc, to show that they contain 10% AAc. The monomer, NIPAm (11.9 mmol) and the crosslinker, BIS (0.700 mmol), were dissolved in deionized water (75 mL) in a beaker with stirring. The mixture was filtered through a 0.2 µm filter affixed to a 20 mL syringe into a 250 mL, 3-neck round bottom flask. An additional 24 mL of deionized water was used to wash the beaker, which was filtered and transferred to the mixture in the round bottom flask. The flask was then fitted with a condenser, temperature probe (thermometer), stir bar, and a N_2 inlet. The temperature was set to 65˚C and N_2 was bubbled through the solution for ~ 1 h, after which AAc (1.4 mmol) was added to the mixture and allowed to stir for a few minutes. To this, 0.197 mmol

APS in 1 mL DI water was added. The mixture was allowed to stir for 4 h, under N_2 atmosphere. The solution was allowed to cool, while stirring overnight.

Following stirring overnight, the microgels were filtered through a type 1 Whatman filter paper, which was then rinsed with deionized water. The microgels were cleaned via centrifugation to remove unreacted monomer and crosslinker, as well as linear polymer from the microgels. To do this, the microgel solution was separated into 15 mL centrifuge tubes obtained from Corning Incorporated (Corning, NY) (~ 12 mL microgel solution/tube) and centrifuged at a speed of ~8400 relative centrifugal force (rcf) in a Baxter, biofuge 17R (Mount Holly, NJ) at 23 °C, for 30 min. Centrifugation yielded a pellet of microgels at the bottom of the centrifuge tube, and the supernatant was removed. ~12 mL of fresh DI water was added and the microgel pellet was redispersed using a Fisher Vortex, Genie 2 vortexer (Pittsburgh, PA). This cleaning protocol was repeated six times.

Synthesis of microgel aggregates. Microgel aggregates were synthesized using three different concentrations of BIS: 2, 10 and 15 mg BIS/mL of total reaction solution (100, 500, and 750 mg total BIS mass, respectively). The first set of aggregates were prepared by adding 10 mL of the above synthesized and cleaned microgels to a filtered solution (filtered through 0.2 μm filter affixed to a 20 mL syringe) of 100 mg of BIS in 39 mL of deionized water, to a beaker and stirred. This solution was transferred into a 250 mL 3-necked round bottom flask that was fitted with a condenser, thermometer, stir bar and a N_2 inlet. The temperature was set to 65˚C and N_2 was bubbled through the solution for ~ 1 h After 1 h, a 1 mL aqueous solution containing 0.0175 mmol of APS was added to this mixture and left to stir for 4 h, under N_2 atmosphere. The solution was allowed to cool with stirring overnight. This process was repeated for the other concentrations of BIS samples as well. The microgel aggregates were cleaned using the same

protocol as mentioned the microgel synthesis section, but without filtering. Representative DIC microscopy images of the 100 mg, 500 mg and 750 mg BIS aggregates are shown in Figure 4-2.
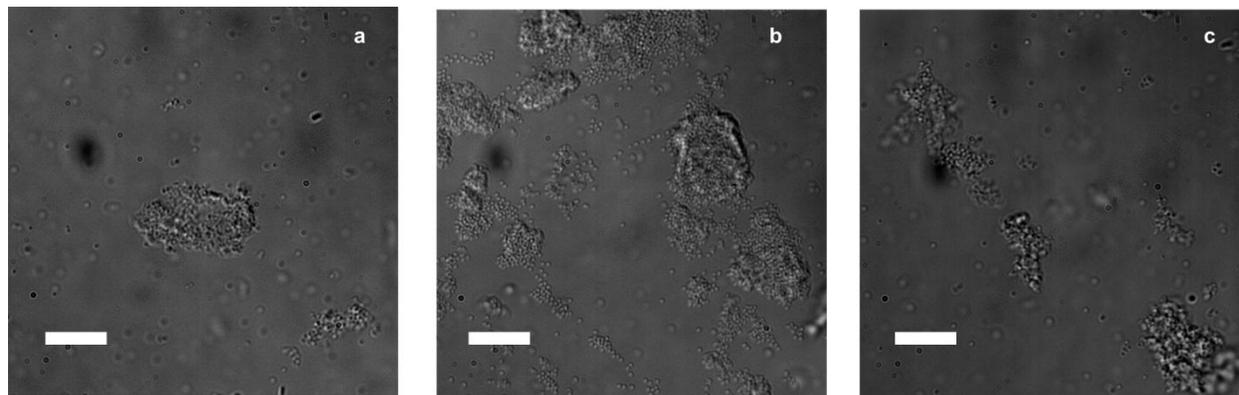
Figure 4-2. DIC microscopy images of microgels aggregates with (a) 100 mg BIS, (B) 500 mg BIS and (C) 750 mg BIS. The scale bar used in all the panels is 5 μm.

Orange II uptake. The individual aggregate solutions were lyophilized to yield a powder, and stock solutions of each were made to contain 5.2 mg aggregates/mL by weighing out 52.1 mg of each aggregate sample into a volumetric flask, and diluting to 10 mL with a pH 7 buffer solution of 0.235 M ionic strength. A stock solution of 0.023 M Orange II in deionized water was prepared. Using a micropipet, 300 μL of the respective aggregate solutions, and 15 μL of Orange II solution, was added to a 15 mL centrifuge tube(Corning Incorporated; Corning, NY) and diluted to 3 mL with the pH 7 buffer solution (final concentrations of aggregates and Orange II were 521 μg/mL and 114 μM, respectively). This sequence of addition of buffer after exposing the dye to the aggregates was maintained for all experiments. This solution was allowed to sit for five minutes and then centrifuged for 30 minutes, at ~8400 rcf to pack the aggregates to the bottom of the centrifuge tube. This centrifugation time was used to ensure that all the dispersed microgels were removed from solution (as confirmed from differential interference contrast

microscopy, data not shown). The supernatant was carefully removed from the tube without disturbing the pellet of aggregates packed at the bottom of the centrifuge tube and transferred to a quartz cuvette. The absorbance was measured using a HP8452A UV-Vis spectrophotometer with a diode array detector (Agilent Technologies, Inc., Santa Clara, CA). Figure 4-3 represents a schematic of uptake studies by the aggregated microgels. The initial concentration of Orange II for all the uptake studies was maintained at 114 µM and it was observed that the pH of Orange II solution was unaffected by the addition of aggregates. The initial absorbance of Orange II was measured in the absence of the aggregates. This measurement was performed before all the studies. It was also observed that the centrifuge tube did not have any effect on the initial absorbance of Orange II, i.e., the tube does not interact with Orange II. To study the uptake of Orange II as a function of temperature, the solution of Orange II and aggregates was held at 50 ˚C, for different intervals of time (microgels deswell) and then cooled down to room temperature (microgels reswell). This solution was then centrifuged and the supernatant was used to perform UV-Vis studies.
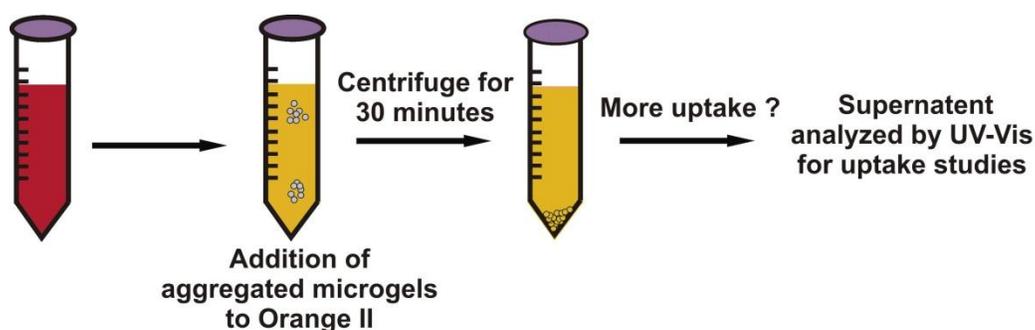
Figure 4-3. Schematic illustrating the uptake of Orange II by the aggregated microgels.

Orange II leaking studies. To evaluate the ability of the microgels to retain Orange II, the concentrations, and volumes from the previous section were scaled up three times. So in this

case, 900 µL of microgels were exposed to 114 µM Orange II in a total volume of 9 mL using the same buffer that was used for the uptake studies. This scaling up was done to get a detectable absorbance signal from the solutions after leaking. As for the Orange II removal studies above, the solution was allowed to sit for five minutes followed by centrifugation for 30 minutes. The supernatant solution was then carefully removed without disturbing the microgels packed at the bottom. To this tube, 9.0 mL of fresh buffer solution (the same buffer that was used for the uptake studies) was added and then the microgels were redispersed by vortexing. This was immediately divided into nine, one mL samples in 1.5 mL Eppendorf tubes obtained from Fisher Scientific, (Ottawa, ON) and the solutions were allowed to incubate for various intervals of times. For example, immediately following splitting up the original solution, one tube was centrifuged for 30 min and the supernatant solution removed and UV-Vis performed on the supernatant solution, this was considered t = 0. We allowed the other tubes to incubate for 10, 20, 30, 40, 50, 60, 70 and 80 minutes respectively, before each was centrifuged.

Counting of aggregates. Solutions containing 41.6 µg/mL of the 100 mg, 500 mg and 750 mg BIS aggregates were prepared. A drop of these samples were placed on a microscope cover slip (25 mm x 25 mm, Fischer Scientific, Ottawa) and pictures of 20 random areas of the sample were obtained using a Olympus IX71 inverted microscope (Markham, Ontario) fitted with a 100 X oil immersion objective, differential interference contrast (DIC) optics and an Andor Technology iXon+ camera (Belfast, Ireland). There were different sizes of aggregates in these samples that were designated as "big", "medium" and "small". When making the designation of size, we measured the apparent diameter of the aggregates in approximately two orthogonal directions. If the two dimensions were ≥ 0.6 µm×1.5 µm < 5.7 µm x 4.5 µm the aggregate was considered small, medium aggregates were ≥ 5.7 µm x 4.5 µm < 10.3 µm×11.5

µm, and large were ≥ 10.3 µm×11.5 µm. Any aggregate < 0.6 µm×1.5 µm was not counted; therefore single particles were not accounted for. A micrometer scale of 50 divisions, each 2 µm in length (Edmund Optics, NJ) was used to measure the sizes of these aggregates.

4.3. Results and Discussion

Effect of aggregation of microgels. In the previous Chapter the efficiency of the microgels to remove Orange II as a function of the concentration of the microgels in solution was evaluated. A maximum uptake of 29.5% for the pNIPAm-*co*-10AAc microgels at room temperature was determined. In this Chapter, the removal efficiency of the pNIPAm-*co*-10AAc microgel aggregates as a function of the amount of aggregates that were present in solution was studied. To do this, the initial absorbance of 3 mL solution of the 114 µM Orange II solution in the absence of microgel aggregates was recorded. This was compared to the absorbance of the supernatant solution after addition of 100, 200, 300 and 400 µ of the 500 mg BIS microgel aggregates to 114 µM Orange II, keeping the total volume of 3 mL consistent from run to run. A calibration curve shown in the previous Chapter, was used to calculate the number of moles of Orange II in solution before and after addition of aggregates. Figure 4-4 shows the percent uptake as a function of concentration of unaggregated pNIPAM-*co*-10AAc microgel (as shown in the previous Chapter) and the percent removal as a function of concentration of the microgel aggregates. The figure shows that the maximum removal efficiency from the aggregates was 45.1% as opposed to 29.5% achieved from the unaggregated microgels. This shows that the aggregation of microgels, significantly improved the removal efficiency.
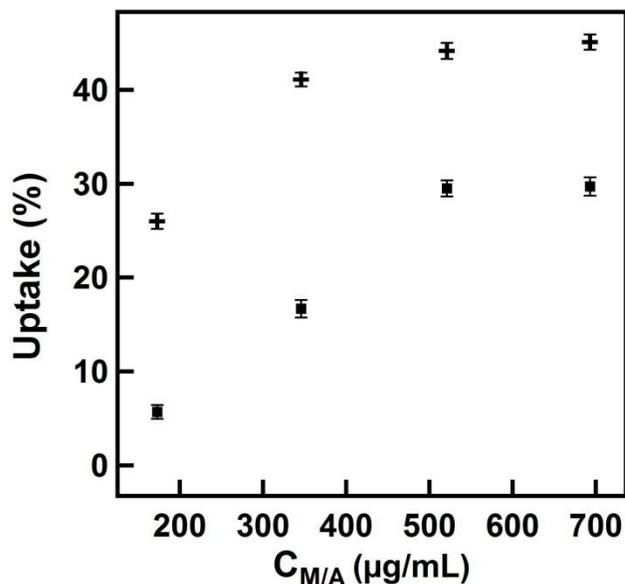
Figure 4-4. Uptake of Orange II as a function of concentration of microgels (C_M), shown by '■' and concentration of microgel aggregates (C_A), shown by '+'. The total volume of all the solutions was maintained at 3 mL in pH 7 buffer. Each point on the plot represents an average of three replicate experiments of uptake studies and the error bars denote the standard deviation.

Furthermore, we calculated the mass of aggregated microgels that would need to be weighed out to result in the same number of microgels in the unaggregated microgel experiment. That is, for a given mass, there are more microgels in the unaggregated sample, then in the aggregated sample. This is because the mass in the aggregated sample comes from a combination of BIS and microgels, while all the mass in the unaggregated case comes from the microgels (the active component). It was found that we had to prepare much higher concentrations of the aggregates in order to equal the particle number in the unaggregated sample. The data for the uptake studies obtained from these concentrations in Figure 4-5 shows that a maximum of 69% removal efficiency is attained at room temperature within an exposure time of five minute. The removal efficiency of an unaggregated sample that has the same number of microgels as in the sample above was 29.5%. So, a sample of aggregated microgels containing the same number of

microgels as in the unaggregated state results in ~ 43.1% increases in uptake. This is a significant improvement compared to the unaggregated case, and supports the hypothesis that the aggregated structure is leading to enhanced removal efficiency.
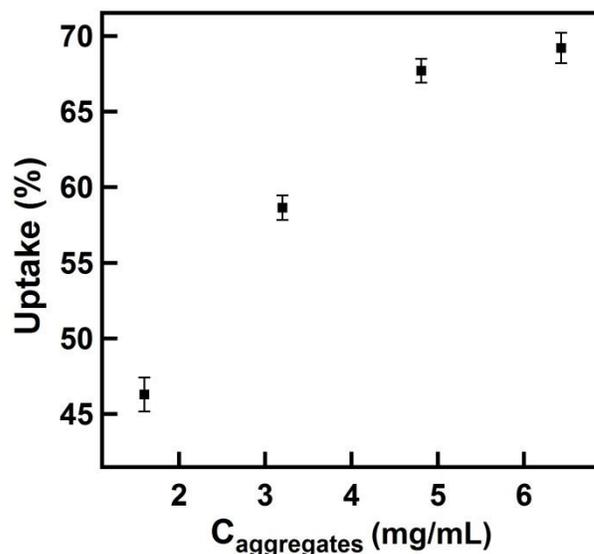
Figure 4-5. The uptake of Orange II as a function of concentration of 500 mg BIS aggregates in a very high aggregate concetration regime. These concentrations were necessary to achieve the same microgels number as the unaggregated microgel case. Each point on the plot represents an average of three replicate experiments and the error bars denote the standard deviation.

This enhancement can be due to: 1) the aggregated microgels have more volume than unaggregated microgels due to the interstitial space between the packed microgels, therefore providing a larger reservoir for Orange II to be trapped in; 2) the aggregates are more hydrophobic than the unaggregated microgels, enhancing the interaction of Orange II with the aggregates; and/or 3) the BIS itself is interacting with the Orange II and removing it from water. A control experiment was performed in which 500 mg BIS was weighed out added to 40 mL DI water and the aggregation was performed using the protocol mentioned in the Experimental, but in the absence of microgels. After the aggregation of BIS, 10 mL of pNIPAM-*co*-10AAc was

added to the mixture; this yields a solution that has the same amount of BIS and microgels as the standard aggregated sample. Uptake studies were performed by monitoring the removal efficiency as a function of the aggregate concentration. The data in Figure 4-6 (a) shows that the aggregates from the control experiment removed only 8.1% of the dye from the solution as opposed to 45.1% removal efficiency by the aggregated microgels. Hence, it is important to have microgels in their aggregated form to result in enhanced removal. This suggests that either the interstitial space argument and/or the hydrophobicity arguments can be valid.
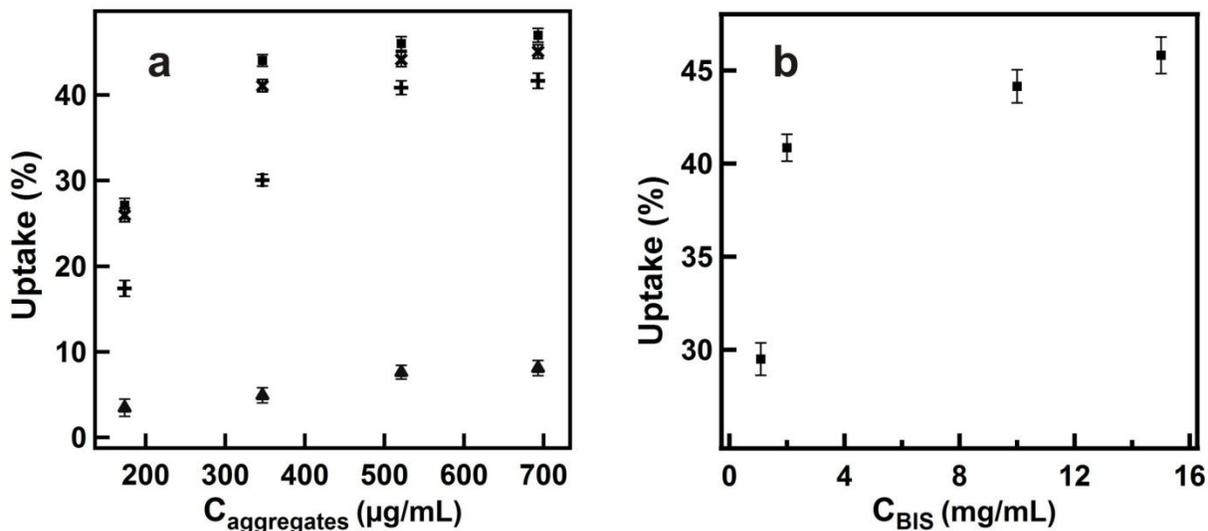
Figure 4-6. Uptake of Orange II as a function of (a) concentration of aggregates from the synthesis using (+) 100 mg, (x) 500 mg and (■) 750 mg BIS and (▲)control experiment using 500 mg BIS aggregates ; (b) concentration of BIS in the aggregates. The first point on (b) is the uptake from unaggregated microgels. Each point on the plot represents an average of three replicate experiments of uptake studies and the error bars denote the standard deviation.

Effect of BIS concentration on removal efficiency. The concentration of BIS (crosslinker) was varied in the microgel aggregates and the uptake studies of Orange II were

performed at room temperature for each of these systems. Figure 4-6 (b) shows the percent uptake as a function of increase in the BIS concentration in the microgel aggregates. The first point on the plot denotes the uptake percent (29.5%) after addition of 300 µl (521 µg/mL) of unaggregated microgels, as reported previously. The remaining data points denote the uptake percent for 100 mg, 500 mg and 750 mg BIS in the synthesis of aggregates for the same concentration of aggregate addition to the Orange II. It was found that the uptake percent was 40.85% for the 100 mg BIS microgel aggregates, and the uptake increased to 44.16% for the 500 mg BIS microgel aggregates. This is only 1.67% lower than the 750 mg BIS microgel aggregates.

The effect of increasing the concentration of the aggregates for the 100 mg 500 mg and 750 mg BIS concentrations was also investigated. Figure 4-6 (a) shows that as the concentration of the aggregates increased from 173 to 521 µg aggregates/mL of reaction solution, the percent uptake of Orange II increased from 17.4% to 40.9% for the 100 mg BIS aggregates; 25.9% to 44.2% for the 500 mg BIS aggregates, and 27.12% to 46.02 % for the 750 mg BIS aggregates. For all the aggregates, there was no significant increase in uptake as the concentration of aggregates was increased from 521 to 693 µg aggregates/mL of reaction solution. We attribute this behavior to an equilibrium process that exists in the system, i.e., only a certain number of moles can be removed from solution due to equilibrium (although drastic changes in concentration does result in enhanced uptake, as indicated above). It should be noted that there is minimal enhancement in uptake as the amount of BIS in the aggregates was increased from 500 mg to 750 mg. The data from these experiments show that the maximum removal efficiency achievable for the microgel aggregates at room temperature improved the uptake efficiency by~17%, compared to the

unaggregated microgels. For the remainder of the studies, we employed the 500 mg BIS aggregates at a concentration of 521 µg aggregates/mL of reaction solution.

We hypothesize that the trend of increased uptake efficiency with increasing concentration of BIS in the aggregates could be due to: 1) a change in the hydrophobicity of the aggregates with BIS concentration used to form the aggregates 2) an increase in the number of aggregates that are in solution; and/or 3) a difference in the size of the aggregates in the respective solutions, which would provide more interstitial volume for Orange II to be trapped. Since it was established above that it is important to have aggregates in solution to achieve enhanced uptake, it stands to reason that if one solution has more aggregates relative to the others, than it should exhibit enhanced uptake.

Table 4-1: Number distribution for different sizes of aggregates in 100 mg, 500 mg and 750 mg BIS concentrations.

Aggregate Size	Number in100 mg BIS	Number in 500 mg BIS	Number in 750 mg BIS
Big	20 ± 3	32 ± 6	35 ± 5
Medium	42 ± 11	35 ± 7	40 ± 13
Small	71 ± 8	135 ± 12	190 ± 7
All sizes	131 ± 12	203 ± 15	265 ± 17

Small aggregates : ≥ 0.6 µm$\times$1.5 µm < 5.7 µm x 4.5 µm; Medium aggregates: ≥ 5.7 µm x 4.5 µm < 10.3 µm$\times$11.5 µm; and Large aggregates: ≥ 10.3 µm$\times$11.5 µm.

A counting experiment was conducted as outlined in the Experimental. In short, solutions containing 41.6 µg/mL of the respective 100 mg, 500 mg and 750 mg BIS aggregates were

prepared and the number of aggregates present in a given volume of these solutions was determined. Table 4-1 that the total number of aggregates increased from 131 ± 12 to 265 ± 17 as the amount of BIS in the aggregates was increased from 100 mg to 750 mg. This is supported by the fact that there were more free, unaggregated particles in the 100 mg BIS sample, compared to the 500 and 750 mg BIS aggregate samples; these were not accounted for in the counting process. Interestingly, when the amount of 100 mg BIS aggregates exposed to Orange II was doubled, to give the same number of aggregates as the 750 mg BIS sample, the uptake efficiency was equal to the uptake efficiency achieved for the 750 mg BIS sample.   When aggregate size is considered, it was observed that there is a higher percent of big aggregates in the 750 mg BIS sample compared to the 100 mg BIS sample, which can also lead to enhanced uptake for the 750 mg BIS aggregates. But, if aggregate size was important, when the 100 mg BIS sample concentration was increased, the 750 mg BIS sample should still result in more uptake, which was not the case. Taken together, it appears that in the low aggregate concentration regime the enhanced uptake for the 750 mg BIS aggregates is due to the increased number of aggregates in the sample, because when the number of aggregates in 100 mg BIS sample was set equal to the 750 mg BIS sample, very similar uptake efficiencies are achieved. It should be noted though that while doubling the mass of the 100 mg BIS sample exposed to the Orange II to result in the same percent uptake as the 750 mg BIS samples, the 750 mg BIS aggregates are still much more efficient at removing Orange II from water on a per mass basis. In the high concentration, or the 'equilibrium' regime, where aggregate number no longer matters, the 500 and 750 mg BIS aggregate samples still result in enhanced uptake efficiency, compared to the 100 mg BIS sample. This can be explained considering the hydrophobicity of these aggregates, which will affect the Orange II partitioning behavior, in turn influencing the equilibrium constant. So,

higher BIS concentrations must result in a higher equilibrium constant, which is operative across all concentration, but most apparent in the high concentration (equilibrium) regime.

***Effect of temperature cycle on removal efficienc*y.** To monitor the effect of single temperature cycle, we added 300 µL of the 500 mg BIS aggregates to 15 µl of Orange II in the same buffer solution as before (3 mL total volume), and heated the solution above 32 ˚C for different intervals of time and cooled it down to room temperature Specifically, we exposed the microgel aggregates to the dye for five minutes and heated to 50 ˚C for 20, 40, 60, 90 and 120 minutes and the solution was cooled down to room temperature (~23 ˚C) for 30 minutes and centrifuged immediately. Figure 4-7 shows the trend for the percent uptake as a function of heating time. The percent uptake at time 0 corresponds to the uptake of the microgel aggregates at room temperature (44.2%). It was observed that the uptake of the dye increased significantly from 47.1% to 67.8 % as the time of heating increased from 20 minutes to 90 minutes. Also, there was minimal increase in the uptake when the solution as heated for 120 minutes (68.1%). The dye removal was also visually confirmed by comparing the intensity of the Orange II solution before and after treatment, Figure 4-8. As can be seen, the solution intensity for the heated sample is significantly reduced. A control experiment was performed as mentioned in the previous Chapter, which confirmed that high temperature alone did not affect the absorbance of Orange II. Hence the reduction in Orange II intensity was due to increased uptake due to the aggregate's thermoresponsive nature.
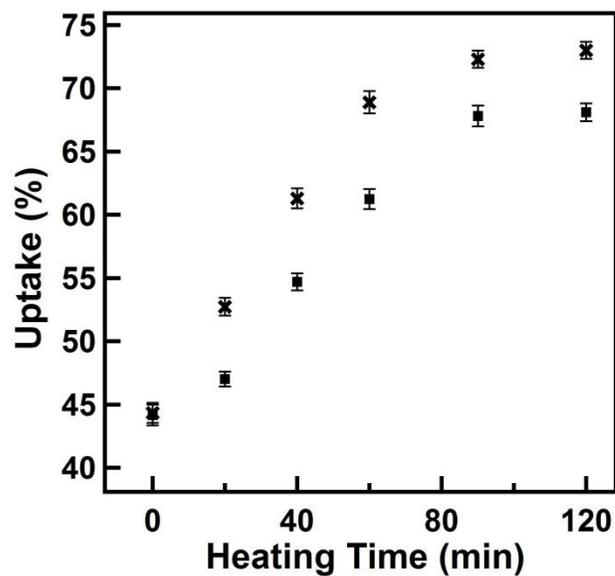
Figure 4-7. Uptake of Orange II as a function of the time the microgels were held at elevated temperature for (■) one and (x) two cycles. Each point on the plot represents an average of three replicate experiments of uptake studies and the error bars denote the standard deviation.
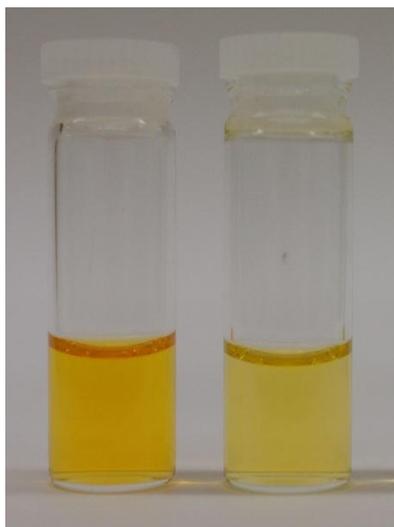
Figure 4-8. Solutions of 114 μM Orange II (left) before and (right) after the addition of 500 mg BIS aggregates. Here, multiple heating cycle (2 cycles) were performed for a period of (90 minutes total hot time)

We also monitored the effect of the multiple heating and cooling cycles on the percent uptake. This was done by exposing the 500 mg BIS aggregates to 15 µL Orange II in the same buffer solution and heated to 50 ˚C and cooled down to room temperature in two cycles, keeping the overall heating and cooling time the same as with the single heating cycle. For example, the solution of aggregates was exposed to the dye and heated to 50 ˚C for 10 minutes and cooled down to room temperature for 15 minutes and heated again to 50 ˚C for another 10 minutes and finally cooled for 15 minutes. So overall the microgels were heated for 20 minutes and cooled for 30 minutes, but over two cycles. This protocol was repeated for all 40, 60, 90 and 120 minutes heating periods. Figure 4-7 shows the effect of increasing the cycle number on the aggregates to remove Orange II from water. It was observed that the maximum uptake of dye increased to 73.01% compared to the single cycle experiment where the maximum uptake was 68.1%. The overall percent uptake of the dye by aggregates was significantly higher than similarly treated unaggregated microgels. We also investigated the effect of cycling between the high and room temperature three times and confirmed that there was no further improvement in the removal efficiency (Figure 4-9).
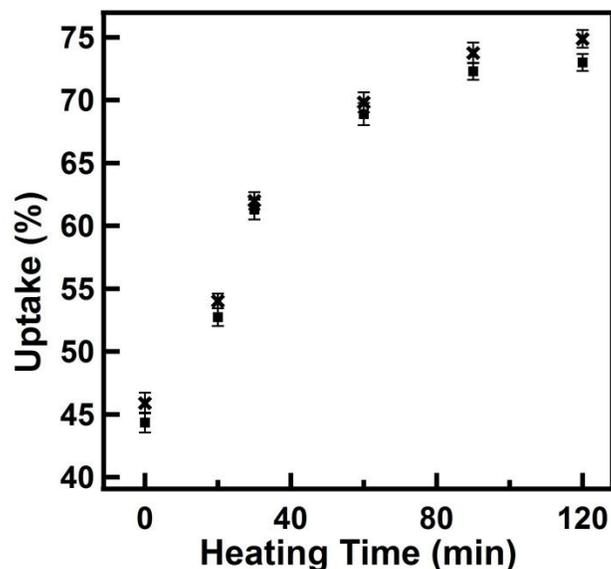
Figure 4-9. Uptake of Orange II as a function of heating and cooling cycles. The uptake of the dye for (**x**) triple heating and cooling cycle is almost the same as the trend observed for the (■) double heating and cooling cycle. Each point on the plot represents an average of three replicate experiments of uptake studies and the error bars denote the standard deviation.

Leaking of Orange II from aggregates. In our previous work we reported that the pNIPAm-*co*-10AAc retained 74.4% of the dye that was removed from the aqueous solution. We followed a similar protocol here to assess the percent of Orange II that was retained in the structures after uptake. This was done by exposing 900 μL of the microgel aggregates to 114 μM Orange II in a total volume of 9 mL pH 7 buffer. This solution was allowed to sit for five minutes and immediately centrifuged (as was done for all uptake experiments at room temperature). The supernatant solution was removed and the microgel aggregates packed at the bottom of the centrifuge tube were redispersed in 9 mL of fresh buffer using a vortexer. This solution was equally divided into 9 Eppendorf tubes and incubated for different intervals of time from 0 to 80 minutes and centrifuged. The supernatant solution from each of these tubes was evaluated for the amount of Orange II present in them and the percent leak of Orange II was determined. As an example, the "10 min" sample tube was incubated for a period of ten minutes

and immediately centrifuged and the supernatant was removed and analyzed for percent leak of Orange II. The "0 min" indicates that the sample was immediately centrifuged without allowing it to incubate. The supernatant from these samples was evaluated for the number of moles of the dye present in it and compared with the number of moles of Orange II originally present in the aggregates. Figure 4-10 represents the percent leak of Orange II from the aggregates as a function of leaking (incubation) time. The percent leak of the dye increased from 18.2% to 24.4% as the incubation time was increased from 10 minutes to 80 minutes. The figure also shows that there was no significant increase in the percent leak of the dye after a period of 50 minutes. Overall, the maximum percent leak of the dye from the aggregates was calculated to be 24.4%. Hence the retention efficiency of the aggregates was 75.6%, which is very similar to the unaggregated microgels. We also monitored if any more the dye leaked out upon addition of fresh buffer. To do this, we picked the sample of aggregates that leaked out highest percent Orange II. As discussed above, the sample was incubated for a period of 80 minutes and centrifuged for 30 minutes. The supernatant solution had 24.4% of the dye that leaked out from the aggregates and was removed. We added fresh 1.0 mL buffer and redispersed the aggregates that remained at the bottom by vortexing. This solution was then incubated for another 80 minutes and centrifuged. The supernatant was analyzed by UV-Vis and we observed that there was no additional leaking. Additionally, we investigated the possibility of the microgels leaking Orange II at elevated temperature due to deswelling of aggregates above their LCST. To do this, we redispersed the microgel aggregates in the supernatant solution containing the leaked Orange II for the 80 minute incubated sample. This solution was incubated for an additional 80 minutes on a hot plate at 50°C and was immediately centrifuged for 30 minutes at 50°C by regulating the

thermostat on the centrifuge. The supernatant was analyzed by UV-Vis and the results from this prove that no more of the dye leaked out from the aggregates.
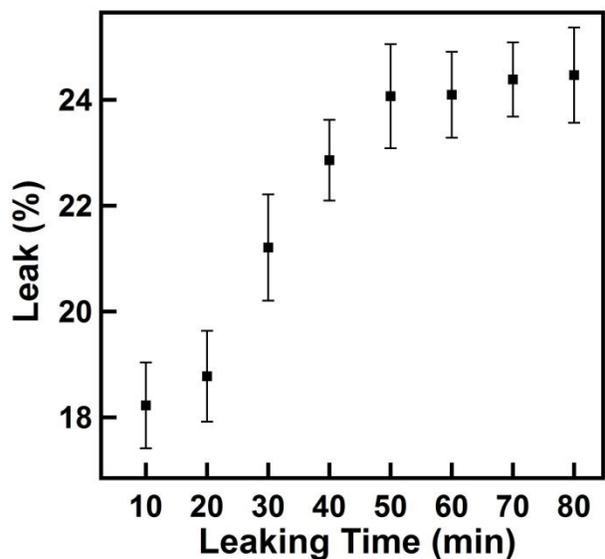
Figure 4-10. The percent leak of Orange II from the microgel aggregates as a function of leak time. Each point on the plot represents an average of three replicate experiments of uptake studies and the error bars denote the standard deviation.

Langmuir sorption isotherm for the removal of Orange II

Figure 4-11 (a) shows the removal efficiency of the microgel aggregates as a function of the concentration of Orange II . Here, we pipetted 5, 10, 15, 20, 25, 30 and 35 µL of Orange II from the stock solution and added 300 µL of the 500 mg (10 mg/mL) BIS aggregates, the total aggregate mass was 1.56 mg. The total volume was maintained at 3 mL for all samples, using the pH 7 buffer solution and the solutions were incubated for five minutes. The solutions were centrifuged for 30 minutes and the supernatant was removed immediately and analyzed for the number of moles of the dye not "sorbed" on the aggregates (as explained in previous sections). A Langmuir isotherm model was used to fit the results from this experiment (equation 1), which gave a good fit with a R^2 of 0.9848. This yielded a maximum sorption of Orange II of 152.8 µmoles/g (0.054 g Orange II/g aggregates) with a Langmuir coefficient of 0.01596 ± 0.00182

L/μmoles. Previously we reported the maximum concentration of Orange II removed by the unaggregated microgels to be 139.9 μmoles/g (0.049 g Orange II/g microgels). We also plotted the sorption isotherm only considering the mass of the microgels in the aggregates, and fit the data with a Langmuir sorption model, which gave a good fit with an R^2 of 0.9853 (Figure 4-11 (b)). In this case, the maximum Orange II sorbed was calculated to be 2871 μmoles/g (1.006 g Orange II/g of microgels). The Langmuir coefficient was calculated as 0.016035 ± 0.0018 L/μmoles. Therefore, the microgels in the aggregates are capable of removing significantly more Orange II/g than the unaggregated microgels.

$$C_{i,s} = C_{i,smax} * K_{ads} * C_{i,mob}/(1 + K_{ads} * C_{i,mob}) \qquad (1)$$

$C_{i,s}$ is the concentration of Orange II in aggregates (sorbent)

$C_{i,mob}$ is the concentration of Orange II in mobile phase (in buffer after centrifugation)

K_{ads} is the Langmuir coefficient

Previously, pNIPAm based gels were used for adsorption of naphthalene disulfonic acid (NS-2). The authors report the loading of NS-2 on the microgels to follow the Langmuir isotherm model, reporting R^2 values of ~ 0.97 and a maximum uptake of 13 mmoles/L of gel (3.747g NS-2/L of gel).[364] Assuming the density of the solution to be 1.000 g/mL, the maximum loading capacity would be 0.0037 g NS-2/g of gel. In comparison, it is evident that the microgel aggregates reported in this submission achieved higher uptake efficiencies and follow Langmuir sorption isotherm more accurately.
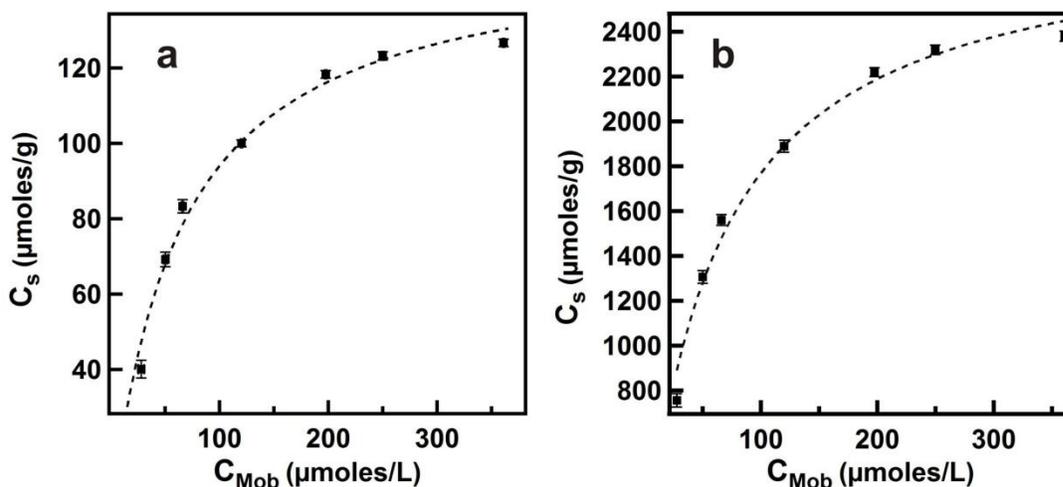
Figure 4-11. Langmuir sorption isotherms for (a) the removal of Orange II by the aggregates and (b) by the microgels alone after correcting for the mass of BIS in the aggregates. C_{mob} is the concentration of the dye remaining in the aqueous phase and C_s is the concentration of Orange II sorbed on the aggregates/microgels. Each point on the plot represents an average of three replicate experiments and the error bars denote the standard deviation.

4.4. Conclusion

We report a system composed of pNIPAm microgel aggregates that are capable of removing a maximum of 73.1% of Orange II from water at elevated temperature. The results indicate that the Orange II uptake efficiency can be enhanced by increasing the BIS concentration from 100 to 500 mg, with minimal enhancement if the concentration of BIS is increased further. The results suggest that both the nature of the aggregate (hydrophobicity) and the aggregate number are important factors that affect uptake efficiency. Also, by exploiting the thermoresponsive nature of these aggregates and by increasing the number of heating/cooling cycles the removal efficiency can be enhanced. The overall retention efficiencies of the aggregates were determined by performing leaking studies, in which we determined that a maximum of 24.4% of the dye that was originally removed leaked out after an incubation time of 80 minutes, but there was minimal additional leaking after 50 minutes. The results for removal

efficiencies as a function of the concentration of dye were fit with the Langmuir model and we evaluated the maximum sorption of Orange II on the aggregates to be 0.054 g Orange II/g aggregates with a Langmuir coefficient of 0.015960 ± 0.00182 L/μmoles. When considering just the mass of the microgels, the Langmuir fit yielded a maximum value of Orange II sorbed of 2871 μmoles/g (1.006 g Orange II/g of microgels). The Langmuir coefficient in this case was calculated as 0.016035 ± 0.0018 L/μmoles.

POLY (*N*-ISOPROPYLACRYLAMIDE) MICROGEL BASED ASSEMBLIES FOR

ORGANIC DYE REMOVAL FROM WATER: MICROGEL DIAMETER EFFECTS

5.1. Introduction [3]

In Chapters 3 and 4, the ability of pNIPAm based microgels and their aggregates to remove the Orange II from aqueous solutions were assessed. It was observed that the aggregated microgels removed significantly more dye from aqueous solutions than unaggregated microgels. It was concluded that the structure or "nature" of the aggregated microgels was responsible for the enhanced uptake. This Chapter discusses the effect of the size of the microgel in the aggregate on the removal efficiency. It was observed that a maximum removal of 85.3% was achieved from the aggregates with microgels of larger diameter at elevated temperature (50 °C). This enhancement could be attributed to the size of the microgels in the aggregates leading to formation of bigger aggregates. Aggregates of larger dimensions would in turn lead to more interstitial volume for the dye to be taken into leading to more uptake of the dye. Overall, this Chapter gives a better understanding of how the properties of the aggregates impact on the removal efficiencies.

5.2. Materials and Methods

Materials. *N*-isopropylacrylamide (monomer) was purchased from TCI (Portland, Oregon) and purified by recrystallization from hexanes (ACS reagent grade, EMD, Gibbstown, NJ). *N,N'*-methylenebisacrylamide (BIS) (~99%), acrylic acid (AAc) (~99%), and ammonium persulphate (APS) (~98%) were obtained from Sigma-Aldrich (Oakville, Ontario) and were used

---

[3] This dissertation has been adapted from references 361, 362 and 363.

as received. Orange II was obtained from Eastman Organic Chemicals (Rochester, NY). All the phosphate salts used for preparing buffer solutions of pH 7 (ionic strength of 0.235 M) were obtained from EMD and were used as received. Deionized (DI) water with a resistivity of 18.2 MΩ·cm was obtained from a Milli-Q Plus system from Millipore (Billerica, MA), and filtered through a 0.2 μm filter, prior to use. Microgel samples were lyophilized using a VirTis benchtop K-manifold freeze dryer (Stone Ridge, NY).

Synthesis of pNIPAm-*co*-AAc-1 microgels (D_H ~321 nm). These were prepared using a previously used protocol.[258] The overall monomer concentration was 65.2 mM (13.05 mmol), and 85% *N*-Isopropylacrylamide (NIPAm, 11.1 mmol), BIS (0.652 mmol), and sodium dodecyl sulphate (SDS, 0.2 mmol) were added to 190 mL deionized water, previously filtered through a 0.2 μm filter. This was then transferred into a 3-neck round bottom flask that was fitted with a reflux condenser, nitrogen inlet, and a thermometer. The solution was purged with N_2 and allowed to heat to 70 °C for ~1 hour. To this 10% AAc (1.30 mmol) was added to the reaction mixture in one aliquot immediately prior to initiation. 0.3 mmol of APS in 10 mL of DI water was added to the monomer solution for initiation. The reaction was allowed to proceed at 70 °C for 4 hours under a nitrogen atmosphere. The resulting suspension was allowed to cool overnight, and then it was filtered through a type 1 Whatman filter paper to remove any large aggregates. Approximately half of the microgel solution was then distributed into rehydrated dialysis tubing (12-14k nominal MWCO, 25 mm flat width, Fisherbrand Regenerated Cellulose, Nepan, ON) for purification. The tubes were placed into two 2 L beakers with deionized water and a stir bar for two weeks and the water was replaced twice daily. Dialysis was used to remove unreacted monomers and crosslinker, and small molecular weight linear polymers, from the microgels. The hydrodynamic diameter (D_H) of these microgels was determined by dynamic

light scattering studies using a ALV/CGS-3 Compact Goniometer System (Hesse, Germany). In brief, a dilute solution of microgels in DI water, maintained at ~23 °C, was irradiated by a 22 mW HeNe laser, and scattered light collected. . Data was analyzed using ALV-5000/EPP correlator software, from which the hydrodynamic diameter was determined. Three sets of samples were analyzed using this protocol and an average D_H of 321 nm ± 8.83 nm was obtained.

Synthesis of pNIPAm-*co*-AAc-2 microgels (~ 1.1 µm). These microgels were prepared by a surfactant free, free radical precipitation polymerization as reported before.[293] These microgels were used even in the previous Chapter. The total monomer concentration was maintained to be 140 mM. Of this, 85% was *N*-isopropylacrylamide (NIPAm), 5% was *N,N'*-methylenebisacrylamide (BIS) crosslinker and 10% was acrylic acid (AAc) . To a clean beaker, NIPAm (11.9 mmol) and the crosslinker, BIS (0.700 mmol), were added and dissolved in deionized water (75 mL) in a beaker with stirring. A 20 mL syringe affixed with a 0.2 µm filter was used to filter the mixture into a clean 250 mL, 3-neck round bottom flask fitted with a condenser, thermometer, stir bar and a N_2 inlet. The beaker was rinsed with 24 mL of deionized water, which was again filtered and transferred to the mixture in the round bottom flask. The temperature was set to 65°C with N_2 bubbling through the solution for ~ 1 h, after which AAc (1.4 mmol) was added to the mixture and stirred for a few minutes. To this, 0.197 mmol APS in 1 mL DI water was added. The mixture was allowed to stir for 4 h, under N_2 atmosphere. The solution was allowed to cool, while stirring overnight.

Following stirring overnight, the microgels were filtered through a type 1 Whatman filter paper, which was then rinsed with deionized water. The microgels were then cleaned via centrifugation to remove unreacted monomer and crosslinker, as well as linear polymer from the microgels. To

do this, the microgel solution was separated into 15 mL centrifuge tubes obtained from Corning Incorporated (Corning, NY) (~ 12 mL microgel solution/tube) and centrifuged at a speed of ~8400 relative centrifugal force (rcf) in a Baxter, biofuge 17R (Mount Holly, NJ) at 23 °C, for 30 min. Centrifugation yielded a pellet of microgels at the bottom of the centrifuge tube, and the supernatant was removed. ~12 mL of fresh DI water was added and the microgel pellet was redispersed using a Fisher Vortex, Genie 2 vortexer (Pittsburgh, PA). This cleaning protocol was repeated six times. The D_H of these microgels was determined by dynamic light scattering to be 1.10 μm ±14.5 nm, as mentioned in previous Chapter.

Synthesis of pNIPAm-*co*-AAc-3 microgels (Diameter ~1.43 μm). These were synthesized following a previously published procedure. [330] The total monomer concentration was 153.8 mM (20 mmol) and 85% *N*-Isopropylacrylamide (NIPAm, 17.0 mmol), 5% *N, N'*-methylenebisacrylamide (BIS, 1.00 mmol) were added to 100 mL of deionized water in a small beaker and stirred. Once dissolved, the solution was filtered through a 0.2 μm filter into a 3-neck round bottom flask. The beaker was rinsed with 25 mL of deionized water and filtered into the flask. The flask was fit with a condenser, a nitrogen inlet, and a temperature probe to provide heating via a feedback-loop controlled hotplate (Torrey Pines Scientific, Carlsbad, CA). The flask was heated in an oil bath to 45 °C while the solution was allowed to stir and purge with N_2 gas for ~1.5 hours. Once the solution reached the set temperature, acrylic acid (AAc, 2.00 mmol, 10% of overall monomer concentration) was added followed by initiation of the reaction by addition of 0.078 M aqueous solution of ammonium persulphate in 5 mL DI water (overall solution volume resulted in 130 mL). After initiation, the reaction solution was then heated at a rate of 30 °C/hour to 65 °C and the reaction was allowed to proceed overnight under nitrogen atmosphere. The resulting suspension was allowed to cool to room temperature, followed by

filtration through a plug of glass wool to remove any coagulum formed during the reaction. The microgels were then cleaned via the same protocol as mentioned in the previous section. To determine the diameter of these microgels, an Olympus IX71 inverted microscope (Markham, Ontario) fitted with a 100 X oil immersion objective, differential interference contrast (DIC) optics and an Andor Technology iXon+ camera (Belfast, Ireland) was used. One drop of a very dilute solution (~100 X dilution) of the cleaned microgels was placed on a microscope cover slip (25 mm x 25 mm, Fischer Scientific, Ottawa) and a number of photographs were obtained at random areas. The photographs were then analyzed using Andor Solis imaging software, to determine microgel diameter. The length scale was determined by photographing a micrometer scale of 50 divisions, each 2 μm in length (Edmund Optics, NJ), at the same magnification that the microgels were photographed at. The apparent diameters of 20 different microgels were measured, and an average diameter of 1.43 μm ± 5.35 nm was determined.

Synthesis of microgel aggregates. Microgel aggregates were synthesized using three different concentrations of BIS- 100 mg (2 mg BIS/mL of total reaction solution), 500 mg (10 mg BIS/mL of total reaction solution) and 750 mg (15 mg BIS/mL of total reaction solution). The aggregates with 100 mg BIS were prepared by directly adding 10 mL of cleaned microgels from the above syntheses to a filtered solution (filtered through 0.2 μm filter affixed to a 20 mL syringe) of 100 mg of BIS in 39 mL of deionized water, to a beaker and stirred. This solution was transferred into a 250 mL 3-necked round bottom flask that was fit with a condenser, thermometer, stir bar and a N_2 inlet. The temperature was set to 65°C and N_2 was bubbled through the solution for ~ 1 h. After 1 h, a 1 mL aqueous solution containing 0.0175 mmol of APS was added to this mixture and left to stir for 4 h, under N_2 atmosphere. The solution was allowed to cool with stirring overnight. This procedure was followed for the synthesis of the 10

mg/mL, and 15 mg/mL BIS aggregate samples, by adding 500 mg and 750 mg BIS to the reaction mixture, respectively. All microgel aggregates were cleaned using the same centrifugation procedure followed for cleaning microgels, but without filtering. Representative DIC microscopy images of "small" "medium" and "big" microgel aggregates with 500 mg BIS are shown in Figure 5-1.
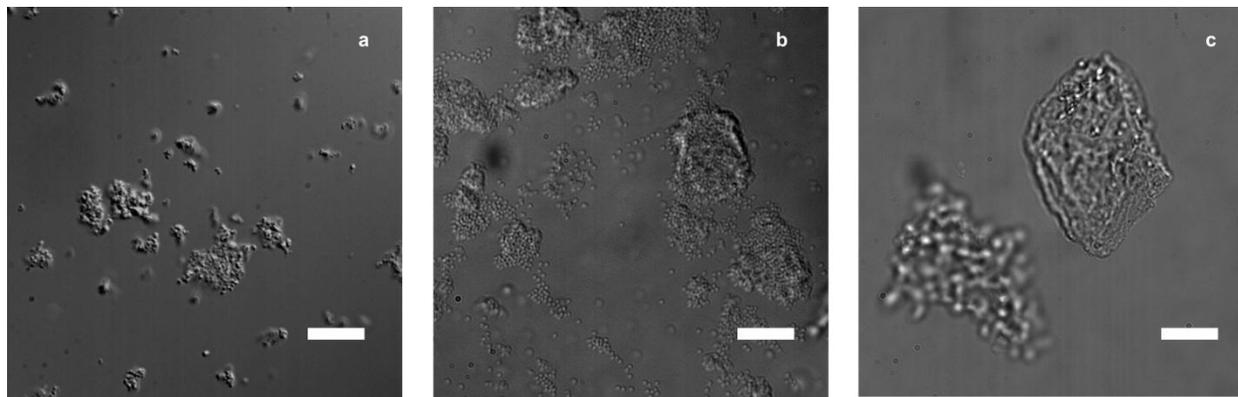
Figure 5-1. DIC microscopy images of 500 mg BIS aggregates of (a) pNIPAm-*co*-AAc-1 (b) pNIPAm-*co*-AAc-2 and (c) pNIPAm-*co*-AAc-3 microgels. The scale bar used in all the panels is 5 μm.

Orange II uptake. All aggregates were lyophilized and stock solutions were made from each sample to contain of 5.2 mg aggregates/mL solution. This was done by redispersing 52.1 mg of each in 10 mL of pH 7 buffer solution of 0.235 M ionic strength in a volumetric flask. A stock solution of Orange II (0.023 M) in deionized water was prepared. Using a micropipette, 300 μL of the aggregate solution and 15 μL of Orange II were transferred into a 15 mL centrifuge tube (Corning Incorporated (Corning, NY)). A buffer solution of pH 7 (ionic strength 0.235 M) was used to bring the volume of the solution up to 3 mL yielding 114 μM Orange II and final concentration of aggregates to be 521 μg aggregates/ml of the reaction solution. This sequence of adding buffer after exposing the dye to the aggregates was maintained for all the

experiments. After five minutes of exposure, this solution was centrifuged for 30 minutes, at ~8400 rcf. This centrifugation time was used to ensure that all the dispersed aggregates were removed from solution (as confirmed from differential interference contrast microscopy, data not shown). The supernatant was carefully removed from the tube without disturbing the pellet of aggregates at the bottom of the tube and transferred to a quartz cuvette. The absorbance was measured using a HP8452A UV-Vis spectrophotometer with a diode array detector (previously Agilent Technologies, Inc., Santa Clara, CA). The initial concentration of Orange II for all the uptake studies was maintained at 114 μM and before very experiment, the initial absorbance of Orange II was measured in the absence of the aggregates. Also, it was observed that centrifuge tube did not have any effect on the initial absorbance of Orange II, as a function of time the solution stayed in the tube.

To study the uptake of Orange II as a function of temperature, the solution of Orange II and aggregates was held at 50 ˚C (microgels deswell), for different intervals of time and then cooled down to room temperature (microgels reswell). The solutions were then centrifuged, and the supernatant was then analyzed by UV-Vis to evaluate the percent uptake of the dye.

Orange II leaking studies:

To evaluate and compare the ability of the aggregates to retain Orange II, 900 μL of microgel aggregates were exposed to 114 μM Orange II in a total volume of 9 mL using the same buffer that was used for the uptake studies. The concentrations and volumes were scaled up three times in order to get a detectable absorbance signal from the solutions after leaking. The aggregates were exposed to the dye for five minutes and centrifuged for 30 minutes. The supernatant solution was then carefully removed without disturbing the aggregates packed at the bottom. To this tube, 9.0 mL of fresh buffer solution (the same buffer that was used for the uptake studies)

was added and the aggregates were redispersed by vortexing. This solution was immediately divided into nine, one mL samples in 1.5 mL Eppendorf tubes obtained from Fisher Scientific, (Ottawa, ON) and the solutions were allowed to incubate for various intervals of time. For example, immediately following splitting up the original solution, one tube was centrifuged for 30 min and the supernatant solution removed and UV-Vis performed on the supernatant solution, this was considered t = 0. Other tubes were incubated for 10, 20, 30, 40, 50, 60, 70 and 80 minutes respectively, before each was centrifuged.

Counting of aggregates Solutions containing 41.6 µg aggregates/mL of the respective aggregates (microgels of all diameters containing 100 mg, 500 mg and 750 mg BIS) were prepared. These solutions were prepared from the same stock solution as above. A drop of each solution was placed on a microscope cover slip (25 mm x 25 mm, Fischer Scientific, Ottawa) and pictures of 10 random areas of the sample were obtained using a Olympus IX71 inverted microscope (Markham, Ontario) fitted with a 100 X oil immersion objective, differential interference contrast (DIC) optics and an Andor Technology iXon+ camera (Belfast, Ireland). There were different sizes of aggregates in these samples that were designated as "big", "medium" and "small". When making the designation of size (detailed in Tables SI1, SI2 and SI3) we measured the apparent diameter of the aggregates in approximately two orthogonal directions. A micrometer scale of 50 divisions, each 2 µm in length (Edmund Optics, NJ) was used to calibrate the microscope, and subsequently used to measure the sizes of these aggregates.

5.3. Results and Discussion

In Chapter 3, we illustrated that pNIPAm based microgels are useful for removing the organic dye molecule Orange II from aqueous solutions. We went on to show that aggregates of

microgels were capable of removing significantly more Orange II from solution than the same mass of unaggregated microgels. We concluded that it was the structure or nature of the aggregated microgels that resulted in the enhanced uptake. Here, we investigate how the uptake depends on the diameter of the microgels that make up the aggregate.

`   ***Effect of BIS concentration on removal efficiency.*** Initially, the effect of varying concentrations of BIS in the various aggregates was investigated. Microgel aggregates were prepared using 100 mg BIS, 500 mg BIS and 750 mg BIS. To conduct this experiment, the initial absorbance of 3 mL of a 114 μM Orange II solution in the absence of microgel aggregates was recorded. This was compared to the absorbance of the supernatant solution after addition of 100, 200, 300 and 400 μL (final concentrations of 173, 347, 521 and 693 μg aggregates/mL of the reaction solution) of the standard aggregate solutions at all BIS concentrations, for all microgel diameters. For all experiments, the initial concentration of Orange II was 114 μM and the total volume of solution was held constant at 3 mL from run to run. A calibration curve (used in previous Chapters) was used to calculate the number of moles of Orange II in solution before and after addition of aggregates. Figure 5-2 shows the uptake data for the 100 mg, 500 mg and 750 mg BIS aggregates made from all sets of microgels. It is evident that for a given microgel diameter, the maximum removal efficiency increases with increasing BIS concentration. For example, at room temperature, the removal efficiency for the pNIPAm-*co*-AAc-1 based aggregates increased from 30.4% to 40.1% as the BIS concentration increased from 100 to 500 mg. A similar trend was observed for the pNIPAm-*co*-AAc-3 microgel aggregates, where the uptake increased from 49.1% to 53.0% when the concentrations of BIS increased from 100 mg to 500 mg, at room temperature. In previous Chapter we reported a similar trend for the pNIPAm-*co*-AAc-2 microgel aggregates , where the removal efficiency increased from 40.8% to 44.1%

when the concentrations of BIS increased from 100 to 500 mg. It should be noted that for all the sets of aggregates there was only a minimal increase in the uptake percent as the concentration of BIS was increased to 750 mg , therefore we did not increase the BIS concentration further.
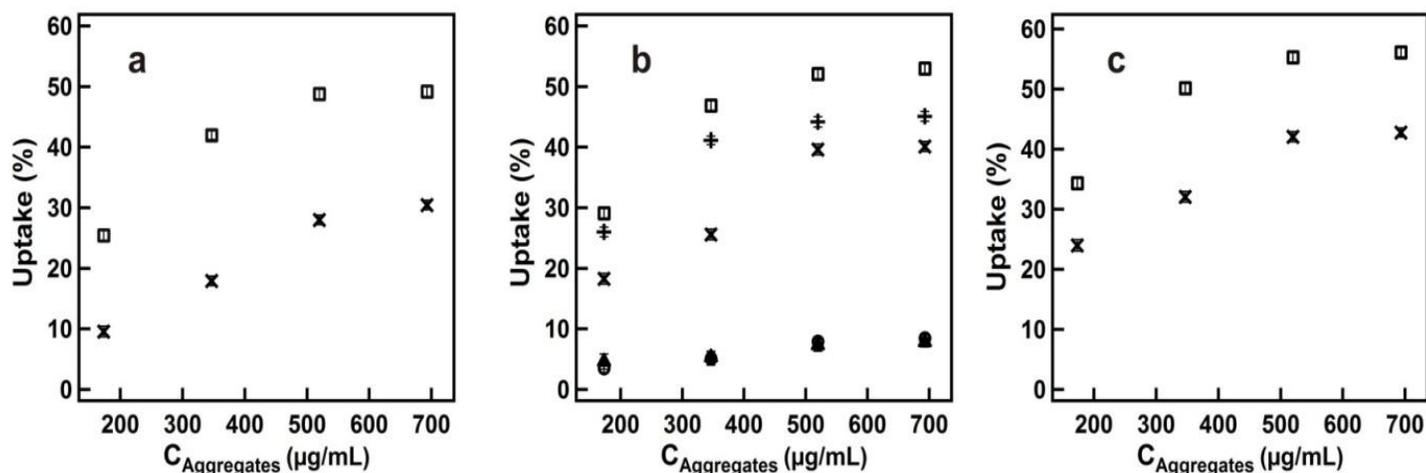
Figure 5-2. Uptake of Orange II as a function of the concentration of aggregates (a) 100 mg BIS aggregates; (b) 500 mg BIS aggregates and ; (c) 750 mg BIS aggregates using (**x**) pNIPAm-*co*-AAc-1 microgels, and (□) pNIPAm-*co*-AAc-3 microgels. Panel (b), shows results for (+) pNIPAm-*co*-AAc-2 microgels.[2] Panel (b) also contains the control experiment results; aggregating BIS, then adding the microgels, from (▲) pNIPAm-*co*-AAc-3 microgels and (■) pNIPAm-*co*-AAc-1 microgels. Each point on the plot represents an average of three replicate experiments of uptake studies and the error bars denote the standard deviation.

We hypothesize that the trend of increased uptake efficiency with increasing concentration of BIS in the aggregates could be due to: 1) an increase in the number or size of aggregates in solution; and/or 2) a change in the hydrophobicity of the aggregates with BIS concentration used to form the aggregates. Similar to our previous Chapter, an aggregate counting experiment was performed to explain the observed trend of higher removal efficiencies for higher concentrations of BIS in the aggregates.   In short, solutions containing 41.6 µg aggregates/mL solution of the 100 mg, 500 mg and 750 mg BIS aggregates, for all the various

microgel diameters, were prepared and the number and size of the aggregates in the given volume were determined (Tables 5-1, 5-2 and 5-3). We observed that for the pNIPAm-*co*AAc-1 aggregates, the aggregate number increased from 33 ± 8 to 49 ± 10 as the amount of BIS increased from 100 mg to 750 mg. For this same change in BIS concentration, the number of pNIPAm-*co*-AAc-2 microgel aggregates increased from 52 ± 10 to 76 ± 15, while the numbers increased from 67 ± 10 to 92 ± 14 for the pNIPAm-*co*-AAc-3 microgel aggregates. From these results, it is evident that the aggregate number increased with BIS concentration for a given microgel diameter. It can also be observed that pNIPAm-*co*-AAc-3 microgel aggregates have the highest overall aggregates number (92 ± 14) compared to 49 ± 10 for the pNIPAm-*co*-AAc-1 microgel aggregates. Furthermore, the pNIPAm-*co*-AAc-3 microgel aggregates were significantly larger than aggregates generated from the smaller diameter microgels.

Table 5-1. Number distribution for different sizes of aggregates with pNIPAm-*co*-AAc-3 in 100 mg, 500 mg and 750 mg (2mg/mL, 10mg/mL and 15mg/mL) BIS concentrations.

Aggregate Size	Number in100 mg BIS	Number in 500 mg BIS	Number in 750 mg BIS
Big	12 ± 5	20 ± 8	23 ± 4
Medium	21 ± 6	19 ± 4	24 ± 7
Small	34 ± 7	43 ± 9	45 ± 11
All sizes	67 ± 10	82 ± 13	92 ± 14

Small aggregates: ≥ 2.3 μm×3.0 μm < 9.3 μm x 8.2 μm; Medium aggregates: ≥ 9.3 μm x 8.2 μm < 14.0 μm×16.5 μm; and Large aggregates: ≥ 14.0 μm×16.5 μm. Any aggregate < 2.3 μm×3.0 μm for pNIPAm-*co*-AAc-1 was not counted.

Table 5-2. Number distribution for different sizes of aggregates with pNIPAm-*co*-AAc-2 microgels in 100 mg, 500 mg and 750 mg (2mg/mL, 10mg/mL and 15mg/mL) BIS concentrations.

Aggregate Size	Number in100 mg BIS	Number in 500 mg BIS	Number in 750 mg BIS
Big	8 ± 4	15 ± 5	19 ± 3
Medium	14 ± 7	17 ± 3	16 ± 9
Small	30 ± 6	34 ± 8	41 ± 12
All sizes	52 ± 10	66 ± 10	76 ± 15

Small aggregates: ≥ 0.6 μm×1.5 μm < 5.7 μm x 4.5 μm; Medium aggregates: ≥ 5.7 μm x 4.5 μm < 10.3 μm×11.5 μm; and Large aggregates: ≥ 10.3 μm×11.5 μm. Any aggregate < 0.6 μm×1.5 μm was not counted.

Table 5-3: Number distribution for different sizes of aggregates with pNIPAm-*co*-AAc-1 in 100 mg, 500 mg and 750 mg (2mg/mL, 10mg/mL and 15mg/mL) BIS concentrations.

Aggregate Size	Number in100 mg BIS	Number in 500 mg BIS	Number in 750 mg BIS
Big	4 ± 2	9 ± 3	12 ± 2
Medium	11 ± 3	8 ± 4	10 ± 5
Small	18 ± 7	21 ± 5	27 ± 8
All sizes	33 ± 8	66 ± 7	49 ± 10

Small aggregates: ≥ 0.9 μm×1.3 μm < 4.1 μm x 3.4 μm; Medium aggregates: ≥ 4.1 μm x 3.4 μm < 8.7 μm×10.1 μm; and Large aggregates: ≥ 8.7 μm×10.1 μm. Any aggregate < 0.9 μm×1.3 μm was not counted.

To understand what factor is most important to affect removal efficiency -- aggregate size or number -- we look to the high aggregate concentration regime in Figure 5-2 (a, b, c). In this

regime, aggregate concentration (i.e., aggregate number) has no impact on uptake efficiency, therefore the differences in uptake efficiency must be due to the nature of the aggregates. In this region, for all BIS concentrations, the uptake efficiency increases with microgel diameter; it appears that aggregate size and/or aggregate hydrophobicity is the most important factor leading to enhanced uptake efficiency. However, since unaggregated "big" microgels remove more organic dye than a given mass of "small" unaggregated microgels, this can also be playing a role. In the lower concentration regime in each of the panels in Figure 5-2, there could be multiple reasons for the observed trend in the uptake efficiencies. These include either or all of the arguments above, which are:-an increase in aggregate number, and/or increase in the aggregate size, and/or hydrophobicity of the aggregates.

As a control, we aggregated 500 mg BIS alone in 40 mL DI water using the protocol mentioned in the Experimental, but in the absence of microgels. After the aggregation of BIS, either 10 mL of pNIPAm-*co*-AAc- 1 or pNIPAm-*co*-AAc- 3 microgels were added to the mixture; this solution has the same amount of BIS and microgels as the standard aggregated sample. Uptake studies were performed by monitoring the removal efficiency as a function of the aggregate concentration from these syntheses. The data in Figure 5-2 (b) shows that the control aggregates from the pNIPAm-*co*-AAc- 1 and 3 removed only 7.8% and 8.5% of the dye from the solution, respectively, as opposed to 40.1% and 53.0% from their aggregated microgel counterparts, at room temperature. This reveals that it is important to have microgels in their aggregated form to result in enhanced removal efficiency, i.e., the presence of aggregated BIS does not lead to enhanced uptake.

   Effect of particle size in the aggregates on the removal efficiency. In our previous Chapters we evaluated the ability of microgels and microgel aggregates to remove Orange II

from water as a function of their concentrations. We reported a maximum uptake of 29.5% for the microgels of ~1.1 μm at room temperature, which increased to 45.1% upon aggregation of these microgels with 500 mg BIS. Here, we investigate the effect of microgel diameter in the aggregates on the removal efficiency. Figure 5-2 (b) shows the percent uptake as a function of concentration of the aggregates with pNIPAm-*co*-AAc-1, pNIPAm-*co*-AAc-2 (data from our previous Chapter) and pNIPAm-*co*-AAc-3 microgels. The figure reveals the maximum removal efficiencies to be a function of the diameter of the microgels used to synthesize the aggregates; a maximum of 40.1% uptake was achieved for pNIPAm-*co*-AAc-1, 45.1% was achieved for pNIPAm-*co*-AAc-2, while 53.0% uptake was achieved for pNIPAm-*co*-AAc-3. From aggregate counting/sizing experiments it was evident that the dimensions of the 500 mg BIS, pNIPAm-*co*-AAc-3 microgel aggregates were much larger than those of pNIPAm-*co*-AAc-1 microgel aggregates. A similar trend of increased uptake efficiency with microgel diameter in the aggregates was also observed at the different BIS concentrations, Figure 5-2 (a, c). This trend is observed at all aggregate concentrations, most importantly, in the high concentration regime. Since, for a given BIS concentration, the big microgel aggregates are larger than the small microgel aggregates, we attribute the enhanced uptake to the size of the aggregate. Larger aggregates have more volume, and therefore more free volume between the aggregated microgels, which can act to remove more dye from the aqueous solution. We hypothesize that the size of microgels within the aggregates affects the size of the aggregates that are formed. In other words, the big particles form bigger aggregates, which in turn achieve higher removal efficiencies. We also studied the uptake efficiency of the unaggregated microgels (with the exception of the pNIPAm-*co*-AAc-1 sample, which were too small to centrifuge) and observed the unaggregated pNIPAm-*co*-AAc-3 microgels to remove 38.0% of Orange II, as opposed to

29.5% for the pNIPAm-*co*-AAc-2 the microgels (Figure 5-3). This fact can also lead to the enhanced uptake for the pNIPAm-*co*-AAc-3 microgel aggregates in the high concentration regime.
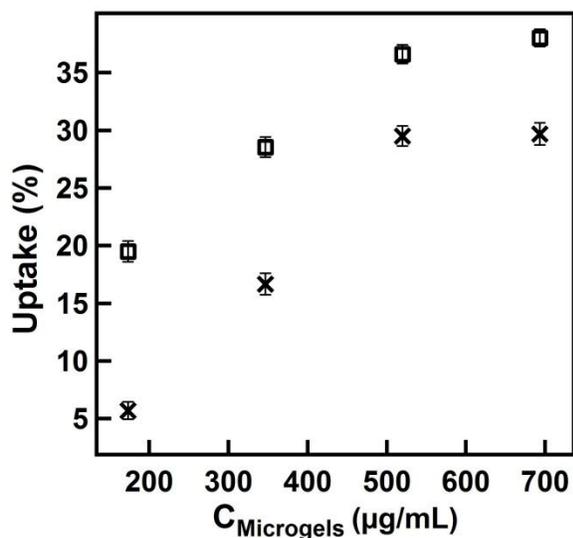
Figure 5-3. Removal of Orange II as a fuction of concentration of (□) unaggregated pNIPAm-*co*-AAc-3microgels and concentration of (**x**) unaggregated pNIPAm-co-AAc-2 microgels from from previous Chapter. Each point on the plot represents an average of three replicate experiments and the error bars denote the standard deviation

It should be pointed out here that even though the unaggregated microgels have more active component (microgels) than the same mass of aggregated microgels, they still remove significantly less Orange II compared to the aggregates. For example, unaggregated pNIPAm-co-AAc-3 microgels remove 38.0% of dye from water compared to 53.0% removal efficiency for the same mass of aggregated pNIPAm-co-AAc-3 microgels. To account for this lack of active component in the aggregates, we adjusted the mass of the aggregates, such that they had the same number of microgels as the unaggregated samples. Figure 5-4 shows that a maximum of 72.8% removal efficiency was achieved at room temperature for the 500 mg BIS pNIPAm-*co*-AAc-3 microgel aggregates.
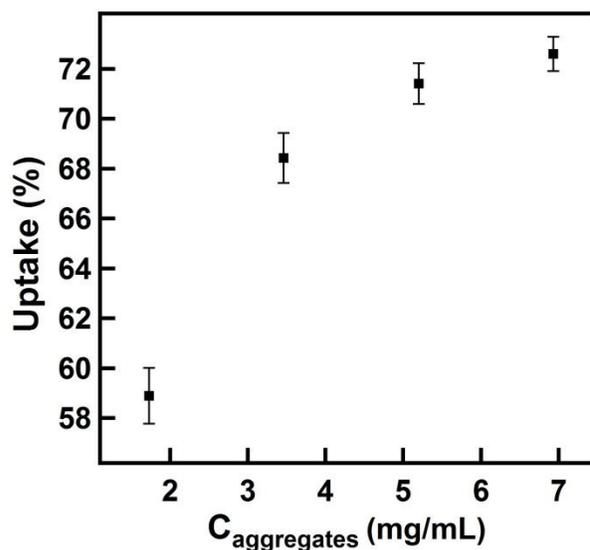
Figure 5-4. The uptake of Orange II as a function of concentration of 500 mg BIS aggregates with pNIPAm-*co*-AAc-1 in a very high aggregate concetration regime. These concentrations were necessary to achieve the same microgels number as the unaggregated microgel case. Each point on the plot represents an average of three replicate experiments and the error bars denote the standard deviation.

Effect of temperature cycle on removal efficiency. To monitor the effect of single temperature cycle, we added 300 μL of the 500 mg BIS aggregates composed of pNIPAm-*co*-AAc-1 and 3 microgels to 15 μl of Orange II in pH 7 (0.235M ionic strength) in a 3 mL total volume. The solution was heated above 32 ˚C for different intervals of time and cooled down to room temperature. Specifically, we exposed the microgel aggregates to the dye solution for five minutes and heated to 50 ˚C for 20, 40, 60, 90 and 120 minutes, the solution was then cooled down to room temperature (~23 ˚C) for 30 minutes and centrifuged immediately. Figure 5-5(a) shows how the percent uptake depends on heating time for the pNIPAm-*co*-AAc-1 and 3

microgels aggregates. The percent uptake at time 0 corresponds to the uptake of the microgel aggregates at room temperature (39.6% and 52.1% for pNIPAm-*co*-AAc-1 and 3 microgel aggregates). It was observed that the uptake of the dye increased significantly from 44.1% to 61.4% and 69.8% to 83.7% for the pNIPAm-*co*-AAc-1 and 3 microgel aggregates, respectively, as the heating time increased from 20 minutes to 60 minutes. Also, there was minimal increase in the uptake when the solution was heated for 90 minutes (~63.1% and 84.6% for the "small" and "big" microgel aggregates respectively). The dye removal by the pNIPAm-*co*-AAc-3 microgel aggregates was very significant (maximum of ~85%) as can be seen visually in Figure 5-6; the solution color for the heated sample is significantly reduced compared to the solution of Orange II in the absence of aggregates, at room temperature. A control experiment as mentioned in previous Chapters confirmed that high temperature alone did not affect the absorbance of Orange II Hence the reduction in Orange II intensity was due to increased uptake due to the aggregate's thermoresponsive nature.
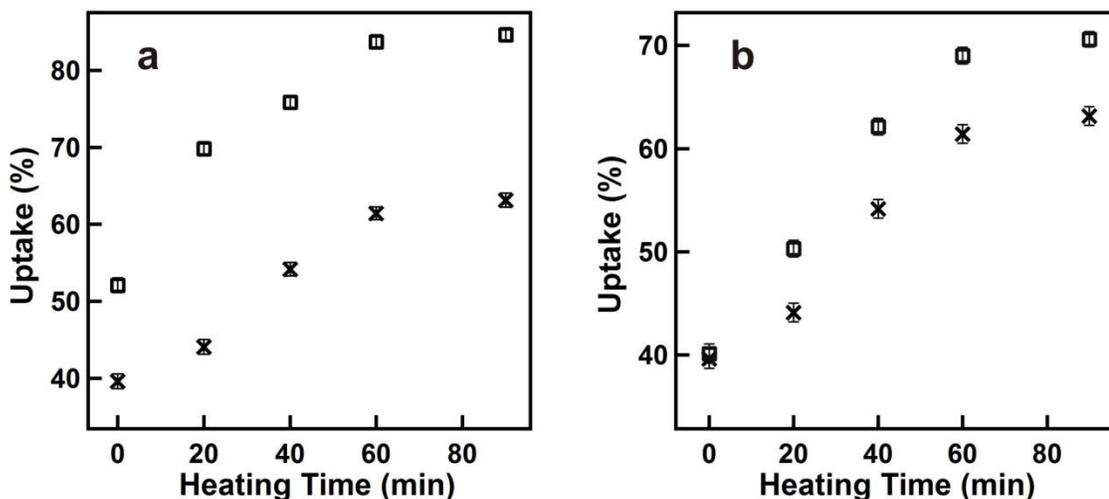
Figure 5-5. (a) Uptake of Orange II as a function of the time the microgels were held at elevated temperature for a single hot cycle (**x**) pNIPAm-*co*-AAc-1 aggregates and (□) pNIPAm-*co*-AAc-3 aggregates. Panel (b), uptake for pNIPAm-*co*-AAc-1 microgel aggregates after (**x**) a single hot cycle and (□) two hot cycles. Each point on the plot represents an average of three replicate experiments of uptake studies and the error bars denote the standard deviation.
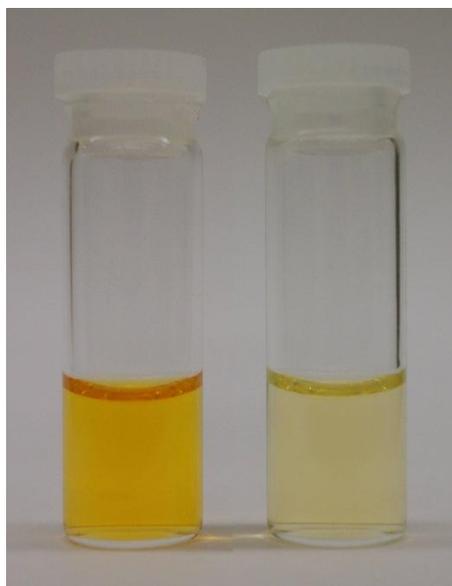
Figure 5-6. Solutions of 114 µM Orange II (left) before and (right) after the addition of 693 µg/mL 500 mg BIS, pNIPAm-*co*-AAc-1 aggregates. Here, single cycle heating cycle was performed for a period of 90 minutes (hot time).

The effect of multiple heating and cooling cycles on the percent uptake of the dye was also investigated. This was done by exposing the 500 mg BIS pNIPAm-*co*-AAc-1 and 3 microgel aggregates (aggregate concentration of 521 µg/mL of reaction solution) to 15 µL Orange II in the pH 7.0 buffer solution used above. This solution was heated to 50 ˚C and cooled down to room temperature in two cycles, keeping the overall heating and cooling time the same as with the single heating cycle. For example, the solution of aggregates was exposed to the dye and heated to 50 ˚C for 10 minutes and cooled down to room temperature for 15 minutes and heated again to 50 ˚C for another 10 minutes and finally cooled for 15 minutes. So overall the microgels were heated for 20 minutes and cooled for 30 minutes, but over two cycles. This protocol was repeated for all 40, 60, 90 and 120 minutes heating periods. Figure 5-5(b) shows that the maximum percent uptake observed for the aggregates of pNIPAm-*co*-AAc-1 microgels increased to 70.6%, compared to the single heating cycle where the maximum uptake observed was 63.1%. But there

was minimal increase for the pNIPAm-*co*-AAc-3 microgel aggregates for an additional hot cycle; the maximum uptake achieved was 85.3% compared to 83.7% uptake for the single heating cycle (Figure 5-7). The overall percent uptake of the dye by the pNIPAm-*co*-AAc-3 microgel aggregates was ~ 10% higher than similarly treated "medium" microgel aggregates, that yielded a maximum of 73.1% at elevated temperature. We also investigated the effect of cycling between high and room temperature three times for the aggregates of pNIPAm-*co*-AAc-1 microgels. There was no further improvement in the removal efficiency.
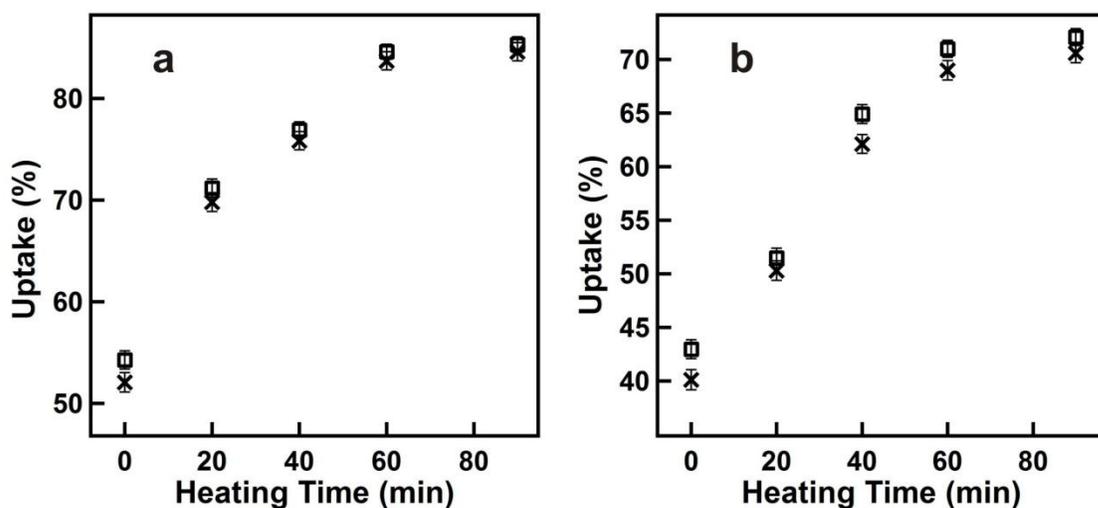
Figure 5-7: Uptake of Orange II as a function of heating and cooling cycles. The uptake of the dye for (a) aggregates with pNIPAm-*co*-AAc-3 for (**x**) single and two (□) cycles and (b) for aggregates with pNIPAm-*co*-AAc-1 for (**x**) two and (□) three cycles. Each point on the plots represent an average of three replicate experiments of uptake studies and the error bars denote the standard deviation.

Leaking of Orange II from aggregates. In our previous Chapter we reported that pNIPAm-*co*-AAc-2 microgel aggregates retained 75.6% of the dye that was removed from the aqueous solution. We studied the ability of the pNIPAm-*co*-AAc-1 and 3 microgel aggregates to retain Orange II as well. This was done by exposing 900 μL of the microgel aggregates to 114

μM Orange II in a total volume of 9 mL pH 7 buffer. This solution was allowed to incubate for five minutes and immediately centrifuged, similar to the other uptake experiments at room temperature. The supernatant solution was removed and the microgel aggregates packed at the bottom of the tube were redispersed in 9 mL fresh buffer (same buffer as above) using a vortexer. This solution was equally divided into 9 Eppendorf tubes and incubated for different intervals of time from 0 to 80 minutes and centrifuged. The supernatant solution from each of these tubes was evaluated for the amount of Orange II present in them and the percent leak of Orange II was determined. As an example, the "10 min" sample was incubated for a period of ten minutes, which was then immediately centrifuged and the supernatant removed. The solution absorbance was then analyzed to evaluate the percent leak. The "0 min" sample was immediately centrifuged without incubation. The supernatant from these samples was evaluated for the number of moles of the dye present in it and compared with the number of moles of Orange II originally present in the aggregates. Figure 5-8 represents the percent leak of Orange II from the aggregates from both the microgels, as a function of leaking (incubation) time. The percent leak of the dye increased from 25.4% to 33.0% and 16.2% to 23.1% for the aggregates from pNIPAm-*co*-AAc-1 and 3 microgel aggregates, respectively, as the incubation time increased from 10 to 80 minutes. The Figure also shows a minimal increase in the percent leak of the dye after a period of 50 minutes. Overall, the maximum percent leak of the dye was calculated to be 33.0% (retention efficiency of 67.0%) and 23.1% (retention efficiency of 76.9%) for the pNIPAm-*co*-AAc-1 and 3 microgel aggregates, respectively. We also monitored if any more dye leaked out upon addition of fresh buffer. To do this, we added fresh buffer to each of these samples that underwent one leaking cycle. Each of these sample aggregates were redispersed in the buffer and incubated for 80 minutes, centrifuged, and the supernatant solution analyzed via

UV-Vis. We observed that there was no additional leaking from the aggregates. Additionally, we investigated the possibility of the microgels leaking Orange II at elevated temperature due to deswelling of aggregates above their LCST. To do this, we redispersed all the aggregate samples that underwent one leaking cycle in their supernatant solutions and incubated them for an additional 80 minutes on a hot plate at 50˚C and was immediately centrifuged for 30 minutes at 50˚C by regulating the thermostat on the centrifuge. The supernatant was analyzed by UV-Vis and no more dye leaked out from the aggregates of both microgels.
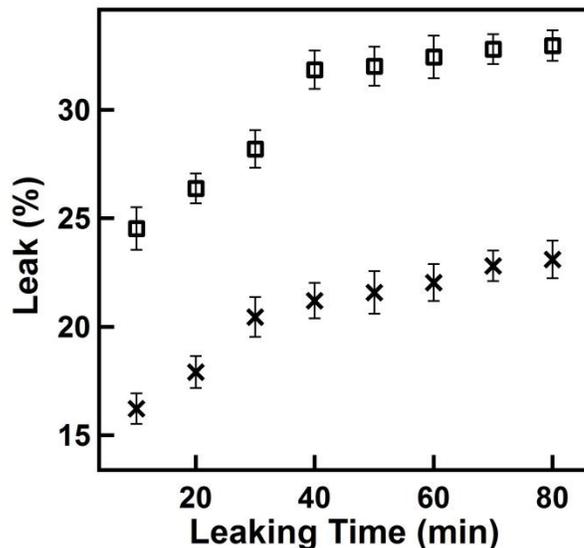
Figure 5-8. The percent leak of Orange II as a function of leak time for (□) pNIPAm-*co*-AAc-1 aggregates, and   (**x**) pNIPAm-*co*-AAc-3 aggregates. Each point on the plot represents an average of three replicate experiments of uptake studies and the error bars denote the standard deviation.

Langmuir sorption isotherm for the removal of Orange II. The removal efficiency for the pNIPAm-*co*-AAc 1 and 3 microgel aggregates as a function of the concentration of Orange II in solution was monitored. To do this, 5, 10, 15, 20, 25, 30 and 35 μL of Orange II solution was

added to 300 µL of the 500 mg BIS from both the aggregates were added. The total volume of this solution was made to be 3 mL using pH 7.0 buffer. This solution was incubated for five minutes similar to other uptake experiments. The solution was then centrifuged for 30 minutes and the supernatant was analyzed for the number of moles of the dye "sorbed" on the aggregates (as explained previously). A Langmuir isotherm model (Figures 5-9 (a) and 5-10 (a)) was used to fit the results from this experiment (equation 1), which gave a good fit with a R^2 of 0.9716 and 0.9934 for the aggregates from pNIPAm-*co*-AAc-1 and 3 microgels, respectively. A maximum sorption of 145.6 µmoles/g (0.051 g Orange II/g aggregates) was achieved from the aggregates from pNIPAm-*co*-AAc-1 microgels with a Langmuir coefficient of 0.0123 ± 0.00212 L/µmoles The aggregates from pNIPAm-*co*-AAc-3 microgels resulted in a maximum sorption of 171.3 µmoles/g (0.06 g Orange II/g aggregates), with a Langmuir coefficient of 0.03202 ± 0.00243 L/µmoles. Previously, for the aggregates from pNIPAm-*co*-AAc-2 microgels, we reported an R^2 of 0.9848 and a maximum sorption of Orange II of 152.8 µmoles/g (0.054 g Orange/ g aggregates). Upon comparison, it is evident that the aggregates from pNIPAm-*co*-AAc-3 resulted in a better fit using the Langmuir sorption and a better system for removal of Orange II/g aggregates.
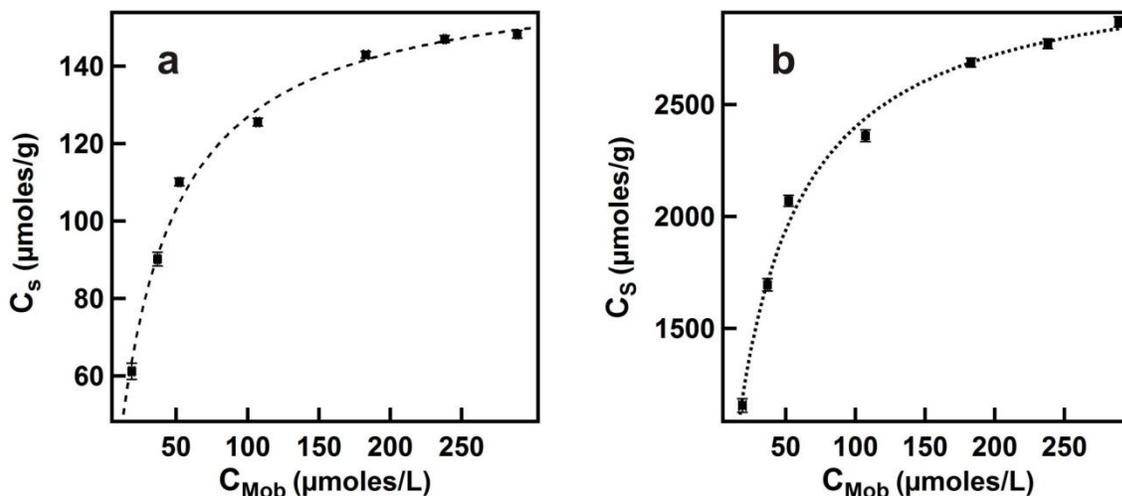
Figure 5-9. Langmuir sorption isotherms for the removal of Orange II by (a) the aggregates with pNIPAm-*co*-AAc-1 microgels and (b) by the microgels alone after correcting for the mass of BIS in the same aggregates. C_{Mob} is the concentration of the dye remaining in the aqueous phase and C_s is the concentration of Orange II sorbed on the aggregates/microgels. Each point on the plot represents an average of three replicate experiments and the error bars denote the standard deviation.
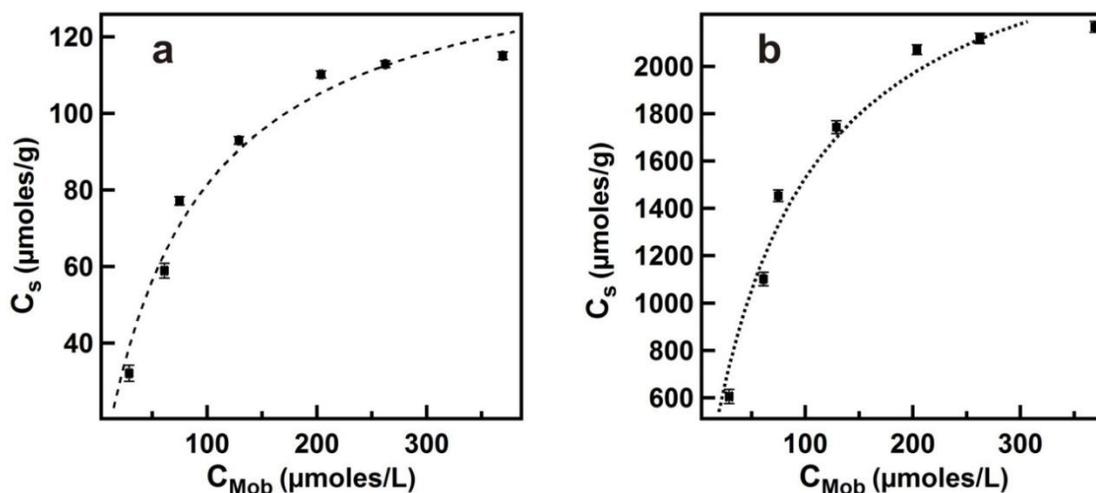
Figure 5-10. Langmuir sorption isotherms for the removal of Orange II by (a) the aggregates with pNIPAm-*co*-AAc-3 microgels and (b) by the microgels alone after correcting for the mass of BIS in the aggregates. C_{Mob} is the concentration of the dye remaining in the aqueous phase and C_s is the concentration of Orange II sorbed on the aggregates/microgels. Each point on the plot represents an average of three replicate experiments and the error bars denote the standard deviation.

We also plotted a Langmuir sorption isotherm by considering only the mass of the microgels in each of these aggregates (Figures 5-9 (b) and 5-10 (b)). The pNIPAm-*co*-AAc-1 system resulted in an R^2 value of 0.9714 and a maximum of 2720 μmoles/g (0.950 g Orange II/g microgels), with a Langmuir coefficient of 0.0123 ± 0.00212. The pNIPAm-*co*-AAc-3 system resulted in an R^2 value of 0.9923 and the maximum Orange II sorbed was calculated to be 3145 μmoles/g (1.10 g Orange II/g of microgels), with a Langmuir coefficient of 0.03217 ± 0.00229 L/μmoles. Whereas, in our previous work, we reported an R^2 value of 0.9853 and maximum of 2871 μmoles/g (1.006 g Orange II/g of microgels) sorbed, for a similar experiment. These results make it evident that the microgels in the aggregates are more efficient in removing Orange II/g than the unaggregated sample. Concheiro and coworkers investigated the uptake of naphthalene disulfonic acid (NS-2) by pNIPAm based systems, and fit their results with a Langmuir isotherm model. They report a maximum loading of 13 mmoles/L of gel, which translates to 3.747g NS-2/L of gel, the fit has a R^2 value of ~ 0.97.[364] If we approximate the density of a water swollen gel as 1.0 g/mL (assuming this density will give the maximum loading capacity), the maximum loading capacity is 0.0037 g NS-2/g of gel. In comparison, the system reported here is far more efficient at removing organic molecules from water.

$$C_{i,s} = C_{i,smax} * K_{ads} * C_{i,m}/(1 + K_{ads} * C_{i,m}) \qquad (1)$$

$C_{i,s}$ is the concentration of Orange II in aggregates (sorbent)

$C_{i,m}$ is the concentration of Orange II in mobile phase (in buffer after centrifugation)

K_{ads} is the Langmuir coefficient

5.4. Conclusion

We report the synthesis of pNIPAm microgel aggregates from pNIPAm-*co*-AAc-1 (D_H ~321 nm), pNIPAm-co-AAc-2 (D_H ~1.1 µm) and pNIPAm-*co*-AAc-3 (diameter ~1.43 µm) microgels and compare their ability to remove the organic, azo dye molecule, Orange II from aqueous solutions. The results indicate that for the aggregates synthesized from "big" microgels, a maximum removal efficiency of 85.3% was achieved while only 70.6% was achieved by the aggregates from "small" microgels at elevated temperature. Also, for aggregates synthesized from the different microgel diameters, the percent uptake of the dye increased as the concentration of BIS was increased from 100 mg to 500 mg, with minimal enhancement as the concentration was increased to 750 mg BIS. The results suggest that the size of the microgels in the aggregates and the size of the aggregates themselves are important factors that affect the uptake efficiencies. Also, by exploiting the thermoresponsive nature of these aggregates and by increasing the number of heating/cooling cycles the removal efficiency can be enhanced. Leaking studies were performed to determine the overall retention efficiencies of the aggregates which resulted in 67.0% and 76.9% for pNIPAm-*co*-AAc-1 and 3 microgel aggregates, respectively. A Langmuir sorption model was fit to our data, and the maximum Orange II sorbed on the aggregates was determined to be 0.051 g Orange II/g aggregates and 0.06 Orange II/g aggregates were achieved by the "small" and "big" microgel aggregates respectively. The Langmuir model was also plotted for the removal efficiencies for the samples by considering the mass of the microgels in the aggregates alone. A maximum of 0.95 g Orange II/g microgels were sorbed in the case of pNIPAm-*co*-AAc-1, with an R^2 value of 0.9714. Whereas, an R^2 value of 0.9923 and the maximum Orange II sorbed on the microgels was determined to be 1.1 g Orange II/g microgel, in the case of pNIPAm-*co*-AAc-3.

CHAPTER 6

REUSABILITY OF MICROGELS AND MICROGEL AGGREGATES FOR REMEDIATION

6.1. Introduction

From the previous Chapters, it is evident that the microgels and microgel aggregates remove significant amounts of Orange II from water. The reusability of pNIPAm-*co*-AAc-2 (~ 1.1 µm) which gave a removal efficiency of 29.5% at room temperature and the microgel aggregates from pNIPAm-*co*-AAc-3 (~ 1.43 µm) which gave a removal efficiency of 83.6% at elevated temperature was tested. Methanol was used as a solvent to extract the dye that was initially removed, and entrapped in the microgel structures. The assemblies were then assessed for their ability to further uptake dye from water. It was observed that after a single extraction of dye from pNIPAm-co-AAc-2 microgels, they were able to subsequently remove 20.9% Orange II from water, as to the original efficiency of 29.5%. Upon multiple extractions, a maximum of 25.7% removal efficiency was achieved for this system at room temperature. In the case of aggregates from pNIPAm-*co*-AAc-3, a maximum of 77.6% uptake efficiency was observed as opposed to the original efficiency of 83.6%.

6.2. Experimental

Materials. *N*-isopropylacrylamide (monomer) was purchased from TCI (Portland, Oregon) and purified by recrystallization from hexanes (ACS reagent grade, EMD, Gibbstown, NJ). *N,N'*-methylenebisacrylamide (BIS) (~99%), acrylic acid (AAc) (~99%), and ammonium persulphate (APS) (~98%) were obtained from Sigma-Aldrich (Oakville, Ontario) and were used as received. Orange II was obtained from Eastman Organic Chemicals (Rochester, NY) and

methanol was (~99.8%) was obtained from Caledon (Georgetown, Ontario). All the phosphate salts used for preparing buffer solutions of pH 7 (ionic strength of 0.235 M) were obtained from EMD and were used as received. Deionized (DI) water with a resistivity of 18.2 MΩ·cm was obtained from a Milli-Q Plus system from Millipore (Billerica, MA), and filtered through a 0.2 μm filter, prior to use. Microgel samples were lyophilized using a VirTis benchtop K-manifold freeze dryer (Stone Ridge, NY).

Synthesis of pNIPAm-*co*-AAc-2 microgels (~ 1.1 μm). These microgels were prepared by a surfactant free, free radical precipitation polymerization as reported before.[293] These were the same set of microgels used in the previous Chapters. The total monomer concentration was maintained to be 140 mM. Of this, 85% was *N*-isopropylacrylamide (NIPAm), 5% was *N,N'*-methylenebisacrylamide (BIS) crosslinker and 10% was acrylic acid (AAc) . To a clean beaker, NIPAm (11.9 mmol) and the crosslinker, BIS (0.700 mmol), were added and dissolved in deionized water (75 mL) in a beaker with stirring. A 20 mL syringe affixed with a 0.2 μm filter was used to filter the mixture into a clean 250 mL, 3-neck round bottom flask fitted with a condenser, thermometer, stir bar and a N_2 inlet. The beaker was rinsed with 24 mL of deionized water, which was again filtered and transferred to the mixture in the round bottom flask. The temperature was set to 65˚C with N_2 bubbling through the solution for ~ 1 h, after which AAc (1.4 mmol) was added to the mixture and stirred for a few minutes. To this, 0.197 mmol APS in 1 mL DI water was added. The mixture was allowed to stir for 4 h, under N_2 atmosphere. The solution was allowed to cool, while stirring overnight.

Following stirring overnight, the microgels were filtered through a type 1 Whatman filter paper, which was then rinsed with deionized water. The microgels were then cleaned via centrifugation to remove unreacted monomer and crosslinker, as well as linear polymer from the microgels. To

do this, the microgel solution was separated into 15 mL centrifuge tubes obtained from Corning Incorporated (Corning, NY) (~ 12 mL microgel solution/tube) and centrifuged at a speed of ~8400 relative centrifugal force (rcf) in a Baxter, biofuge 17R (Mount Holly, NJ) at 23 °C, for 30 min. Centrifugation yielded a pellet of microgels at the bottom of the centrifuge tube, and the supernatant was removed. ~12 mL of fresh DI water was added and the microgel pellet was redispersed using a Fisher Vortex, Genie 2 vortexer (Pittsburgh, PA). This cleaning protocol was repeated six times. The D_H of these microgels was determined by dynamic light scattering to be 1.10 μm ±14.5 nm, as mentioned in Chapter 3.

Synthesis of pNIPAm-*co*-AAc-3 microgels (Diameter ~1.43 μm). These were synthesized following a previously published procedure. [330] These were the same set of microgels used in the previous Chapters. The total monomer concentration was 153.8 mM (20 mmol) and 85% *N*-Isopropylacrylamide (NIPAm, 17.0 mmol), 5% *N*, *N'*- methylenebisacrylamide (BIS, 1.00 mmol) were added to 100 mL of deionized water in a small beaker and stirred. Once dissolved, the solution was filtered through a 0.2 μm filter into a 3-neck round bottom flask. The beaker was rinsed with 25 mL of deionized water and filtered into the flask. The flask was fit with a condenser, a nitrogen inlet, and a temperature probe to provide heating via a feedback-loop controlled hotplate (Torrey Pines Scientific, Carlsbad, CA). The flask was heated in an oil bath to 45 °C while the solution was allowed to stir and purge with N_2 gas for ~1.5 hours. Once the solution reached the set temperature, acrylic acid (AAc, 2.00 mmol, 10% of overall monomer concentration) was added followed by initiation of the reaction by addition of 0.078 M aqueous solution of ammonium persulphate in 5 mL DI water (overall solution volume resulted in 130 mL). After initiation, the reaction solution was then heated at a rate of 30 °C/hour to 65 °C and the reaction was allowed to proceed overnight under nitrogen atmosphere. The resulting

suspension was allowed to cool to room temperature, followed by filtration through a plug of glass wool to remove any coagulum formed during the reaction. The microgels were then cleaned via the same protocol as mentioned in the previous section. A diameter of 1.43 μm ± 5.35 nm was determined by microscopy as detailed in the previous Chapter.

Synthesis of microgel aggregates. Microgel aggregates were synthesized using three different concentrations of BIS- 100 mg (2 mg BIS/mL of total reaction solution), 500 mg (10 mg BIS/mL of total reaction solution) and 750 mg (15 mg BIS/mL of total reaction solution). The aggregates with 100 mg BIS were prepared by directly adding 10 mL of cleaned microgels from the above syntheses to a filtered solution (filtered through 0.2 μm filter affixed to a 20 mL syringe) of 100 mg of BIS in 39 mL of deionized water, to a beaker and stirred. This solution was transferred into a 250 mL 3-necked round bottom flask that was fit with a condenser, thermometer, stir bar and a N_2 inlet. The temperature was set to 65˚C and N_2 was bubbled through the solution for ~ 1 h. After 1 h, a 1 mL aqueous solution containing 0.0175 mmol of APS was added to this mixture and left to stir for 4 h, under N_2 atmosphere. The solution was allowed to cool with stirring overnight. This procedure was followed for the synthesis of the 10 mg/mL, and 15 mg/mL BIS aggregate samples, by adding 500 mg and 750 mg BIS to the reaction mixture, respectively. All microgel aggregates were cleaned using the same centrifugation procedure followed for cleaning microgels, but without filtering.

Orange II uptake. PNIPAm-*co*-AAc-2 microgels and aggregates from pNIPAm-co-AAc-3 were lyophilized and stock solutions were made from each sample to contain of 5.2 mg /mL solution. This was done by redispersing 52.1 mg of each in 10 mL of pH 7 buffer solution of 0.235 M ionic strength in a volumetric flask. A stock solution of Orange II (0.023 M) in deionized water was prepared. Using a micropipette, 300 μL of the microgels and aggregate

solution and 15 μL of Orange II were transferred into a 15 mL centrifuge tube (Corning Incorporated (Corning, NY)). A buffer solution of pH 7 (ionic strength 0.235 M) was used to bring the volume of the solution up to 3 mL yielding 114 μM Orange II and final concentration of aggregates to be and 521 μg microgels/ml of the reaction solution and 521 μg aggregates/ml of the reaction solution. After five minutes of exposure, this solution was centrifuged for 30 minutes, at ~8400 rcf. This centrifugation time was used to ensure that all the dispersed microgels and aggregates were removed from solution (as confirmed from differential interference contrast microscopy, data not shown). The supernatant was carefully removed from the tube without disturbing the pellet at the bottom of the tube and transferred to a quartz cuvette. The absorbance was measured using a HP8452A UV-Vis spectrophotometer with a diode array detector (previously Agilent Technologies, Inc., Santa Clara, CA). The initial concentration of Orange II for all the uptake studies was maintained at 114 μM and before very experiment, the initial absorbance of Orange II was measured in the absence of the microgels and aggregates. Also, it was observed that centrifuge tube did not have any effect on the initial absorbance of Orange II, as a function of time the solution stayed in the tube.

To study the uptake of Orange II as a function of temperature, the solution of Orange II and aggregates was held at 50 ˚C (microgels deswell), for different intervals of time and then cooled down to room temperature (microgels reswell). The solutions were then centrifuged, and the supernatant was then analyzed by UV-Vis to evaluate the percent uptake of the dye.

Extraction studies. The uptake studies on the pNIPAm-co-AAc-2 microgels were performed as detailed in the above section. The microgels were then exposed to MeOHfor and this solution was allowed to shake on a Fisher Vortex, Genie 2 vortexer (Pittsburgh, PA) fitted

with a shaker for 15 minutes. The solution was then centrifuged for 30 minutes at ~8400 rcf. The supernatant was then transferred into a small glass vial and the methanol was evaporated using a rotary evaporator (Brinkmann Buchi RE-111, New Jersy, NJ). The dye in the vial was then redissolved in 3 mL of DI water and the absorbance was measured, and moles extracted calculated. Similarly, the microgels pellets were dried using the rotary evaporator to remove any methanol present in them.

To the dried microgels, an uptake study was performed using the same protocol mentioned previously. In order to do another extraction, fresh 3 ml of methanol was added to the dried microgels after the first extraction and they were then redispersed in methanol and centrifuged in the same way as mentioned above. For further extractions, the above sequence was repeated the desired number of times and then the uptake studies were performed on the dried microgels accordingly.

The extraction experiments for aggregates from pNIPAm-*co*-AAc-3 were performed in the similar way, but after exposing fresh solution of dye to the dried aggregates subsequent to the extractions, the solution was heated to 50 ˚C, for 90 minutes and cooled down to room temperature for 30 minutes before determining their uptake efficiencies.

6.3. Results and Discussion

Reusability studies on pNIPAm-co-AAc-2 microgels. PNIPAm-co-AAc-2 microgel were investigated for their reusability by performing an uptake Orange II uptake experiment, at room temperature as detailed in the experimental. Briefly, the initial absorbance of 3 mL solution of 114 µM Orange II was recorded in the absence of the microgels. This was then compared to the absorbance from the supernatant after addition of 300 µL of the microgels (from a stock of 5.2 mg/mL) and 15 µL of Orange II (from a stock solution of 0.023 M in DI

water) in an overall volume of 3 mL. The percent removal efficiency of these microgels was confirmed to be 29.5% as reported in Chapter 3. To the microgels loaded with the dye, 3 mL methanol was added and the supernatant was transferred to a vial and dried. 3 mL of fresh DI water was added to the vial and the number of moles of dyes extracted after this step was determined by UV-Vis analysis and the extraction efficiency was calculated to be 72.5%. The microgels packed at the bottom were also dried to remove any methanol present in them and a fresh uptake study was performed using the protocol detailed in the experimental. It was observed that after the 1st extraction experiment, the microgels exhibited a removal efficiency of 20.9%. This in turn means that the microgels can be reused to remove 20.9% of the dye from aqueous solutions after one MeOH extraction. In order to study the effect of increasing the number of extractions on the reusability, a series of experiments were performed where the removal efficiency of the microgels after 2, 3, 4 and 5 extractions was monitored. The extraction efficiencies for extractions 2 through 5 were not determined because the concentration of Orange II was too low to be detected by UV-VIS. Figure 6-1 shows that as the number of extractions increases from 1 to 4, the uptake efficiency increased from 20.9% to 25.4% and upon increasing the number of extractions to 5, the efficiency increased only to 25.7%. Therefore, a maximum of 25.7% uptake can be expected from the microgels.
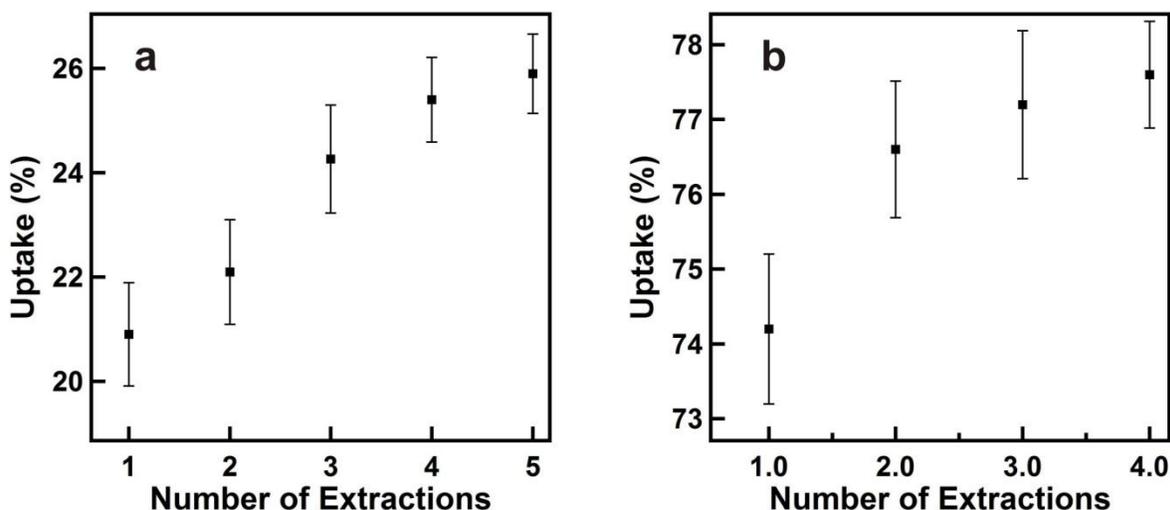
Figure 6-1. Trend of percent uptake of Orange II as a function of the number of MeOH extraction cycles for a) the microgels pNIPAm-co-AAc-2 and b) pNIPAm-co-AAc-3 microgel aggregates after a single temeprature cycle of 90 minutes heating and 30 minutes cooling.Each point on the plot represents an average of three replicate experiments of uptake studies and the error bars denote the standard deviation.

Reusability studies on aggregates from pNIPAm-co-AAc-3 microgels. Initial uptake studies on pNIPAm-co-AAc-1 microgel aggregates were performed at elevated temperature using the protocol detailed in the experimental. Briefly, 300 μL of the 500 mg BIS aggregates of pNIPAm-*co*-AAc-3 were added to 15 μl of Orange II in pH 7 (0.235M ionic strength) in a 3 mL total volume, and heated the solution to 52 ˚C for 90 minutes and cooled down to room temperature for 30 minutes. This solution was then centrifuged immediately and the absorbance of the supernatant was analyzed by UV-Vis. The uptake efficiency was calculated to be 83.6% as reported previously in Chapter 5. To study the reusability of these aggregates, the supernatant was discarded and 3 mL methanol was added to the aggregates and centrifuged. The supernatant from this sample was transferred into a vial and the methanol was evaporated using a rotary evaporator. To this vial, 3 mL DI water was added and the number of moles of Orange II present

in the vial was determined by UV-Vis analysis. The extraction efficiency was determined to be 71.1%. MeOH was removed from the aggregates by drying via a rotary evaporator. To this, fresh solution of Orange II was added to monitor the uptake efficiency at elevated temperatures as detailed before. The solution was heated to 52 ˚C for 90 minutes and then cooled back to room temperature for 30 minutes and this solution was immediately centrifuged and the supernatant was analyzed by UV-Vis. The aggregates after one time treatment with methanol, gave an uptake efficiency of 74.2%. In order to determine the possibility of improving the reusability of these aggregates, multiple extractions were performed using methanol. The protocol for uptake studies after multiple extractions are detailed in the experimental. The extraction efficiencies for multiple extractions were again not recorded due to low concentrations of Orange II present in the supernatant of the extracted solutions. Figure 6-1 indicates that as the number of extractions increased from 1 to 4, the uptake efficiencies increased from 74.2% to 77.2%, which is fairly close to the original uptake efficiency of these aggregates before treating them with methanol. The increase in the uptake efficiency after 5 times extractions was only minimal which was determined to be 77.6%.

6.4. Conclusion

The reusability of microgels and microgel aggregates for water remediation was investigated. The unaggregated pNIPAm-*co*-AAc-2 microgels at room temperature originally gave a maximum uptake of 29.5% while the pNIPAm-*co*-AAc-3 microgel aggregates at elevated temperatures, removed 83.6% of the dye from aqueous solutions, which was established in the previous Chapters. Methanol was used as a solvent to extract the dye loaded inside these systems. It was observed that after 5 extractions, a maximum uptake efficiency of 25.7% was

obtained for the unaggregated pNIPAm-co-AAc-2 microgels at room temperature, and a maximum removal efficiency of 77.6% was obtained for the pNIPAm-co-AAc-3 microgel aggregates at elevated temperatures. These results indicate that the microgels and microgel aggregates systems can be reused further to remove significant amounts of Orange II, fairly close to the original efficiency values.

CHAPTER 7

FUTURE DIRECTIONS

The projects discussed in the previous Chapters lead to an understanding of how microgels and microgel based aggregates can be used for removing significant amounts of Orange II from aqueous solutions. This led to an understanding that function directly influences function. Many experiments can be performed with these systems to make them more versatile for removal of many other organic compounds that are of major threat to the environment. Some of these experiments have been mentioned in this Chapter.

- In Chapter 3, pNIPAm microgels with the higher concentrations of AAc were found to be the system that achieved the highest removal efficiency. It was also established that the removal of Orange II by these microgels followed a Langmuir isotherm model, which in turn means that dye removal by these microgels could be due a sorption process. These microgels can be further modified with various other comonomers (vinyl acrylic acid, methacrylic acid, methyl methacrylate, and so on) and various pH conditions used to specifically remove contaminants, for example, silver, naphthenic acids, PCBs and PAHs..

- In Chapters 4 and 5, it was established that the aggregated microgels with high concentrations of crosslinker and the microgel with larger diameters achieved very significant removal efficiencies. These systems can also be chemically modified and make them more versatile to remove specific contaminants from water. Furthermore, these systems were fit by Langmuir isotherm model more accurately. Keeping the size of the aggregate in mind, we performed preliminary studies on macrogel systems of

pNIPAm modified with an adsorbent material, nanocrystalline cellulose (NCC). It was observed that at room temperature, these systems removed about 25% of the dye from water, which is fairly close to what was achieved by the microgels in Chapter 3 at room temperature. These systems can be further modified by further increasing the concentration of NCC present in the microgels and perform more detailed analysis of how temperature and pH can affect the removal efficiencies of these systems. Also, other common adsorbents, activated carbon can be added to these microgels and monitor the uptake studies. These systems can also be monitored for their ability to remove several other organic contaminants.

- In Chapters 3, 4 and 5, leaking studies were performed to determine the efficiencies of these systems to retain the Orange II that was initially remove from water. This can be used as a basis to design efficient drug delivery systems that are dependent on the release profile of drug molecules from the microgels.

- In Chapter 6, initial results of reusability of the microgels and their aggregates using methanol was discussed. It was established that higher number of extractions resulted in better reusability of the microgels. Further experiments can be performed on these systems using more suitable solvents to reuse microgels to their full and original potential for removal of the dye. Several other treatment methods can be performed after isolating the aggregates or the microgels from the contaminant sample to make these systems more reusable.

REFERENCES

1.   Theron, J.; Walker, J. A.; Cloete, T. E., Nanotechnology and water treatment: Applications and emerging opportunities. *Critical Reviews in Microbiology* **2008,** *34* (1), 43-69.

2.   Crittenden, J. C.; Trussell, R. R.; Hand, D. W.; Howe, K. J.; Tchobanoglous, G., Water treatment - Principles and design (2nd Edition). John Wiley & Sons.

3.   Homem, V.; Santos, L., Degradation and removal methods of antibiotics from aqueous matrices - A review. *Journal of Environmental Management* **2011,** *92* (10), 2304-2347.

4.   Adams, C.; Wang, Y.; Loftin, K.; Meyer, M., Removal of antibiotics from surface and distilled water in conventional water treatment processes. *Journal of Environmental Engineering-Asce* **2002,** *128* (3), 253-260.

5.   Tchobanoglous, G.; Burton, F.; Stensel, D.; Wastewater engineering- Treatment and reuse (4th edition). Metcalf & Eddy, Inc.

6.   Senta, I.; Matosic, M.; Jakopovic, H. K.; Terzic, S.; Curko, J.; Mijatovic, I.; Ahel, M., Removal of antimicrobials using advanced wastewater treatment. *Journal of Hazardous Materials* **2011,** *192* (1), 319-328.

7.   Yangali-Quintanilla, V.; Maeng, S. K.; Fujioka, T.; Kennedy, M.; Amy, G., Proposing nanofiltration as acceptable barrier for organic contaminants in water reuse. *Journal of Membrane Science* **2010,** *362* (1-2), 334-345.

8.   Fu, F.; Wang, Q., Removal of heavy metal ions from wastewaters: A review. *Journal of Environmental Management* **2011,** *92* (3), 407-418.

9.   Kurniawan, T. A.; Lo, W. H.; Chan, G. Y. S., Physico-chemical treatments for removal of recalcitrant contaminants from landfill leachate. *Journal of Hazardous Materials* **2006,** *129* (1-3), 80-100.

10.   Lee, M.; Paik, I. S.; Kim, I.; Kang, H.; Lee, S., Remediation of heavy metal contaminated groundwater originated from abandoned mine using lime and calcium carbonate. *Journal of Hazardous Materials* **2007,** *144* (1-2), 208-214.

11.   Erdem, E.; Karapinar, N.; Donat, R., The removal of heavy metal cations by natural zeolites. *Journal of Colloid and Interface Science* **2004,** *280* (2), 309-314.

12.   Babel, S.; Kurniawan, T. A., Low-cost adsorbents for heavy metals uptake from contaminated water: a review. *Journal of Hazardous Materials* **2003,** *97* (1-3), 219-243.

13.   Mohan, D.; Pittman, C. U., Arsenic removal from water/wastewater using adsorbents - A critical review. *Journal of Hazardous Materials* **2007,** *142* (1-2), 1-53.

14.   Matilainen, A.; Vepsalainen, M.; Sillanpaa, M., Natural organic matter removal by coagulation during drinking water treatment: A review. *Advances in Colloid and Interface Science* **2010,** *159* (2), 189-197.

15.   Cai, Z. X.; Kim, J. S.; Benjamin, M. M., NOM removal by adsorption and membrane filtration using heated aluminum oxide particles. *Environmental Science & Technology* **2008,** *42* (2), 619-623.

16.   Berube, D.; Dorea, C. C., Optimizing alum coagulation for turbidity, organics, and residual Al reductions. *Water Science and Technology: Water Supply* **2008,** *8* (5), 505-511.

17.   Korth, A.; Fiebiger, C.; Bornmann, K.; Schmidt, W., NOM increase in drinking water reservoirs - relevance for drinking water production. *Natural Organic Material Research: Innovations and Applications for Drinking Water* **2004,** *4* (4), 55-60.

18.   Homem, V.; Santos, L., Degradation and removal methods of antibiotics from aqueous matrices - A review. *Journal of environmental management* **2011,** *92* (10), 2304-47.

19.   Pera-Titus, M.; Garcia-Molina, V.; Banos, M. A.; Gimenez, J.; Esplugas, S., Degradation of chlorophenols by means of advanced oxidation processes: a general review. *Applied Catalysis B-Environmental* **2004,** *47* (4), 219-256.

20.   Borba, C. E.; Guirardello, R.; Silva, E. A.; Veit, M. T.; Tavares, C. R. G., Removal of nickel(II) ions from aqueous' solution by biosorption in a fixed bed column: Experimental and theoretical breakthrough curves. *Biochemical Engineering Journal* **2006,** *30* (2), 184-191.

21.   Namasivayam, C.; Kadirvelu, K., Uptake of mercury (II) from wastewater by activated carbon from an unwanted agricultural solid by-product: coirpith. *Carbon* **1999,** *37* (1), 79-84.

22.   Naseem, R.; Tahir, S. S., Removal of Pb(II) from aqueous/acidic solutions by using bentonite as an adsorbent. *Water Research* **2001,** *35* (16), 3982-3986.

23.   Mirbagheri, S. A.; Hosseini, S. N., Pilot plant investigation on petrochemical wastewater treatment for the removal of copper and chromium with the objective of reuse. *Desalination* **2005,** *171* (1), 85-93.

24.   Charerntanyarak, L., Heavy metals removal by chemical coagulation and precipitation. *Water Science and Technology* **1999,** *39* (10-11), 135-138.

25.   Chang, Q.; Wang, G., Study on the macromolecular coagulant PEX which traps heavy metals. *Chemical Engineering Science* **2007,** *62* (17), 4636-4643.

26.   Chang, Q.; Zhang, M.; Wang, J. X., Removal of Cu(2+) and turbidity from wastewater by mercaptoacetyl chitosan. *Journal of Hazardous Materials* **2009,** *169* (1-3), 621-625.

27.   Bratskaya, S. Y.; Pestov, A. V.; Yatluk, Y. G.; Avramenko, V. A., Heavy metals removal by flocculation/precipitation using N-(2-carboxyethyl)chitosans. *Colloids and Surfaces a-Physicochemical and Engineering Aspects* **2009,** *339* (1-3), 140-144.

28.   El Samrani, A. G.; Lartiges, B. S.; Villieras, F., Chemical coagulation of combined sewer overflow: Heavy metal removal and treatment optimization. *Water Research* **2008,** *42* (4-5), 951-960.

29.   Hankins, N. P.; Lu, N.; Hilal, N., Enhanced removal of heavy metal ions bound to humic acid by polyelectrolyte flocculation. *Separation and Purification Technology* **2006,** *51* (1), 48-56.

30.   Duan, J. C.; Lu, Q.; Chen, R. W.; Duan, Y. Q.; Wang, L. F.; Gao, L.; Pan, S. Y., Synthesis of a novel flocculant on the basis of crosslinked Konjac glucomannan-graft-polyacrylamide-co-sodium xanthate and its application in removal of Cu(2+) ion. *Carbohydrate Polymers* **2010,** *80* (2), 436-441.

31.   Mohan, D.; Pittman, C. U., Activated carbons and low cost adsorbents for remediation of tri- and hexavalent chromium from water. *Journal of Hazardous Materials* **2006,** *137* (2), 762-811.

32.   Jusoh, A.; Shiung, L. S.; Ali, N.; Noor, M., A simulation study of the removal efficiency of granular activated carbon on cadmium and lead. *Desalination* **2007,** *206* (1-3), 9-16.

33.   Kurniawan, T. A.; Chan, G. Y. S.; Lo, W. H.; Babel, S., Physico-chemical treatment techniques for wastewater laden with heavy metals. *Chemical Engineering Journal* **2006,** *118* (1-2), 83-98.

34.   Leyva Ramos, R.; Bernal Jacome, L. A.; Mendoza Barron, J.; Fuentes Rubio, L.; Guerrero Coronado, R. M., Adsorption of zinc(II) from an aqueous solution onto activated carbon. *Journal of Hazardous Materials* **2002,** *90* (1), 27-38.

35.   Monser, L.; Adhoum, N., Modified activated carbon for the removal of copper, zinc, chromium and cyanide from wastewater. *Separation and Purification Technology* **2002,** *26* (2-3), 137-146.

36.   Ouki, S. K.; Neufeld, R. D., Use of activated carbon for the recovery of chromium from industrial wastewaters. *Journal of Chemical Technology and Biotechnology* **1997,** *70* (1), 3-8.

37.   Vaca Mier, M.; Lopez Callejas, R.; Gehr, R.; Jimenez Cisneros, B. E.; Alvarez, P. J. J., Heavy metal removal with Mexican clinoptilolite: Multi-component ionic exchange. *Water Research* **2001,** *35* (2), 373-378.

38.   Panday, K. K.; Prasad, G.; Singh, V. N., Copper (II) remocal from aqueous-solutions by fly-ash. *Water Research* **1985,** *19* (7), 869-873.

39.   Schmuhl, R.; Krieg, H. M.; Keizer, K., Adsorption of Cu(II) and Cr(VI) ions by chitosan: Kinetics and equilibrium studies. *Water Sa* **2001,** *27* (1), 1-7.

40.   Sen, A. K.; De, A. K., Adsorption of mercury (II) by coal fly-ash. *Water Research* **1987,** *21* (8), 885-888.

41.   Sharma, D. C.; Forster, C. F., Removal of hexavalent chromium using sphagnum moss peat. *Water Research* **1993,** *27* (7), 1201-1208.

42.   Bhattacharyya, K. G.; Sen Gupta, S., Adsorption of a few heavy metals on natural and modified kaolinite and montmorillonite: A review. *Advances in Colloid and Interface Science* **2008,** *140* (2), 114-131.

43.   Jiang, M. Q.; Jin, X. Y.; Lu, X. Q.; Chen, Z. L., Adsorption of Pb(II), Cd(II), Ni(II) and Cu(II) onto natural kaolinite clay. *Desalination* **2010,** *252* (1-3), 33-39.

44.   Kang, S. Y.; Lee, J. U.; Moon, S. H.; Kim, K. W., Competitive adsorption characteristics of Co2+, Ni2+, and Cr3+ by IRN-77 cation exchange resin in synthesized wastewater. *Chemosphere* **2004,** *56* (2), 141-147.

45.   Gode, F.; Pehlivan, E., Removal of chromium(III) from aqueous solutions using Lewatit S 100: The effect of pH, time, metal concentration and temperature. *Journal of Hazardous Materials* **2006,** *136* (2), 330-337.

46.   Abo-Farha, S. A.; Abdel-Aal, A. Y.; Ashour, I. A.; Garamon, S. E., Removal of some heavy metal cations by synthetic resin purolite C100. *Journal of Hazardous Materials* **2009,** *169* (1-3), 190-194.

47.   Motsi, T.; Rowson, N. A.; Simmons, M. J. H., Adsorption of heavy metals from acid mine drainage by natural zeolite. *International Journal of Mineral Processing* **2009,** *92* (1-2), 42-48.

48.   Ostroski, I. C.; Barros, M.; Silva, E. A.; Dantas, J. H.; Arroyo, P. A.; Lima, O. C. M., A comparative study for the ion exchange of Fe(III) and Zn(II) on zeolite NaY. *Journal of Hazardous Materials* **2009,** *161* (2-3), 1404-1412.

49.   Taffarel, S. R.; Rubio, J., On the removal of Mn(2+) ions by adsorption onto natural and activated Chilean zeolites. *Minerals Engineering* **2009,** *22* (4), 336-343.

50.   Moreno, N.; Querol, X.; Ayora, C., Utilization of zeolites synthesized from coal fly ash for the purification of acid mine waters. *Environmental Science & Technology* **2001,** *35* (17), 3526-3534.

51.   Alvarez-Ayuso, E.; Garcia-Sanchez, A.; Querol, X., Purification of metal electroplating waste waters using zeolites. *Water Research* **2003,** *37* (20), 4855-4862.

52.   Landaburu-Aguirre, J.; Garcia, V.; Pongracz, E.; Keiski, R. L., The removal of zinc from synthetic wastewaters by micellar-enhanced ultrafiltration: statistical design of experiments. *Desalination* **2009,** *240* (1-3), 262-269.

53.   Samper, E.; Rodriguez, M.; De la Rubia, M. A.; Prats, D., Removal of metal ions at low concentration by micellar-enhanced ultrafiltration (MEUF) using sodium dodecyl sulphate (SDS) and linear alkylbenzene sulfonate (LAS). *Separation and Purification Technology* **2009,** *65* (3), 337-342.

54.   Li, X.; Zeng, G. M.; Huang, J. H.; Zhang, C.; Fang, Y. Y.; Qu, Y. H.; Luo, F.; Lin, D.; Liu, H. L., Recovery and reuse of surfactant SDS from a MEUF retentate containing Cd(2+) or Zn(2+) by ultrafiltration. *Journal of Membrane Science* **2009,** *337* (1-2), 92-97.

55.   Molinari, R.; Poerio, T.; Argurio, P., Selective separation of copper(II) and nickel(II) from aqueous media using the complexation-ultrafiltration process. *Chemosphere* **2008,** *70* (3), 341-348.

56.   Aroua, M. K.; Zuki, F. M.; Sulaiman, N. M., Removal of chromium ions from aqueous solutions by polymer-enhanced ultrafiltration. *Journal of Hazardous Materials* **2007,** *147* (3), 752-758.

57.   Trivunac, K.; Stevanovic, S., Removal of heavy metal ions from water by complexation-assisted ultrafiltration. *Chemosphere* **2006,** *64* (3), 486-491.

58.   Kim, H. J.; Baek, K.; Kim, B. K.; Yang, J. W., Humic substance-enhanced ultrafiltration for removal of cobalt. *Journal of Hazardous Materials* **2005,** *122* (1-2), 31-36.

59.   Shahalam, A. M.; Al-Harthy, A.; Al-Zawhry, A., Feed water pretreatment in RO systems: unit processes in the Middle East. *Desalination* **2002,** *150* (3), 235-245.

60.   Dialynas, E.; Diamadopoulos, E., Integration of a membrane bioreactor coupled with reverse osmosis for advanced treatment of municipal wastewater. *Desalination* **2009,** *238* (1-3), 302-311.

61.   Mohsen-Nia, M.; Montazeri, P.; Modarress, H., Removal of Cu2+ and Ni2+ from wastewater with a chelating agent and reverse osmosis processes. *Desalination* **2007,** *217* (1-3), 276-281.

62.   Murthy, Z. V. R.; Chaudhari, L. B., Separation of binary heavy metals from aqueous solutions by nanofiltration and characterization of the membrane using Spiegler-Kedem model. *Chemical Engineering Journal* **2009,** *150* (1), 181-187.

63.   Muthukrishnan, M.; Guha, B. K., Effect of pH on rejection of hexavalent chromium by nanofiltration. *Desalination* **2008,** *219* (1-3), 171-178.

64.   Murthy, Z. V. R.; Chaudhari, L. B., Application of nanofiltration for the rejection of nickel ions from aqueous solutions and estimation of membrane transport parameters. *Journal of Hazardous Materials* **2008,** *160* (1), 70-77.

65.   Csefalvay, E.; Pauer, V.; Mizsey, P., Recovery of copper from process waters by nanofiltration and reverse osmosis. *Desalination* **2009,** *240* (1-3), 132-142.

66.   Figoli, A.; Cassano, A.; Criscuoli, A.; Mozumder, M. S. I.; Uddin, M. T.; Islam, M. A.; Drioli, E., Influence of operating parameters on the arsenic removal by nanofiltration. *Water Research* **2010,** *44* (1), 97-104.

67.   Eriksson, P., Nanofiltration extends the range of membrane filtration. *Environmental Progress* **1988,** *7* (1), 58-62.

68.   Chen, G. H., Electrochemical technologies in wastewater treatment. *Separation and Purification Technology* **2004,** *38* (1), 11-41.

69.   Heidmann, I.; Calmano, W., Removal of Zn(II), Cu(II), Ni(II), Ag(I) and Cr(VI) present in aqueous solutions by aluminium electrocoagulation. *Journal of Hazardous Materials* **2008,** *152* (3), 934-941.

70.   Savage, N.; Diallo, M. S., Nanomaterials and water purification: Opportunities and challenges. *Journal of Nanoparticle Research* **2005,** *7* (4-5), 331-342.

71.   Zhang, W. X., Nanoscale iron particles for environmental remediation: An overview. *Journal of Nanoparticle Research* **2003,** *5* (3-4), 323-332.

72.   Tratnyek, P. G.; Johnson, R. L., Nanotechnologies for environmental cleanup. *Nano Today* **2006,** *1* (2), 44-48.

73.   Klabunde, K. J.; Stark, J.; Koper, O.; Mohs, C.; Park, D. G.; Decker, S.; Jiang, Y.; Lagadic, I.; Zhang, D. J., Nanocrystals as stoichiometric reagents with unique surface chemistry. *Journal of Physical Chemistry* **1996,** *100* (30), 12142-12153.

74.   Nurmi, J. T.; Tratnyek, P. G.; Sarathy, V.; Baer, D. R.; Amonette, J. E.; Pecher, K.; Wang, C. M.; Linehan, J. C.; Matson, D. W.; Penn, R. L.; Driessen, M. D., Characterization and properties of metallic iron nanoparticles: Spectroscopy, electrochemistry, and kinetics. *Environmental Science & Technology* **2005,** *39* (5), 1221-1230.

75.   Ponder, S. M.; Darab, J. G.; Mallouk, T. E., Remediation of Cr(VI) and Pb(II) aqueous solutions using supported, nanoscale zero-valent iron. *Environmental Science & Technology* **2000,** *34* (12), 2564-2569.

76. Kanel, S. R.; Manning, B.; Charlet, L.; Choi, H., Removal of arsenic(III) from groundwater by nanoscale zero-valent iron. *Environmental Science & Technology* **2005,** *39* (5), 1291-1298.

77. Li, X. Q.; Zhang, W. X., Iron nanoparticles: the core-shell structure and unique properties for Ni(II) sequestration. *Langmuir* **2006,** *22* (10), 4638-4642.

78. Wang, H. J.; Zhou, A. L.; Peng, F.; Yu, H.; Yang, J., Mechanism study on adsorption of acidified multiwalled carbon nanotubes to Pb(II). *Journal of Colloid and Interface Science* **2007,** *316* (2), 277-283.

79. Kabbashi, N. A.; Atieh, M. A.; Al-Mamun, A.; Mirghami, M. E. S.; Alam, M. D. Z.; Yahya, N., Kinetic adsorption of application of carbon nanotubes for Pb(II) removal from aqueous solution. *Journal of Environmental Sciences-China* **2009,** *21* (4), 539-544.

80. Kuo, C. Y.; Lin, H. Y., Adsorption of aqueous cadmium (II) onto modified multi-walled carbon nanotubes following microwave/chemical treatment. *Desalination* **2009,** *249* (2), 792-796.

81. Pillay, K.; Cukrowska, E. M.; Coville, N. J., Multi-walled carbon nanotubes as adsorbents for the removal of parts per billion levels of hexavalent chromium from aqueous solution. *Journal of Hazardous Materials* **2009,** *166* (2-3), 1067-1075.

82. Li, Y. H.; Liu, F. Q.; Xia, B.; Du, Q. J.; Zhang, P.; Wang, D. C.; Wang, Z. H.; Xia, Y. Z., Removal of copper from aqueous solution by carbon nanotube/calcium alginate composites. *Journal of Hazardous Materials* **2010,** *177* (1-3), 876-880.

83. Kandah, M. I.; Meunier, J. L., Removal of nickel ions from water by multi-walled carbon nanotubes. *Journal of Hazardous Materials* **2007,** *146* (1-2), 283-288.

84.   Ormad, M. P.; Miguel, N.; Claver, A.; Matesanz, J. M.; Ovelleiro, J. L., Pesticides removal in the process of drinking water production. *Chemosphere* **2008,** *71* (1), 97-106.

85.   Oller, I.; Malato, S.; Sanchez-Perez, J. A., Combination of Advanced Oxidation Processes and biological treatments for wastewater decontamination-A review. *The Science of the total environment* **2011,** *409* (20), 4141-66.

86.   Steber, J.; Wierich, P., Properties of hydroxyethane diphosphonate affecting its environmental fate: Degradability, sludge adsorption, mobility in soils, and bioconcentration. *Chemosphere* **1986,** *15* (7), 929-945.

87.   Muñoz, R.; Guieysse, B., Algal–bacterial processes for the treatment of hazardous contaminants: A review. *Water Research* **2006,** *40* (15), 2799-2815.

88.   Lapertot, M.; Pulgarín, C.; Fernández-Ibáñez, P.; Maldonado, M. I.; Pérez-Estrada, L.; Oller, I.; Gernjak, W.; Malato, S., Enhancing biodegradability of priority substances (pesticides) by solar photo-Fenton. *Water Research* **2006,** *40* (5), 1086-1094.

89.   Katsoyiannis, A.; Samara, C., Persistent organic pollutants (POPS) in the sewage treatment plant of Thessaloniki, northern Greece: occurrence and removal. *Water Research* **2004,** *38* (11), 2685-2698.

90.   Doll, T. E.; Frimmel, F. H., Removal of selected persistent organic pollutants by heterogeneous photocatalysis in water. *Catalysis Today* **2005,** *101* (3-4), 195-202.

91.   Balcioglu, I. A.; Arslan, I.; Sacan, M. T., Homogenous and heterogenous advanced oxidation of two commercial reactive dyes. *Environmental Technology* **2001,** *22* (7), 813-822.

92.   Gonze, E.; Commenges, N.; Gonthier, Y.; Bernis, A., High frequency ultrasound as a pre- or a post-oxidation for paper mill wastewaters and landfill leachate treatment. *Chemical Engineering Journal* **2003,** *92* (1-3), 215-225.

93.   Bhatkhande, D. S.; Pangarkar, V. G.; Beenackers, A. A. C. M., Photocatalytic degradation for environmental applications – a review. *Journal of Chemical Technology & Biotechnology* **2002,** *77* (1), 102-116.

94.   García-Montaño, J.; Ruiz, N.; Muñoz, I.; Domènech, X.; García-Hortal, J. A.; Torrades, F.; Peral, J., Environmental assessment of different photo-Fenton approaches for commercial reactive dye removal. *Journal of Hazardous Materials* **2006,** *138* (2), 218-225.

95.   Hernandez, R.; Zappi, M.; Colucci, J.; Jones, R., Comparing the performance of various advanced oxidation processes for treatment of acetone contaminated water. *Journal of Hazardous Materials* **2002,** *92* (1), 33-50.

96.   Bautitz, I. R.; Nogueira, R. F. P., Degradation of tetracycline by photo-Fenton process - Solar irradiation and matrix effects. *Journal of Photochemistry and Photobiology a-Chemistry* **2007,** *187* (1), 33-39.

97.   Andreozzi, R.; Caprio, V.; Insola, A.; Marotta, R., Advanced oxidation processes (AOP) for water purification and recovery. *Catalysis Today* **1999,** *53* (1), 51-59.

98.   Andreozzi, R.; Canterino, M.; Marotta, R.; Paxeus, N., Antibiotic removal from wastewaters: The ozonation of amoxicillin. *Journal of Hazardous Materials* **2005,** *122* (3), 243-250.

99.   Balcioglu, I. A.; Otker, M., Treatment of pharmaceutical wastewater containing antibiotics by O-3 and O-3/H2O2 processes. *Chemosphere* **2003,** *50* (1), 85-95.

100.   Arslan-Alaton, I.; Caglayan, A. E., Ozonation of Procaine Penicillin G formulation effluent - Part I: Process optimization and kinetics. *Chemosphere* **2005,** *59* (1), 31-39.

101.   Qiang, Z.; Liu, C.; Dong, B.; Zhang, Y., Degradation mechanism of alachlor during direct ozonation and O3/H2O2 advanced oxidation process. *Chemosphere* **2010,** *78* (5), 517-526.

102.   Wang, C.; Yediler, A.; Lienert, D.; Wang, Z.; Kettrup, A., Ozonation of an azo dye C.I. Remazol Black 5 and toxicological assessment of its oxidation products. *Chemosphere* **2003,** *52* (7), 1225-1232.

103.   Germirli Babuna, F.; Camur, S.; Alaton, I. A.; Okay, O.; Iskender, G., The application of ozonation for the detoxification and biodegradability improvement of a textile auxiliary: Naphtalene sulphonic acid. *Desalination* **2009,** *249* (2), 682-686.

104.   Gan, S.; Lau, E. V.; Ng, H. K., Remediation of soils contaminated with polycyclic aromatic hydrocarbons (PAHs). *Journal of Hazardous Materials* **2009,** *172* (2-3), 532-549.

105.   González, O.; Sans, C.; Esplugas, S., Sulfamethoxazole abatement by photo-Fenton. Toxicity, inhibition and biodegradability assessment of intermediates. *Journal of Hazardous Materials* **2007,** *146* (3), 459-464.

106.   Trovó, A. G.; Melo, S. A. S.; Nogueira, R. F. P., Photodegradation of the pharmaceuticals amoxicillin, bezafibrate and paracetamol by the photo-Fenton process-Application to sewage treatment plant effluent. *Journal of Photochemistry and Photobiology A: Chemistry* **2008,** *198* (2-3), 215-220.

107.   Trovó, A. G.; Nogueira, R. F. P.; Agüera, A.; Sirtori, C.; Fernández-Alba, A. R., Photodegradation of sulfamethoxazole in various aqueous media: Persistence, toxicity and photoproducts assessment. *Chemosphere* **2009,** *77* (10), 1292-1298.

108.   Arslan-Alaton, I.; Gurses, F., Photo-fenton-like and photo-fenton-like oxidation of Procaine Penicillin G formulation effluent. *Journal of Photochemistry and Photobiology A: Chemistry* **2004,** *165* (1-3), 165-175.

109.   Arslan-Alaton, I.; Dogruel, S., Pre-treatment of penicillin formulation effluent by advanced oxidation processes. *Journal of Hazardous Materials* **2004,** *112* (1-2), 105-113.

110.   Elmolla, E.; Chaudhuri, M., Improvement of biodegradability of synthetic amoxicillin wastewater by photo-Fenton process. *World Appl. Sci. J.* **2009,** *5*, 53-58.

111.   Elmolla, E.; Chaudhuri, M., Optimization of Fenton process for treatment of amoxicillin, ampicillin and cloxacillin antibiotics in aqueous solution. *Journal of Hazardous Materials* **2009,** *170* (2-3), 666-672.

112.   Bobu, M.; Yediler, A.; Siminiceanu, I.; Schulte-Hostede, S., Degradation studies of ciprofloxacin on a pillared iron catalyst. *Applied Catalysis B: Environmental* **2008,** *83* (1-2), 15-23.

113.   Guinea, E.; Brillas, E.; Centellas, F.; Cañizares, P.; Rodrigo, M. A.; Sáez, C., Oxidation of enrofloxacin with conductive-diamond electrochemical oxidation, ozonation and Fenton oxidation. A comparison. *Water Research* **2009,** *43* (8), 2131-2138.

114.   Pérez-Moya, M.; Graells, M.; Castells, G.; Amigó, J.; Ortega, E.; Buhigas, G.; Pérez, L. M.; Mansilla, H. D., Characterization of the degradation performance of the sulfamethazine antibiotic by photo-Fenton process. *Water Research* **2010,** *44* (8), 2533-2540.

115.   Pérez, M.; Torrades, F.; Domènech, X.; Peral, J., Fenton and photo-Fenton oxidation of textile effluents. *Water Research* **2002,** *36* (11), 2703-2710.

116.   Torrades, F.; García-Montaño, J.; Antonio García-Hortal, J.; Domènech, X.; Peral, J., Decolorization and mineralization of commercial reactive dyes under solar light assisted photo-Fenton conditions. *Solar Energy* **2004,** *77* (5), 573-581.

117.   Amat, A. M.; Arques, A.; Miranda, M. A.; Seguí, S., Photo-Fenton reaction for the abatement of commercial surfactants in a solar pilot plant. *Solar Energy* **2004,** *77* (5), 559-566.

118.   Liu, R.; Chiu, H. M.; Shiau, C.-S.; Yeh, R. Y.-L.; Hung, Y.-T., Degradation and sludge production of textile dyes by Fenton and photo-Fenton processes. *Dyes and Pigments* **2007,** *73* (1), 1-6.

119.   Ay, F.; Catalkaya, E. C.; Kargi, F., A statistical experiment design approach for advanced oxidation of Direct Red azo-dye by photo-Fenton treatment. *Journal of Hazardous Materials* **2009,** *162* (1), 230-236.

120.   Torrades, F.; Pérez, M.; Mansilla, H. D.; Peral, J., Experimental design of Fenton and photo-Fenton reactions for the treatment of cellulose bleaching effluents. *Chemosphere* **2003,** *53* (10), 1211-1220.

121.   Schrank, S. G.; José, H. J.; Moreira, R. F. P. M.; Schröder, H. F., Applicability of fenton and H2O2/UV reactions in the treatment of tannery wastewaters. *Chemosphere* **2005,** *60* (5), 644-655.

122.   Schrank, S. G.; José, H. J.; Moreira, R. F. P. M.; Schröder, H. F., Elucidation of the behavior of tannery wastewater under advanced oxidation conditions. *Chemosphere* **2004,** *56* (5), 411-423.

123.   Sauer, T. P.; Casaril, L.; Oberziner, A. L. B.; José, H. J.; Moreira, R. d. F. P. M., Advanced oxidation processes applied to tannery wastewater containing Direct Black 38-Elimination and degradation kinetics. *Journal of Hazardous Materials* **2006,** *135* (1-3), 274-279.

124.   Millioli, V. S.; Freire, D. D. C.; Cammarota, M. C., Petroleum oxidation using Fenton's reagent over beach sand following a spill. *Journal of Hazardous Materials* **2003,** *103* (1-2), 79-91.

125.   Lapertot, M.; Ebrahimi, S.; Dazio, S.; Rubinelli, A.; Pulgarin, C., Photo-Fenton and biological integrated process for degradation of a mixture of pesticides. *Journal of Photochemistry and Photobiology a-Chemistry* **2007,** *186* (1), 34-40.

126.   Farre, M. J.; Domenech, X.; Peral, J., Assessment of photo-Fenton and biological treatment coupling for Diuron and Linuron removal from water. *Water Research* **2006,** *40* (13), 2533-2540.

127.   Kastanek, F.; Maleterova, Y.; Kastanek, P., Combination of advanced oxidation and/or reductive dehalogenation and biodegradation for the decontamination of waters contaminated with chlorinated organic compounds. *Separation Science and Technology* **2007,** *42* (7), 1613-1625.

128.   Boreen, A. L.; Arnold, W. A.; McNeill, K., Photochemical fate of sulfa drugs in then aquatic environment: Sulfa drugs containing five-membered heterocyclic groups. *Environmental Science and Technology* **2004,** *38* (14), 3933-3940.

129.   Giokas, D. L.; Vlessidis, A. G., Application of a novel chemometric approach to the determination of aqueous photolysis rates of organic compounds in natural waters. *Talanta* **2007,** *71* (1), 288-295.

130.   Jiao, S.; Zheng, S.; Yin, D.; Wang, L.; Chen, L., Aqueous oxytetracycline degradation and the toxicity change of degradation compounds in photoirradiation process. *Journal of Environmental Sciences* **2008,** *20* (7), 806-813.

131.   Kümmerer, K., Antibiotics in the aquatic environment - A review - Part I. *Chemosphere* **2009,** *75* (4), 417-434.

132.   Shemer, H.; Kunukcu, Y. K.; Linden, K. G., Degradation of the pharmaceutical Metronidazole via UV, Fenton and photo-Fenton processes. *Chemosphere* **2006,** *63* (2), 269-276.

133.   Calza, P.; Medana, C.; Pazzi, M.; Baiocchi, C.; Pelizzetti, E., Photocatalytic transformations of sulphonamides on titanium dioxide. *Applied Catalysis B: Environmental* **2004,** *53* (1), 63-69.

134.   Addamo, M.; Augugliaro, V.; Di Paola, A.; García-López, E.; Loddo, V.; Marcì, G.; Palmisano, L., Removal of drugs in aqueous systems by photoassisted degradation. *Journal of Applied Electrochemistry* **2005,** *35* (7-8), 765-774.

135.   Baran, W.; Sochacka, J.; Wardas, W., Toxicity and biodegradability of sulfonamides and products of their photocatalytic degradation in aqueous solutions. *Chemosphere* **2006,** *65* (8), 1295-1299.

136.   Reyes, C.; Fernández, J.; Freer, J.; Mondaca, M. A.; Zaror, C.; Malato, S.; Mansilla, H. D., Degradation and inactivation of tetracycline by TiO2 photocatalysis. *Journal of Photochemistry and Photobiology A: Chemistry* **2006,** *184* (1-2), 141-146.

137.   Hu, L.; Flanders, P. M.; Miller, P. L.; Strathmann, T. J., Oxidation of sulfamethoxazole and related antimicrobial agents by TiO2 photocatalysis. *Water Research* **2007,** *41* (12), 2612-2626.

138.   Abellán, M. N.; Bayarri, B.; Giménez, J.; Costa, J., Photocatalytic degradation of sulfamethoxazole in aqueous suspension of TiO2. *Applied Catalysis B: Environmental* **2007,** *74* (3-4), 233-241.

139.   Palominos, R.; Freer, J.; Mondaca, M. A.; Mansilla, H. D., Evidence for hole participation during the photocatalytic oxidation of the antibiotic flumequine. *Journal of Photochemistry and Photobiology A: Chemistry* **2008,** *193* (2-3), 139-145.

140.   Klauson, D.; Babkina, J.; Stepanova, K.; Krichevskaya, M.; Preis, S., Aqueous photocatalytic oxidation of amoxicillin. *Catalysis Today* **2010,** *151* (1-2), 39-45.

141. Kaniou, S.; Pitarakis, K.; Barlagianni, I.; Poulios, I., Photocatalytic oxidation of sulfamethazine. *Chemosphere* **2005,** *60* (3), 372-380.

142. Chatzitakis, A.; Berberidou, C.; Paspaltsis, I.; Kyriakou, G.; Sklaviadis, T.; Poulios, I., Photocatalytic degradation and drug activity reduction of Chloramphenicol. *Water Research* **2008,** *42* (1-2), 386-394.

143. Sreedhar Ready, S.; Kotaiah, B., Decolorization of simulated spent reactive dye bath using solar/TiO2/H2O2. *International Journal of Environmental Science and Technology* **2005,** *2* (3), 245-251.

144. Liu, H. L.; Chiou, Y. R., Optimal decolorization efficiency of Reactive Red 239 by UV/TiO2 photocatalytic process coupled with response surface methodology. *Chemical Engineering Journal* **2005,** *112* (1-3), 173-179.

145. Pérez, M.; Torrades, F.; Peral, J.; Lizama, C.; Bravo, C.; Casas, S.; Freer, J.; Mansilla, H. D., Multivariate approach to photocatalytic degradation of a cellulose bleaching effluent. *Applied Catalysis B: Environmental* **2001,** *33* (2), 89-96.

146. Saien, J.; Nejati, H., Enhanced photocatalytic degradation of pollutants in petroleum refinery wastewater under mild conditions. *Journal of Hazardous Materials* **2007,** *148* (1-2), 491-495.

147. Kuburovic, N.; Todorovic, M.; Raicevic, V.; Orlovic, A.; Jovanovic, L.; Nikolic, J.; Kuburovic, V.; Drmanic, S.; Solevic, T., Removal of methyl tertiary butyl ether from wastewaters using photolytic, photocatalytic and microbiological degradation processes. *Desalination* **2007,** *213* (1-3), 123-128.

148. Goel, M.; Chovelon, J. M.; Ferronato, C.; Bayard, R.; Sreekrishnan, T. R., The remediation of wastewater containing 4-chlorophenol using integrated photocatalytic and biological treatment. *Journal of Photochemistry and Photobiology B-Biology* **2010,** *98* (1), 1-6.

149. Iijima, S.; Ichihashi, T., Single-shell carbon nanotubes of 1-nm diameter. *Nature* **1993,** *363* (6430), 603-605.

150. Balasubramanian, K.; Burghard, M., Chemically functionalized carbon nanotubes. *Small* **2005,** *1* (2), 180-192.

151. Lu, C.; Chung, Y. L.; Chang, K. F., Adsorption of trihalomethanes from water with carbon nanotubes. *Water Research* **2005,** *39* (6), 1183-1189.

152. Bull, R. J.; Birnbaum, L. S.; Cantor, K. P.; Rose, J. B.; Butterworth, B. E.; Pegram, R.; Tuomisto, J., Water chlorination: Essential process or cancer hazard? *Fundamental and Applied Toxicology* **1995,** *28* (2), 155-166.

153. Rook, J. J., Formation of haloforms during chlorination of natural waters. *Water Treat. Exam.* **1974,** *23* (2), 234-243.

154. Salipira, K. L.; Mamba, B. B.; Krause, R. W.; Malefetse, T. J.; Durbach, S. H., Carbon nanotubes and cyclodextrin polymers for removing organic pollutants from water. *Environmental Chemistry Letters* **2007,** *5* (1), 13-17.

155. Long, R. Q.; Yang, R. T., Carbon nanotubes as superior sorbent for dioxin removal [1]. *Journal of the American Chemical Society* **2001,** *123* (9), 2058-2059.

156. Zhou, Q.; Xiao, J.; Wang, W.; Liu, G.; Shi, Q.; Wang, J., Determination of atrazine and simazine in environmental water samples using multiwalled carbon nanotubes as the adsorbents for preconcentration prior to high performance liquid chromatography with diode array detector. *Talanta* **2006,** *68* (4), 1309-1315.

157.   Zhou, Q.; Xiao, J.; Wang, W., Using multi-walled carbon nanotubes as solid phase extraction adsorbents to determine dichlorodiphenyltrichloroethane and its metabolites at trace level in water samples by high performance liquid chromatography with UV detection. *Journal of Chromatography A* **2006,** *1125* (2), 152-158.

158.   Zhou, Q.; Xiao, J.; Wang, W., Comparison of multiwalled carbon nanotubes and a conventional absorbent on the enrichment of sulfonylurea herbicides in water samples. *Analytical Sciences* **2007,** *23* (2), 189-192.

159.   Zhang, W. X.; Wang, C. B.; Lien, H. L., Treatment of chlorinated organic contaminants with nanoscale bimetallic particles. *Catalysis Today* **1998,** *40* (4), 387-395.

160.   Zhang, Z.; Wang, C. C.; Zakaria, R.; Ying, J. Y., Role of particle size in nanocrystalline TiOi-based photocatalysts. *Journal of Physical Chemistry B* **1998,** *102* (52), 10871-10878.

161.   Wang, C. B.; Zhang, W. X., Synthesizing nanoscale iron particles for rapid and complete dechlorination of TCE and PCBs. *Environmental Science and Technology* **1997,** *31* (7), 2154-2156.

162.   He, F.; Zhao, D., Preparation and characterization of a new class of starch-stabilized bimetallic nanoparticles for degradation of chlorinated hydrocarbons in water. *Environmental Science and Technology* **2005,** *39* (9), 3314-3320.

163.   Cheng, S. F.; Wu, S. C., The enhancement methods for the degradation of TCE by zero-valent metals. *Chemosphere* **2000,** *41* (8), 1263-1270.

164.   Cheng, S. F.; Wu, S. C., Feasibility of using metals to remediate water containing TCE. *Chemosphere* **2001,** *43* (8), 1023-1028.

165. Shin, E. J.; Keane, M. A., Detoxification of dichlorophenols by catalytic hydrodechlorination using a nickel/silica catalyst. *Chemical Engineering Science* **1999,** *54* (8), 1109-1120.

166. Lien, H. L.; Zhang, W. X., Transformation of chlorinated methanes by nanoscale iron particles. *Journal of Environmental Engineering* **1999,** *125* (11), 1042-1047.

167. Lien, H. L.; Zhang, W. X., Nanoscale iron particles for complete reduction of chlorinated ethenes. *Colloids and Surfaces A: Physicochemical and Engineering Aspects* **2001,** *191* (1-2), 97-105.

168. Schrick, B.; Blough, J. L.; Jones, A. D.; Mallouk, T. E., Hydrodechlorination of trichloroethylene to hydrocarbons using bimetallic nickel-iron nanoparticles. *Chemistry of Materials* **2002,** *14* (12), 5140-5147.

169. Zhu, B. W.; Lim, T. T.; Feng, J., Reductive dechlorination of 1,2,4-trichlorobenzene with palladized nanoscale Fe0 particles supported on chitosan and silica. *Chemosphere* **2006,** *65* (7), 1137-1145.

170. Wei, J.; Xu, X.; Liu, Y.; Wang, D., Catalytic hydrodechlorination of 2,4-dichlorophenol over nanoscale Pd/Fe: Reaction pathway and some experimental parameters. *Water Research* **2006,** *40* (2), 348-354.

171. Košutić, K.; Dolar, D.; Ašperger, D.; Kunst, B., Removal of antibiotics from a model wastewater by RO/NF membranes. *Separation and Purification Technology* **2007,** *53* (3), 244-249.

172. Radjenović, J.; Petrović, M.; Ventura, F.; Barceló, D., Rejection of pharmaceuticals in nanofiltration and reverse osmosis membrane drinking water treatment. *Water Research* **2008,** *42* (14), 3601-3610.

173. Koyuncu, I.; Arikan, O. A.; Wiesner, M. R.; Rice, C., Removal of hormones and antibiotics by nanofiltration membranes. *Journal of Membrane Science* **2008,** *309* (1-2), 94-101.

174. Li, S. Z.; Li, X. Y.; Wang, D. Z., Membrane (RO-UF) filtration for antibiotic wastewater treatment and recovery of antibiotics. *Separation and Purification Technology* **2004,** *34* (1-3), 109-114.

175. Méndez-Díaz, J. D.; Prados-Joya, G.; Rivera-Utrilla, J.; Leyva-Ramos, R.; Sánchez-Polo, M.; Ferro-García, M. A.; Medellín-Castillo, N. A., Kinetic study of the adsorption of nitroimidazole antibiotics on activated carbons in aqueous phase. *Journal of Colloid and Interface Science* **2010,** *345* (2), 481-490.

176. Kim, S. H.; Shon, H. K.; Ngo, H. H., Adsorption characteristics of antibiotics trimethoprim on powdered and granular activated carbon. *Journal of Industrial and Engineering Chemistry* **2010,** *16* (3), 344-349.

177. Putra, E. K.; Pranowo, R.; Sunarso, J.; Indraswati, N.; Ismadji, S., Performance of activated carbon and bentonite for adsorption of amoxicillin from wastewater: Mechanisms, isotherms and kinetics. *Water Research* **2009,** *43* (9), 2419-2430.

178. Lambert, S. D.; Graham, N. J. D.; Sollars, C. J.; Fowler, G. D., Evaluation of inorganic adsorbents for the removal of problematic textile dyes and pesticides. In *Water Science and Technology*, 1997; Vol. 36, pp 173-180.

179. Nath, K.; Bhakhar, M. S., Microbial regeneration of spent activated carbon dispersed with organic contaminants: mechanism, efficiency, and kinetic models. *Environmental Science and Pollution Research* **2011,** *18* (4), 534-546.

180.   Yin, C. Y.; Aroua, M. K.; Daud, W. M. A. W., Review of modifications of activated carbon for enhancing contaminant uptakes from aqueous solutions. *Separation and Purification Technology* **2007,** *52* (3), 403-415.

181.   Song, Z.; Williams, C. J.; Edyvean, R. G. J., Treatment of tannery wastewater by chemical coagulation. *Desalination* **2004,** *164* (3), 249-259.

182.   Matilainen, A.; Lindqvist, N.; Tuhkanen, T., Comparison of the effiency of aluminium and ferric sulphate in the removal of natural organic matter during drinking water treatment process. *Environmental Technology* **2005,** *26* (8), 867-875.

183.   Golob, V.; Vinder, A.; Simonic, M., Efficiency of the coagulation/flocculation method for the treatment of dyebath effluents. *Dyes and Pigments* **2005,** *67* (2), 93-97.

184.   Lee, J. W.; Choi, S. P.; Thiruvenkatachari, R.; Shim, W. G.; Moon, H., Evaluation of the performance of adsorption and coagulation processes for the maximum removal of reactive dyes. *Dyes and Pigments* **2006,** *69* (3), 196-203.

185.   Gaydardzhiev, S.; Karthikeyan, J.; Ay, P., Colour removal from model solutions by coagulation - Surface charge and floc characterisation aspects. *Environmental Technology* **2006,** *27* (2), 193-199.

186.   Canizares, P.; Martinez, F.; Jimenez, C.; Lobato, J.; Rodrigo, M. A., Coagulation and electrocoagulation of wastes polluted with dyes. *Environmental Science & Technology* **2006,** *40* (20), 6418-6424.

187.   Mishra, A.; Bajpai, M., Flocculation behaviour of model textile wastewater treated with a food grade polysaccharide. *Journal of Hazardous Materials* **2005,** *118* (1-3), 213-217.

188.   Zemaitaitiene, R. J.; Zliobaite, E.; Klimaviciute, R.; Zemaitaitis, A., The role of anionic substances in removal of textile dyes from solutions using cationic flocculant. *Colloids and Surfaces a-Physicochemical and Engineering Aspects* **2003,** *214* (1-3), 37-47.

189.   Forgacs, E.; Cserhati, T.; Oros, G., Removal of synthetic dyes from wastewaters: a review. *Environment International* **2004,** *30* (7), 953-971.

190.   Gupta, G. S.; Shukla, S. P.; Prasad, G.; Singh, V. N., China-clay as an adsorbent for dye house wastewaters. *Environmental Technology* **1992,** *13* (10), 925-936.

191.   Kabdasli, I.; Tunay, O.; Orhon, D., Wastewater control and management in a leather tanning district. *Water Science and Technology* **1999,** *40* (1), 261-267.

192.   Ivanov, K.; Gruber, E.; Schempp, W.; Kirov, D., Possibilities of using zeolite as filler and carrier for dyestuffs in paper. *Papier* **1996,** *50* (7-8), 456-&.

193.   Bhat, R. V.; Mathur, P., Changing scenario of food colours in India. *Current Science* **1998,** *74* (3), 198-202.

194.   Cook, S. M. F.; Linden, D. R., Use of rhodamine WT to facilitate dilution and analysis of atrazine samples in short-term transport studies. *Journal of Environmental Quality* **1997,** *26* (5), 1438-1440.

195.   Martinez-Huitle, C. A.; Brillas, E., Decontamination of wastewaters containing synthetic organic dyes by electrochemical methods: A general review. *Applied Catalysis B-Environmental* **2009,** *87* (3-4), 105-145.

196.   Crini, G., Non-conventional low-cost adsorbents for dye removal: A review. *Bioresource Technology* **2006,** *97* (9), 1061-1085.

197.   Karadag, D.; Tok, S.; Akgul, E.; Ulucan, K.; Evden, H.; Kaya, M. A., Combining adsorption and coagulation for the treatment of azo and anthraquinone dyes from aqueous solution. *Industrial & Engineering Chemistry Research* **2006,** *45* (11), 3969-3973.

198.   Chen, H. Z.; Xu, H. Y.; Heinze, T. M.; Cerniglia, C. E., Decolorization of water and oil-soluble azo dyes by Lactobacillus acidophilus and Lactobacillus fermentum. *Journal of Industrial Microbiology & Biotechnology* **2009,** *36* (12), 1459-1466.

199.   Raghavacharya, C., Colour removal from industrial effluents. *Chemical Engineering World* **1997,** *32* (7), 53-54.

200.   Nassar, M. M.; El-Geundi, M. S., Comparative cost of colour removal from textile effluents using natural adsorbents. *Journal of Chemical Technology and Biotechnology* **1991,** *50* (2), 257-264.

201.   Rao, K. C. L. N.; Krishnaiah, K.; Ashutosh, Colour removal from a dyestuff industry effluent using activated carbon. *Indian Journal of Chemical Technology* **1994,** *1* (1), 13-19.

202.   McKay, G., Adsorption of dyestuffs from aqueous solutions using activated carbon. III. Interparticle diffusion processes. *Journal of Chemical Technology and Biotechnology, Chemical Technology* **1983,** *33 A* (4), 196-204.

203.   Chern, J. M.; Huang, S. N., Study of nonlinear wave propagation theory. 1. Dye adsorption by activated carbon. *Industrial and Engineering Chemistry Research* **1998,** *37* (1), 253-257.

204.   Wu, F. C.; Tseng, R. L.; Juang, R. S., Preparation of activated carbons from bamboo and their adsorption abilities for dyes and phenol. *Journal of Environmental Science and Health - Part A Toxic/Hazardous Substances and Environmental Engineering* **1999,** *34* (9), 1753-1775.

205.   Allen, S. J.; Gan, Q.; Matthews, R.; Johnson, P. A., Comparison of optimised isotherm models for basic dye adsorption by kudzu. *Bioresource Technology* **2003,** *88* (2), 143-152.

206.   Aksu, Z.; Tezer, S., Biosorption of reactive dyes on the green alga Chlorella vulgaris. *Process Biochemistry* **2005,** *40* (3-4), 1347-1361.

207.   Martin, M. J.; Artola, A.; Balaguer, M. D.; Rigola, M., Activated carbons developed from surplus sewage sludge for the removal of dyes from dilute aqueous solutions. *Chemical Engineering Journal* **2003,** *94* (3), 231-239.

208.   Sanghi, R.; Bhattacharya, B., Review on decolorisation of aqueous dye solutions by low cost adsorbents. *Coloration Technology* **2002,** *118* (5), 256-269.

209.   Gupta, V. K.; Suhas, Application of low-cost adsorbents for dye removal - A review. *Journal of Environmental Management* **2009,** *90* (8), 2313-2342.

210.   Do, J. S.; Chen, M. L., Decolourization of dye-containing solutions by electrocoagulation. *Journal of Applied Electrochemistry* **1994,** *24* (8), 785-790.

211.   Stackelberg, P. E.; Gibs, J.; Furlong, E. T.; Meyer, M. T.; Zaugg, S. D.; Lippincott, R. L., Efficiency of conventional drinking-water-treatment processes in removal of pharmaceuticals and other organic compounds. *Science of the Total Environment* **2007,** *377* (2-3), 255-272.

212.   Robinson, T.; McMullan, G.; Marchant, R.; Nigam, P., Remediation of dyes in textile effluent: a critical review on current treatment technologies with a proposed alternative. *Bioresource Technology* **2001,** *77* (3), 247-255.

213.   dos Santos, A. B.; Cervantes, F. J.; van Lier, J. B., Review paper on current technologies for decolourisation of textile wastewaters: Perspectives for anaerobic biotechnology. *Bioresource Technology* **2007,** *98* (12), 2369-2385.

214. Hao, O. J.; Kim, H.; Chiang, P. C., Decolorization of wastewater. *Critical Reviews in Environmental Science and Technology* **2000,** *30* (4), 449-505.

215. Gutiérrez, M. C.; Crespi, M., A review of electrochemical treatments for colour elimination. *Journal of the Society of Dyers and Colourists* **1999,** *115* (11), 342-345.

216. Naim, M. M.; El Abd, Y. M., Removal and recovery of dyestuffs from dyeing wastewaters. *Separation and Purification Methods* **2002,** *31* (1), 171-228.

217. Kariyajjanavar, P.; Jogttappa, N.; Nayaka, Y. A., Studies on degradation of reactive textile dyes solution by electrochemical method. *Journal of Hazardous Materials* **2011,** *190* (1-3), 952-961.

218. Bekiari, V.; Sotiropoulou, M.; Bokias, G.; Lianos, P., Use of poly(N,N-dimethylacrylamide-co-sodium acrylate) hydrogel to extract cationic dyes and metals from water. *Colloids and Surfaces a-Physicochemical and Engineering Aspects* **2008,** *312* (2-3), 214-

219. Solpan, D.; Duran, S.; Saraydin, D.; Guven, O., Adsorption of methyl violet in aqueous solutions by poly(acrylamide-co-acrylic acid) hydrogels. *Radiation Physics and Chemistry* **2003,** *66* (2), 117-127.

220. Solpan, D.; Duran, S.; Torun, M., Removal of cationic dyes by poly(acrylamide-co-acrylic acid) hydrogels in aqueous solutions. *Radiation Physics and Chemistry* **2008,** *77* (4), 447-452.

221. Solpan, D.; Kolge, Z., Adsorption of methyl violet in aqueous solutions by poly(N-vinylpyrrolidone-co-methacrylic acid) hydrogels. *Radiation Physics and Chemistry* **2006,** *75* (1), 120-128.

222.   Thivaios, I.; Bokias, G., Adsorption of nile red by poly(N-isopropylacrylamide) gels in binary water/tetrahydrofuran mixtures. *Journal of Applied Polymer Science* **2010,** *116* (3), 1509-1514.

223.   Ozkahraman, B.; Acar, I.; Emik, S., Removal of cationic dyes from aqueous solutions with poly (N-isopropylacrylamide-co-itaconic acid) hydrogels. *Polymer Bulletin* **2011,** *66* (4), 551-570.

224.   Abdel-Aziz, H. M.; Siyam, T., Radiation synthesis of poly(acrylamide-acrylic acid-dimethylaminoethyl methacrylate) resin and its use for binding of some anionic dyes. *Water Air and Soil Pollution* **2011,** *218* (1-4), 165-174.

225.   Li, S. F., Removal of crystal violet from aqueous solution by sorption into semi-interpenetrated networks hydrogels constituted of poly(acrylic acid-acrylamide-methacrylate) and amylose. *Bioresource Technology* **2010,** *101* (7), 2197-2202.

226.   Li, S. F.; Yan, S. L.; Yu, J. Y., Removal of cationic dyes from aqueous solution by hydrophobically modified poly(acrylic Acid) hydrogels. *Polymer-Plastics Technology and Engineering* **2011,** *50* (8), 783-790.

227.   Kasgoz, H., Aminofunctionalized acrylamide-maleic acid hydrogels: Adsorption of indigo carmine. *Colloids and Surfaces a-Physicochemical and Engineering Aspects* **2005,** *266* (1-3), 44-50.

228.   Kasgoz, H.; Durmus, A., Dye removal by a novel hydrogel-clay nanocomposite with enhanced swelling properties. *Polymers for Advanced Technologies* **2008,** *19* (7), 838-845.

229.   Yun, J.; Im, J. S.; Oh, A.; Jin, D. H.; Bae, T. S.; Lee, Y. S.; Kim, H. I., pH-sensitive photocatalytic activities of TiO(2)/poly(vinyl alcohol)/poly(acrylic acid) composite hydrogels.

Materials Science and Engineering B-Advanced Functional Solid-State Materials **2011,** *176* (3), 276-281.

230.   Sari, M. M., Removal of acidic indigo carmine textile dye from aqueous solutions using radiation induced cationic hydrogels. *Water Science and Technology* **2010,** *61* (8), 2097-2104.

231.   Akkaya, M. C.; Emik, S.; Guclu, G.; Iyim, T. B.; Ozgumus, S., Removal of basic dyes from aqueous solutions by crosslinked-acrylic acid/acrylamidopropane sulfonic acid hydrogels. *Journal of Applied Polymer Science* **2009,** *114* (2), 1150-1159.

232.   Senkal, B. F.; Yavuz, E., Preparation of poly(vinyl pyrrolidone) grafted sulfonamide based polystyrene resin and its use for the removal of dye from water. *Polymers for Advanced Technologies* **2006,** *17* (11-12), 928-931.

233.   Jin, X. Y.; Jiang, M. Q.; Shan, X. Q.; Pei, Z. G.; Chen, Z. L., Adsorption of methylene blue and orange II onto unmodified and surfactant-modified zeolite. *Journal of Colloid and Interface Science* **2008,** *328* (2), 243-247.

234.   Laszlo, J. A., Regeneration of dye-saturated quaternized cellulose by bisulfite-mediated borohydride reduction of dye azo droops: An improved process for decolorization of textile wastewaters. *Environmental Science & Technology* **1997,** *31* (12), 3647-3653.

235.   Anandan, S.; Lee, G. J.; Chen, P. K.; Fan, C.; Wu, J. J., Removal of orange II dye in water by visible light assisted photocatalytic ozonation using Bi2O3 and Au/Bi2O3 nanorods. *Industrial & Engineering Chemistry Research* **2010,** *49* (20), 9729-9737.

236.   Nayak, S.; Lyon, L. A., Soft nanotechnology with soft nanoparticles. *Angewandte Chemie-International Edition* **2005,** *44* (47), 7686-7708.

237.   Hennink, W. E.; van Nostrum, C. F., Novel crosslinking methods to design hydrogels. *Advanced Drug Delivery Reviews* **2002,** *54* (1), 13-36.

238.   Hamidi, M.; Azadi, A.; Rafiei, P., Hydrogel nanoparticles in drug delivery. *Advanced Drug Delivery Reviews* **2008,** *60* (15), 1638-1649.

239.   Hoffman, A. S., Hydrogels for biomedical applications. *Advanced Drug Delivery Reviews* **2002,** *54* (1), 3-12.

240.   Gehrke, S. H., Synthesis, equilibrium swelling, kinetics, permeability and applications of environmentally responsive gels. *Advances in Polymer Science* **1993,** *110*, 80-144.

241.   Drury, J. L.; Mooney, D. J., Hydrogels for tissue engineering: Scaffold design variables and applications. *Biomaterials* **2003,** *24* (24), 4337-4351.

242.   Dhara, D.; Nisha, C. K.; Chatterji, P. R., Super absorbent hydrogels: Interpenetrating networks of poly(acrylamide-co-acrylic acid) and poly(vinyl alcohol): Swelling behavior and structural parameters. *Journal of Macromolecular Science - Pure and Applied Chemistry* **1999,** *36 A* (2), 197-210.

243.   Oh, J. K.; Drumright, R.; Siegwart, D. J.; Matyjaszewski, K., The development of microgels/nanogels for drug delivery applications. *Progress in Polymer Science* **2008,** *33* (4), 448-477.

244.   Gombotz, W. R.; Wee, S. F., Protein release from alginate matrices. *Advanced Drug Delivery Reviews* **1998,** *31* (3), 267-285.

245.   Goosen, M. F. A.; O'Shea, G. M.; Gharapetian, H. M.; Chou, C.; Sun, A. M., Optimization of microencapsulation parameters: semipermeable microcapsules as a bioartificial pancreas. *Biotechnology and Bioengineering* **1985,** *27* (2), 146-150.

246.   Lutolf, M. P.; Raeber, G. P.; Zisch, A. H.; Tirelli, N.; Hubbell, J. A., Cell-responsive synthetic hydrogels. *Advanced Materials* **2003,** *15* (11), 888-892.

247.   Dai, W. S.; Barbari, T. A., Hollow fiber-supported hydrogels with mesh-size asymmetry. *Journal of Membrane Science* **2000,** *171* (1), 79-86.

248.   Kikuchi, A.; Okano, T., Pulsatile drug release control using hydrogels. *Advanced Drug Delivery Reviews* **2002,** *54* (1), 53-77.

249.   Kim, S. W.; Bae, Y. H.; Okano, T., Hydrogels: swelling, drug loading, and release. *Pharmaceutical Research* **1992,** *9* (3), 283-290.

250.   Qiu, Y.; Park, K., Environment-sensitive hydrogels for drug delivery. *Advanced Drug Delivery Reviews* **2001,** *53* (3), 321-339.

251.   Park, T. G., Temperature modulated protein release from pH/temperature-sensitive hydrogels. *Biomaterials* **1999,** *20* (6), 517-521.

252.   Miyata, T.; Uragami, T.; Nakamae, K., Biomolecule-sensitive hydrogels. *Advanced Drug Delivery Reviews* **2002,** *54* (1), 79-98.

253.   Li, Y.; Tanaka, T., Study of the universality class of the gel network system. *The Journal of Chemical Physics* **1989,** *90* (9), 5161-5166.

254.   Li, Y.; Tanaka, T., Kinetics of swelling and shrinking of gels. *The Journal of Chemical Physics* **1990,** *92* (2), 1365-1371.

255.   Tanaka, T.; Wang, C.; Pande, V.; Grosberg, A. Y.; English, A.; Masamune, S.; Gold, H.; Levy, R.; King, K., Polymer gels that can recognize and recover molecules. *Faraday Discussions* **1995,** *101*, 201-206.

256.   Gan, D.; Lyon, L. A., Interfacial nonradiative energy transfer in responsive core-shell hydrogel nanoparticles. *Journal of the American Chemical Society* **2001,** *123* (34), 8203-8209.

257.   Gan, D.; Lyon, L. A., Tunable swelling kinetics in core - shell hydrogel nanoparticles. *Journal of the American Chemical Society* **2001,** *123* (31), 7511-7517.

258. Jones, C. D.; Lyon, L. A., Synthesis and characterization of multiresponsive core-shell microgels. *Macromolecules* **2000,** *33* (22), 8301-8306.

259. Gan, D.; Lyon, L. A., Fluorescence nonradiative energy transfer analysis of crosslinker heterogeneity in core-shell hydrogel nanoparticles. *Analytica Chimica Acta* **2003,** *496* (1-2), 53-63.

260. Tanaka, T., Collapse of gels and the critical endpoint. *Physical Review Letters* **1978,** *40* (12), 820-823.

261. Dusek, K.; Patterson, D., Transition in swollen polymer networks induced by intramolecular condensation. *J. Polym. Sci.* **1968,** *6* (6), 1209-1216.

262. Moselhy, J.; Wu, X. Y.; Nicholov, R.; Kodaria, K., In vitro studies of the interaction of poly(NIPAm/MAA) nanoparticles with proteins and cells. *Journal of Biomaterials Science, Polymer Edition* **2000,** *11* (2), 123-147.

263. Gupta, P.; Vermani, K.; Garg, S., Hydrogels: from controlled release to pH-responsive drug delivery. *Drug Discovery Today* **2002,** *7* (10), 569-579.

264. Gil, E. S.; Hudson, S. M., Stimuli-reponsive polymers and their bioconjugates. *Progress in Polymer Science* **2004,** *29* (12), 1173-1222.

265. Jeong, B.; Gutowska, A., Lessons from nature: stimuli-responsive polymers and their biomedical applications. *Trends in Biotechnology* **2002,** *20* (7), 305-311.

266. Duracher, D.; Sauzedde, F.; Elaissari, A.; Perrin, A.; Pichot, C., Cationic amino-containing N-isopropyl-acrylamide-styrene copolymer latex particles: 1-Particle size and morphology vs. polymerization process. *Colloid and Polymer Science* **1998,** *276* (3), 219-231.

267.   Snowden, M. J.; Chowdhry, B. Z.; Vincent, B.; Morris, G. E., Colloidal copolymer microgels of N-isopropylacrylamide and acrylic acid: pH, ionic strength and temperature effects. *Journal of the Chemical Society-Faraday Transactions* **1996,** *92* (24), 5013-5016.

268.   Sershen, S. R.; Westcott, S. L.; Halas, N. J.; West, J. L., Temperature-sensitive polymer-nanoshell composites for photothermally modulated drug delivery. *Journal of Biomedical Materials Research* **2000,** *51* (3), 293-298.

269.   Sershen, S. R.; Westcott, S. L.; Halas, N. J.; West, J. L., Independent optically addressable nanoparticle-polymer optomechanical composites. *Applied Physics Letters* **2002,** *80* (24), 4609-4611.

270.   Nayak, S.; Debord, S. B.; Lyon, L. A., Investigations into the deswelling dynamics and thermodynamics of thermoresponsive microgel composite films. *Langmuir* **2003,** *19* (18), 7374-7379.

271.   Plunkett, K. N.; Kraft, M. L.; Yu, Q.; Moore, J. S., Swelling kinetics of disulfide cross-linked microgels. *Macromolecules* **2003,** *36* (11), 3960-3966.

272.   Serpe, M. J.; Rivera, M.; Kersey, F. R.; Clark, R. L.; Craig, S. L., Time and distance dependence of reversible polymer bridging followed by single-molecule force spectroscopy. *Langmuir* **2008,** *24* (9), 4738-4742.

273.   Nayak, S.; Lyon, L. A., Photoinduced phase transitions in poly(N-isopropylacrylamide) microgels. *Chemistry of Materials* **2004,** *16* (13), 2623-2627.

274.   Lutz, J. F.; Weichenhan, K.; Akdemir, O.; Hoth, A., About the phase transitions in aqueous solutions of thermoresponsive copolymers and hydrogels based on 2-(2-methoxyethoxy)ethyl methacrylate and oligo(ethylene glycol) methacrylate. *Macromolecules* **2007,** *40* (7), 2503-2508.

275. Amalvy, J. I.; Wanless, E. J.; Li, Y.; Michailidou, V.; Armes, S. P.; Duccini, Y., Synthesis and characterization of novel pH-responsive microgels based on tertiary amine methacrylates. *Langmuir* **2004,** *20* (21), 8992-8999.

276. Suzuki, A.; Tanaka, T., Phase transition in polymer gels induced by visible light. *Nature* **1990,** *346* (6282), 345-347.

277. Shibayama, M.; Tanaka, T., Volume phase transition and related phenomena of polymer gels. *Adv. Polym. Sci.* **1993,** *109*, 1-62.

278. Argentiere, S.; Blasi, L.; Morello, G.; Gigli, G., A Novel pH-responsive nanogel for the controlled uptake and release of hydrophobic and cationic solutes. *Journal of Physical Chemistry C* **2011,** *115* (33), 16347-16353.

279. Popescu, M. T.; Mourtas, S.; Pampalakis, G.; Antimisiaris, S. G.; Tsitsilianis, C., pH-Responsive hydrogel/liposome soft nanocomposites for tuning drug release. *Biomacromolecules* **2011,** *12* (8), 3023-3030.

280. Riedinger, A.; Leal, M. P.; Deka, S. R.; George, C.; Franchini, I. R.; Falqui, A.; Cingolani, R.; Pellegrino, T., "Nanohybrids" based on pH-responsive hydrogels and inorganic nanoparticles for drug delivery and sensor applications. *Nano Letters* **2011,** *11* (8), 3136-3141.

281. Bajpai, A. K.; Shukla, S. K.; Bhanu, S.; Kankane, S., Responsive polymers in controlled drug delivery. *Progress in Polymer Science* **2008,** *33* (11), 1088-1118.

282. Peppas, N. A., Hydrogels and drug delivery. *Current Opinion in Colloid & Interface Science* **1997,** *2* (5), 531-537.

283. Fu, G.; Soboyejo, W. O., Investigation of swellable poly (N-isopropylacrylamide) based hydrogels for drug delivery. *Materials Science & Engineering C-Materials for Biological Applications* **2011,** *31* (5), 1084-1090.

284. Bajpai, A. K.; Bajpai, J.; Saini, R.; Gupta, R., Responsive polymers in biology and technology. *Polymer Reviews* **2011,** *51* (1), 53-97.

285. Mart, R. J.; Osborne, R. D.; Stevens, M. M.; Ulijn, R. V., Peptide-based stimuli-responsive biomaterials. *Soft Matter* **2006,** *2* (10), 822-835.

286. Roy, I.; Gupta, M. N., Smart polymeric materials: emerging biochemical applications. *Chemistry & Biology* **2003,** *10* (12), 1161-1171.

287. Ben-Moshe, M.; Alexeev, V. L.; Asher, S. A., Fast responsive crystalline colloidal array photonic crystal glucose sensors. *Analytical Chemistry* **2006,** *78* (14), 5149-5157.

288. Frisman, I.; Shachaf, Y.; Seliktar, D.; Biancdo-Peled, H.; Stimuli responsive hydrogels made from biosynthetic fibrinogen conjugates for tissue engineering, *Langmuir* **2011,** *27* (11), 6977-6986.

289. Schild, H. G., Poly (N-isopropylacrylamide) - experiment, theory and application. *Progress in Polymer Science* **1992,** *17* (2), 163-249.

290. Wu, C., A comparison between the 'coil-to-globule' transition of linear chains and the "volume phase transition" of spherical microgels. *Polymer* **1998,** *39* (19), 4609-4619.

291. Wu, C.; Zhou, S. Q., Internal motions of both poly(N-isopropylacrylamide) linear chains and spherical microgel particles in water. *Macromolecules* **1996,** *29* (5), 1574-1578.

292. Matsuo, E. S.; Tanaka, T., Kinetics of discontinuous volume-phase transition of gels. *The Journal of Chemical Physics* **1988,** *89* (3), 1695-1703.

293. Serpe, M. J.; Jones, C. D.; Lyon, L. A., Layer-by-layer deposition of thermoresponsive microgel thin films. *Langmuir* **2003,** *19* (21), 8759-8764.

294.   Sorrell, C. D.; Carter, M. C. D.; Serpe, M. J., Color tunable poly (N-isopropylacrylamide)-co-acrylic acid microgel-Au hybrid assemblies. *Advanced Functional Materials* **2011,** *21* (3), 425-433.

295.   Zavgorodnya, O.; Serpe, M., Assembly of poly(N-isopropylacrylamide)-co-acrylic acid microgel thin films on polyelectrolyte multilayers: Effects of polyelectrolyte layer thickness, surface charge, and microgel solution pH. *Colloid & Polymer Science* **2011,** *289* (5), 591-602.

296.   Sorrell, C. D.; Serpe, M. J., Reflection order selectivity of color-tunable poly(N-isopropylacrylamide) microgel based etalons. *Advanced materials* **2011,** *23* (35), 4088-92.

297.   Gong, X. J.; Wu, C.; Ngai, T., Surface interaction forces mediated by poly(N-isopropylacrylamide) (pNIPAM) polymers: effects of concentration and temperature. *Colloid and Polymer Science* **2010,** *288* (10-11), 1167-1172.

298.   Hu, T. J.; You, Y. Z.; Pan, C. Y.; Wu, C., The coil-to-globule-to-brush transition of linear thermally sensitive poly(N-isopropylacrylamide) chains grafted on a spherical microgel. *Journal of Physical Chemistry B* **2002,** *106* (26), 6659-6662.

299.   Pelton, R., Temperature-sensitive aqueous microgels. *Advances in Colloid and Interface Science* **2000,** *85* (1), 1-33.

300.   Saunders, B. R.; Vincent, B., Microgel particles as model colloids: theory, properties and applications. *Advances in Colloid and Interface Science* **1999,** *80* (1), 1-25.

301.   Heskins, M.; Guillet, J. E., Solution properties of poly(N-isopropylacrylamide). *J. Macromol. Sci. Chem.* **1968,** *A2* (8), 1441-1455.

302.   Halperin, A.; Kroger, M., Collapse of thermoresponsive brushes and the tuning of protein adsorption. *Macromolecules* **2011,** *44* (17), 6986-7005.

303.   Tanaka, T., Kinetics of phase transition in polymer gels. *Physica A: Statistical Mechanics and its Applications* **1986,** *140* (1-2), 261-268.

304.   Tanaka, T.; Nishio, I.; Sun, S. T.; Ueno-Nishio, S., Collapse of gels in an electric field. *Science* **1982,** *218* (4571), 467-469.

305.   Tanaka, T.; Fillmore, D. J., Kinetics of swelling of gels. *The Journal of Chemical Physics* **1979,** *70* (3), 1214-1218.

306.   Tanaka, T.; Fillmore, D.; Sun, S. T.; Nishio, I.; Swislow, G.; Shah, A., Phase transitions in ionic gels. *Physical Review Letters* **1980,** *45* (20), 1636-1639.

307.   Yan, Q.; Hoffman, A. S., Synthesis of macroporous hydrogels with rapid swelling and deswelling properties for delivery of macromolecules. *Polymer* **1995,** *36* (4), 887-889.

308.   Wu, X. S.; Hoffman, A. S.; Yager, P., Synthesis and characterization of thermally reversible macroporous poly(N-isopropylacrylamide) hydrogels. *Journal of Polymer Science Part a-Polymer Chemistry* **1992,** *30* (10), 2121-2129.

309.   Wang, J.; Gan, D.; Lyon, L. A.; El-Sayed, M. A., Temperature-jump investigations of the kinetics of hydrogel nanoparticle volume phase transitions. *Journal of the American Chemical Society* **2001,** *123* (45), 11284-11289.

310.   Wu, C.; Zhou, S., Volume phase transition of swollen gels: Discontinuous or continuous? *Macromolecules* **1997,** *30* (3), 574-576.

311.   Daly, E.; Saunders, B. R., Temperature-dependent electrophoretic mobility and hydrodynamic radius measurements of poly(N-isopropylacrylamide) microgel particles: structural insights. *Physical Chemistry Chemical Physics* **2000,** *2* (14), 3187-3193.

312. Ohshima, H.; Makino, K.; Kato, T.; Fujimoto, K.; Kondo, T.; Kawaguchi, H., Electrophoretic mobility of latex particles covered with temperature-sensitive hydrogel layers. *Journal of Colloid And Interface Science* **1993,** *159* (2), 512-514.

313. Karg, M.; Pastoriza-Santos, I.; Rodriguez-Gonzalez, B.; von Klitzing, R.; Wellert, S.; Hellweg, T., Temperature, pH, and ionic strength induced changes of the swelling behavior of pNIPAM-poly(allylacetic acid) copolymer microgels. *Langmuir* **2008,** *24* (12), 6300-6306.

314. Andersson, M.; Maunu, S. L., Volume phase transition and structure of poly(N-isopropylacrylamide) microgels studied with H-1-NMR spectroscopy in D2O. *Colloid and Polymer Science* **2006,** *285* (3), 293-303.

315. Lyon, L. A.; Debord, J. D.; Debord, S. B.; Jones, C. D.; McGrath, J. G.; Serpe, M. J., Microgel colloidal crystals. *Journal of Physical Chemistry B* **2004,** *108* (50), 19099-19108.

316. Hoare, T.; Pelton, R., Functional group distributions in carboxylic acid containing poly(N-isopropylacrylamide) microgels. *Langmuir* **2004,** *20* (6), 2123-2133.

317. Brugger, B.; Richtering, W., Emulsions stabilized by stimuli-sensitive poly(N-isopropylacrylamide)-co-methacrylic acid polymers: microgels versus low molecular weight polymers. *Langmuir* **2008,** *24* (15), 7769-7777.

318. Hoare, T.; Pelton, R., Highly pH and temperature responsive microgels functionalized with vinylacetic acid. *Macromolecules* **2004,** *37* (7), 2544-2550.

319. Schmidt, S.; Hellweg, T.; von Klitzing, R., Packing density control in p(NIPAM-co-AAc) microgel monolayers: effect of surface charge, pH, and preparation technique. *Langmuir* **2008,** *24* (21), 12595-12602.

320.   Kratz, K.; Hellweg, T.; Eimer, W., Influence of charge density on the swelling of colloidal poly(N-isopropylacrylamide-co-acrylic acid) microgels. *Colloids and Surfaces a-Physicochemical and Engineering Aspects* **2000,** *170* (2-3), 137-149.

321.   Braun, O.; Selb, J.; Candau, F., Synthesis in microemulsion and characterization of stimuli-responsive polyelectrolytes and polyampholytes based on N-isopropylacrylamide. *Polymer* **2001,** *42* (21), 8499-8510.

322.   Dowding, P. J.; Vincent, B.; Williams, E., Preparation and swelling properties of poly(NIPAM) 'minigel' particles prepared by inverse suspension polymerization. *Journal of Colloid and Interface Science* **2000,** *221* (2), 268-272.

323.   Guo, Z.; Wang, J.; Zhu, H., Preparation of temperature sensitive ultrafine particles of poly(N-isopropyl acrylamide) by microemulsion polymerization. *Acta Polymerica Sinica* **2001,** (4), 492-493.

324.   Ming, W.; Zhao, Y.; Cui, J.; Fu, S.; Jones, F. N., Formation of irreversible nearly transparent physical polymeric hydrogels during a modified microemulsion polymerization. *Macromolecules* **1999,** *32* (2), 528-530.

325.   Neyret, S.; Vincent, B., The properties of polyampholyte microgel particles prepared by microemulsion polymerization. *Polymer* **1997,** *38* (25), 6129-6134.

326.   Motornov, M.; Roiter, Y.; Tokarev, I.; Minko, S., Stimuli-responsive nanoparticles, nanogels and capsules for integrated multifunctional intelligent systems. *Progress in Polymer Science* **2010,** *35* (1-2), 174-211.

327.   Pich, A.; Richtering, W., Microgels by precipitation polymerization: synthesis, characterization, and functionalization. *Chemical Design of Responsive Microgels* **2010,** *234*, 1-37.

328.   Murray, M. J.; Snowden, M. J., The preparation, characterization and applications of colloidal microgels. *Advances in Colloid and Interface Science* **1995,** *54*, 73-91.

329.   Suzuki, D.; McGrath, J. G.; Kawaguchi, H.; Lyon, L. A., Colloidal crystals of thermosensitive, core/shell hybrid microgels. *Journal of Physical Chemistry C* **2007,** *111* (15), 5667-5672.

330.   Meng, Z. Y.; Smith, M. H.; Lyon, L. A., Temperature-programmed synthesis of micron-sized multi-responsive microgels. *Colloid and Polymer Science* **2009,** *287* (3), 277-285.

331.   Guan, Y.; Zhang, Y. J., PNIPAM microgels for biomedical applications: from dispersed particles to 3D assemblies. *Soft Matter* **2011,** *7* (14), 6375-6384.

332.   Su, S. X.; Ali, M.; Filipe, C. D. M.; Li, Y. F.; Pelton, R., Microgel-based inks for paper-supported biosensing applications. *Biomacromolecules* **2008,** *9* (3), 935-941.

333.   Suzuki, D.; Kawaguchi, H., Hybrid microgels with reversibly changeable multiple brilliant color. *Langmuir* **2006,** *22* (8), 3818-3822.

334.   Wu, W. T.; Zhou, T.; Zhou, S. Q., Tunable photolumineseence of Ag nanocrystals in multiple-sensitive hybrid microgels. *Chemistry of Materials* **2009,** *21* (13), 2851-2861.

335.   Welsch, N.; Ballauff, M.; Lu, Y., Microgels as nanoreactors: applications in catalysis. *Chemical Design of Responsive Microgels* **2010,** *234*, 129-163.

336.   Lu, Y.; Ballauff, M., Thermosensitive core-shell microgels: From colloidal model systems to nanoreactors. *Progress in Polymer Science* **2011,** *36* (6), 767-792.

337.   Du, Y. A.; Lo, E.; Ali, S.; Khademhosseini, A., Directed assembly of cell-laden microgels for fabrication of 3D tissue constructs. *Proceedings of the National Academy of Sciences of the United States of America* **2008,** *105* (28), 9522-9527.

338.   Das, M.; Mardyani, S.; Chan, W. C. W.; Kumacheva, E., Biofunctionalized pH-responsive microgels for cancer cell targeting: Rational design. *Advanced Materials* **2006,** *18* (1), 80-83.

339.   Petras, R. A.; Ropp, P. A.; DeSimone, J. M., Reductively labile PRINT particles for the delivery of doxorubicin to HeLa cells. *Journal of the American Chemical Society* **2008,** *130* (15), 5008-5009.

340.   Ghugare, S. V.; Mozetic, P.; Paradossi, G., Temperature-sensitive poly(vinyl alcohol)/poly(methacrylate-co-N-isopropyl acrylamide) microgels for doxorubicin delivery. *Biomacromolecules* **2009,** *10* (6), 1589-1596.

341.   Cavalieri, F.; Chiessi, E.; Villa, R.; Viganò, L.; Zaffaroni, N.; Telling, M. F.; Paradossi, G., Novel PVA-based hydrogel microparticles for doxorubicin delivery. *Biomacromolecules* **2008,** *9* (7), 1967-1973.

342.   Oh, J. K.; Siegwart, D. J.; Matyjaszewski, K., Synthesis and biodegradation of nanogels as delivery carriers for carbohydrate drugs. *Biomacromolecules* **2007,** *8* (11), 3326-3331.

343.   Goh, S. L.; Murthy, N.; Xu, M.; Fréchet, J. M. J., Cross-linked microparticles as carriers for the delivery of plasmid DNA for vaccine development. *Bioconjugate Chemistry* **2004,** *15* (3), 467-474.

344.   Murthy, N.; Xu, M.; Schuck, S.; Kunisawa, J.; Shastri, N.; Fréchet, J. M. J., A macromolecular delivery vehicle for protein-based vaccines: acid-degradable protein-loaded microgels. *Proceedings of the National Academy of Sciences of the United States of America* **2003,** *100* (9), 4995-5000.

345.   Shi, L.; Khondee, S.; Linz, T. H.; Berkland, C., Poly(*N*-vinylformamide) nanogels capable of pH-sensitive protein release. *Macromolecules* **2008,** *41* (17), 6546-6554.

346. Bharali, D. J.; Sahoo, S. K.; Mozumdar, S.; Maitra, A., Cross-linked polyvinylpyrroelidone nanoparticles: A potential carrier for hydrophilic drugs. *Journal of Colloid and Interface Science* **2003,** *258* (2), 415-423.

347. Gupta, V. K.; Jain, R.; Nayak, A.; Agarwal, S.; Shrivastava, M., Removal of the hazardous dye-Tartrazine by photodegradation on titanium dioxide surface. *Materials Science & Engineering C-Materials for Biological Applications* **2011,** *31* (5), 1062-1067.

348. Salazar, R.; Garcia-Segura, S.; Ureta-Zanartu, M. S.; Brillas, E., Degradation of disperse azo dyes from waters by solar photoelectro-Fenton. *Electrochimica Acta* **2011,** *56* (18), 6371-6379.

349. Elias, B.; Guihard, L.; Nicolas, S.; Fourcade, F.; Amrane, A., Effect of electro-fenton application on azo dyes biodegradability. *Environmental Progress & Sustainable Energy* **2011,** *30* (2), 160-167.

350. Pearce, C. I.; Lloyd, J. R.; Guthrie, J. T., The removal of colour from textile wastewater using whole bacterial cells: a review. *Dyes and Pigments* **2003,** *58* (3), 179-196.

351. Panswad, T.; Luangdilok, W., Decolorization of reactive dyes with different molecular structures under different environmental conditions. *Water Research* **2000,** *34* (17), 4177-4184.

352. Sponza, D. T.; Isik, M., Decolorization and azo dye degradation by anaerobic/aerobic sequential process. *Enzyme and Microbial Technology* **2002,** *31* (1-2), 102-110.

353. El-Desoky, H. S.; Ghoneim, M. M.; Zidan, N. M., Decolorization and degradation of Ponceau S azo-dye in aqueous solutions by the electrochemical advanced Fenton oxidation. *Desalination* **2010,** *264* (1-2), 143-150.

354.   Bayram, E.; Ayranci, E., Electrochemically enhanced removal of polycyclic aromatic basic dyes from dilute aqueous solutions by activated carbon cloth electrodes. *Environmental Science & Technology* **2010,** *44* (16), 6331-6336.

355.   Guilherme, M. R.; Silva, R.; Girotto, E. M.; Rubira, A. F.; Muniz, E. C., Hydrogels based on pAAm network with pNIPAAm included: hydrophilic-hydrophobic transition measured by the partition of Orange II and Methylene Blue in water. *Polymer* **2003,** *44* (15), 4213-4219.

356.   Guilherme, M. R.; da Silva, R.; Rubira, A. F.; Geuskens, G.; Muniz, E. C., Thermo-sensitive hydrogels membranes from PAAm networks and entangled PNIPAAm: effect of temperature, cross-linking and PNIPAAm contents on the water uptake and permeability. *Reactive & Functional Polymers* **2004,** *61* (2), 233-243.

357.   Zhao, H. T.; Joseph, J.; Zhang, H.; Karoui, H.; Kalyanaraman, B., Synthesis and biochemical applications of a solid cyclic nitrone spin trap: A relatively superior trap for detecting superoxide anions and glutathiyl radicals. *Free Radical Biology and Medicine* **2001,** *31* (5), 599-606.

358.   Zhao, H. T.; Joseph, J.; Fales, H. M.; Sokoloski, E. A.; Levine, R. L.; Vasquez-Vivar, J.; Kalyanaraman, B., Detection and characterization of the product of hydroethidine and intracellular superoxide by HPLC and limitations of fluorescence. *Proceedings of the National Academy of Sciences of the United States of America* **2005,** *102* (16), 5727-5732.

359.   Xu, Y. K.; Kalyanaraman, B., Synthesis and ESR studies of a novel cyclic nitrone spin trap attached to a phosphonium group-a suitable trap for mitochondria-generated ROS? *Free Radical Research* **2007,** *41* (1), 1-7.

360.   Shi, H. L.; Timmins, G.; Monske, M.; Burdick, A.; Kalyanaraman, B.; Liu, Y.; Clement, J. L.; Burchiel, S.; Liu, K. J., Evaluation of spin trapping agents and trapping conditions for

detection of cell-generated reactive oxygen species. *Archives of Biochemistry and Biophysics* **2005,** *437* (1), 59-68.

361.   Parasuraman, D.; Serpe, M. J., Poly (N-isopropylacrylamide) microgels for organic dye removal from water. *ACS Applied Materials & Interfaces* **2011**, *3*, 2732.

362.   Parasuraman, D.; Serpe, M. J., Poly (N-isopropylacrylamide) microgel based assemblies for organic dye removal from water. *ACS Applied Materials & Interfaces* **2011,** DOI: 10.1021/am201132x.

363.   Parasuraman, D.; Serpe, M. J., Poly (N-isopropylacrylamide) microgel based assemblies for organic dye removal from water: Microgel diameter effects. *ACS Applied Materials & Interfaces* **2011,** Submitted.

364. Alvarez-Lorenzo, C.; Concheiro, A., Reversible adsorption by a pH-and temperature-sensitive acrylic hydrogel. *Journal of Controlled Release* **2002,** *80* (1-3), 247-257.